# Pixels to Parameters

*Automated Bronchial Tree Analysis in Low-Dose CT for Normative Lung Imaging Biomarkers*

**Ivan Dudurych**

# Pixels to Parameters

## Automated Bronchial Tree Analysis in Low-Dose CT for Normative Lung Imaging Biomarkers

Ivan Dudurych

university of groningen

# Pixels to Parameters

Automated Bronchial Tree Analysis in Low-Dose CT for Normative Lung Imaging Biomarkers

**PhD thesis**

to obtain the degree of PhD of the

University of Groningen

on the authority of the

Rector Magnificus Prof. J.M.A. Scherpen

and in accordance with

the decision by the College of Deans.

This thesis will be defended in public on

Wednesday 11 December 2024 at 16:15 hours

by

Ivan Dudurych

born on 6th July 1993

**Supervisors**

Prof. R. Vliegenthart

Prof. M. de Bruijne

**Assessment Committee**

Prof. P.M.A. van Ooijen

Prof. G.H. Koppelman

Prof. P.A. de Jong

***Look closely. The beautiful may be small.***

# Table of Contents

# PART 1

## BRONCHIAL PARAMETERS ON CHEST CT IN CONTEXT

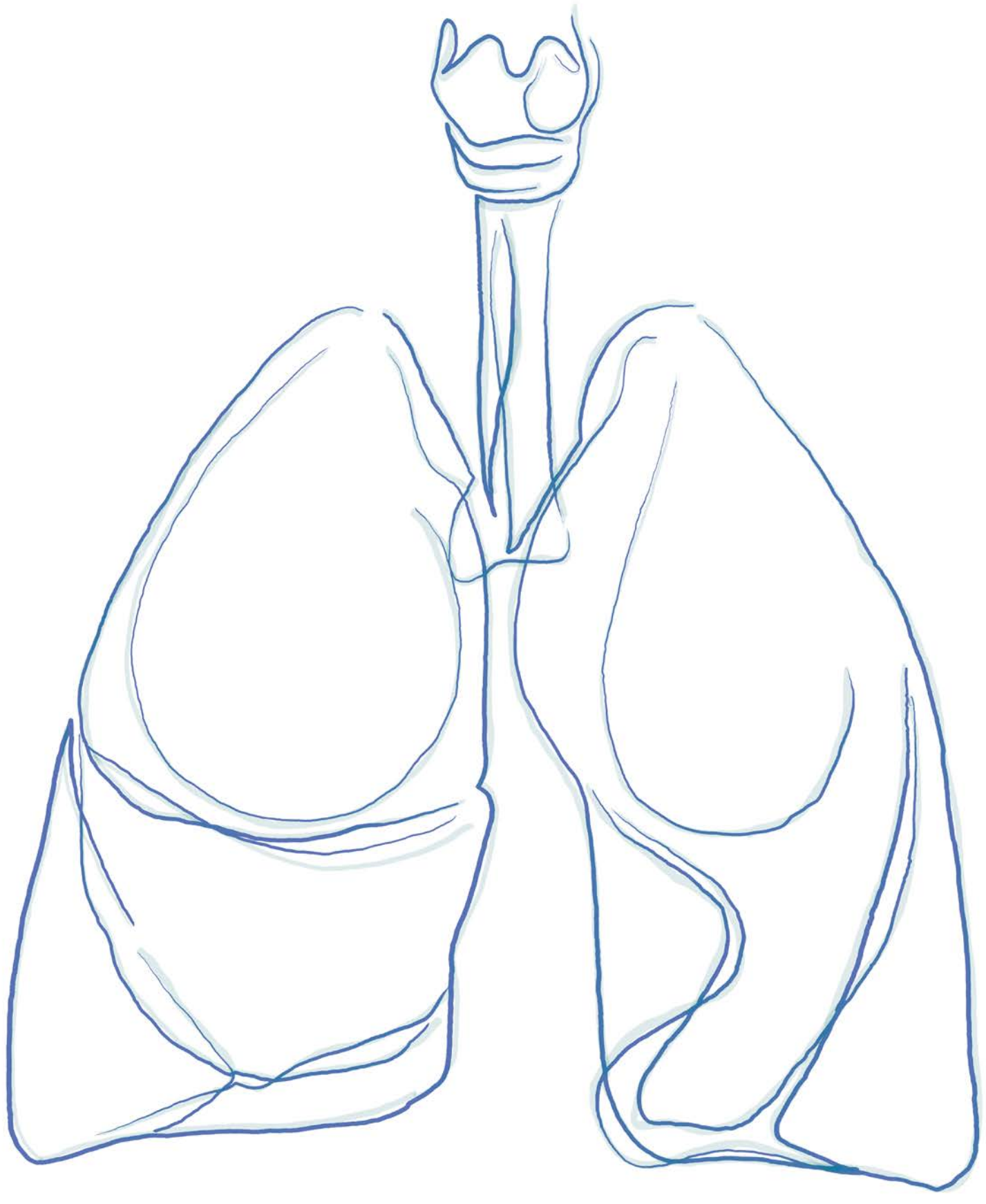

# CHAPTER 1

## Introduction

Modern medical imaging, enhanced by advancements in computer vision, is transforming our ability to extract detailed data from each scan. Analysing complex structures like the airway tree has historically been limited by labour-intensive measurement processes. However, the emergence of advanced computer vision methods facilitates large-scale analysis of numerous scans. This advancement in technology has led to significant insights from scans of the lungs into the pathophysiology of respiratory diseases. Nonetheless, defining what constitute "normal" airway measurements has remained challenging due to the lack of large-scale population-based cohorts. In this thesis, we apply state-of-the-art imaging analysis techniques to establish normal distributions of bronchial values in the general population, and we explore how these parameters correlate with smoking habits and respiratory illnesses.

## Background

### Respiratory System

The primary function of the respiratory system is the exchange of gases between the atmosphere and the circulatory system. This process involves oxygenating the blood and eliminating waste carbon dioxide, by way of the lungs.[1] The respiratory system can be categorised into the upper and lower respiratory systems. Air is brought into the lungs via the respiratory tract which is split into upper and lower sections.

The upper respiratory tract consists of the nose, mouth, and pharynx, while the lower respiratory tract begins at the larynx and continues as the trachea and main bronchi to the terminal bronchioles and alveoli. The airways have a tree-like structure with about 25 divisions from trachea to alveoli. Each division is distinguished by the size and composition of the airway.[2] The first 7 divisions are termed bronchi and are composed of cartilage, smooth muscle, and a lining of epithelial cells interspersed with mucous-producing goblet cells and endocrine cells. The divisions thereafter are termed bronchioles, distinct from bronchi by the lack of cartilage, a progressively thinner muscular layer and a single-layer epithelium of ciliated (hair-like) cells with scattered additional

cells that produce surfactant and mucous. Branches less than 2mm in diameter are often called "small airways".[3]

The lower respiratory system contains a juxtaposed vascular system that follows the airways to the alveoli, including pulmonary arteries bringing de-oxygenated blood from the heart to the gas-exchange surfaces of the alveoli, and the pulmonary veins delivering oxygenated blood back to the heart. Both airways and vessels are supported by the interstitium, which is tissue providing structure and elasticity to the lungs. The combination of terminal airways, vessels, alveoli and interstitium is often referred to as the lung parenchyma.

The lungs expose a vast surface area of between 40-80m² to the environment for gas exchange. This surface is thus also exposed to toxic gases, smoke particles, and infective agents, which can damage the lungs. Damage can build up over time and cause fundamental changes to the composition and structure of the airways and the parenchyma, for example thickening of the airway walls, mucous hypersecretion, and destruction of the alveoli (Figure 1.1 & Figure 1.2). This damage and resulting changes can lead to respiratory disease. When these changes become prominent enough, they can be visualised using medical imaging and eventually cause symptoms.

## Imaging of Airways

Radiological imaging of the airways is possible through a variety of means. While magnetic resonance imaging (MRI) is advancing, its application mainly encompasses functional assessments rather than detailed anatomical evaluations of the bronchi, due to MRI's limitations with regard to visualization of lung parenchyma and breathing motion artifacts.[4,5] Currently, computed tomography (CT) is the main technique used for visualizing and measuring airways. CT comprises a series of cross-sectional "slices", with 200-600 slices together forming a typical volume for a scan of the thorax. Each slice is made by reconstructing the detected attenuation of multiple x-ray beams from different angles around the subject. As CT uses ionising radiation, which is potentially damaging to cells, it is clinically important to aim for the lowest doses of x-ray that provide adequate image quality for a target purpose, such as clinical diagnostic imaging, lung-cancer screening, or interventional procedures. The dose correlates directly with the quality of the resulting image with higher doses providing clearer images with less noise. In a screening setting, low-dose CT has been shown to be useful for lung nodule detection; however, airway segmentation on low-dose CT poses challenges due to the lower quality of the image.

Segmenting and measuring the airways can be difficult and time-consuming.[6] At maximum inspiration the lungs consist of 80-90% air, resulting in a low-intensity structure without clear delineations between the smallest branches and the adjacent air-spaces due to resolution limitations and partial volume effects.[7]

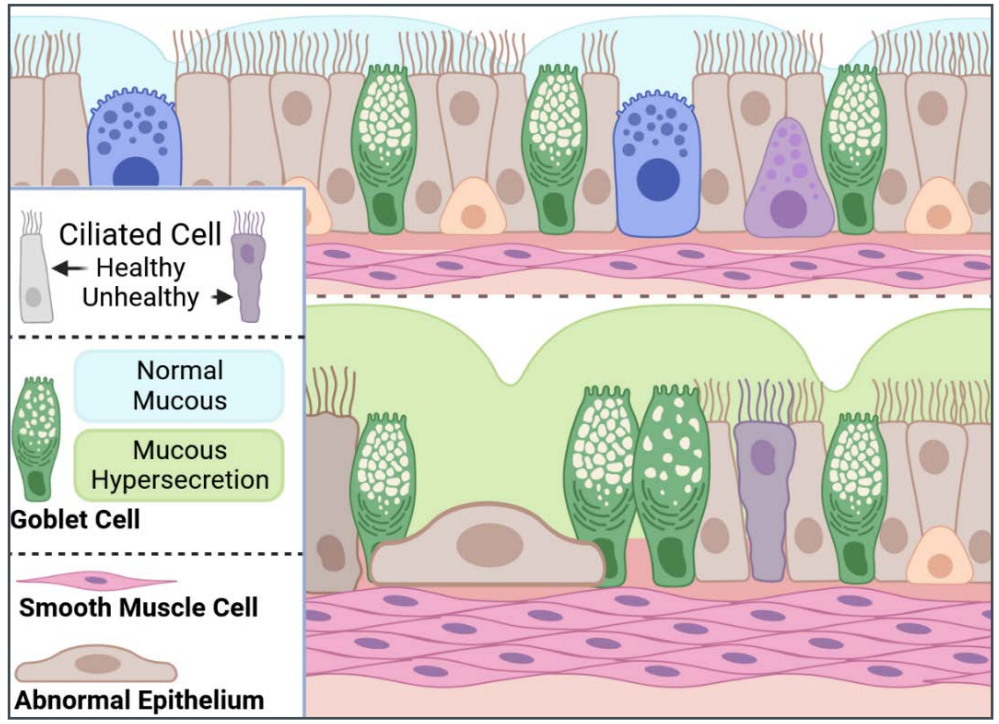


***Figure 1.1*** *– Structure of a healthy and unhealthy airway of the lower respiratory tract. The healthy airway (top) has a densely coupled ciliated epithelium with a few mucous-secreting goblet and other supporting cells. The smooth muscle layer and supporting extracellular matrix are of normal thickness. The unhealthy airway (bottom) has a reduction of ciliated epithelial cells, which can be replaced with abnormal epithelial cells. Goblet cells and mucous hypersecretion proliferate, and the smooth muscle layer alongside the extracellular matrix is hypertrophied and thickened.*

While many solutions are being investigated for lumen segmentation, accurate wall segmentation remains an underexplored area. The size of the airways becomes smaller as we move from the central to peripheral branches and eventually approaches a size like the spatial resolution of the scan, making it increasingly difficult to visualize and measure smaller airway structures. This step is difficult but important to accurately understand the health of the airway wall, particularly in populations presumed healthy, where subtle

abnormalities can signal early disease.

Many automated techniques for airway lumen segmentation have been emerging with the rise of efficient deep-learning systems.[8] However, they rely on the availability of high-quality training datasets with extensive and accurate airway segmentations, which are costly and time intensive to obtain.[9]

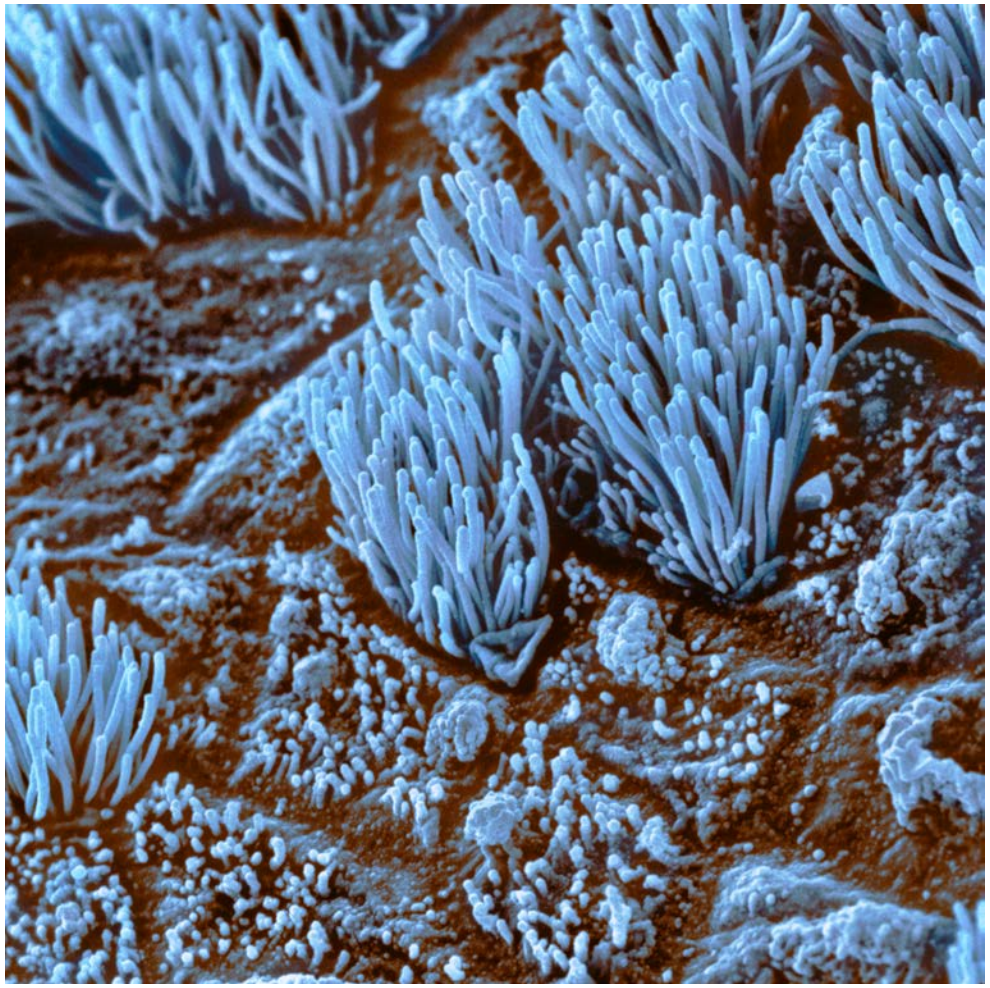

***Figure 1.2*** *- Coloured scanning electron micrograph of bronchial mucosa of a smoker. Many of the epithelial cells have had their hair-like cilia (blue) destroyed by smoke.*

The main advantage of deep-learning approaches is that they can learn the image features that distinguish the lumen of an airway from the rest of the lung, which enables automatic segmentation of airways. This allows the deep-learning models to be trained on a specific dataset to provide good, automated, results tailored to that dataset. Once the lumen of the airway is segmented, the outer wall can be measured using a variety of means such as manually tracing the outlines, full-width half-max (Figure 1.3A), graph-cut (Figure 1.3B), and intensity-integration (Figure 1.3C), typically done using a cross-section of the airway perpendicular to its centreline (Figure 1.3D).[10–12]

Airway tree segmentation from CT images is useful to assess lung diseases that are characterized by structural changes of the airway tree. The measurements of the lumen and wall of an airway can be used to quantify the burden of disease, and if tracked over time, to monitor response to disease treatment.[13,14] Directly measuring the airways can provide novel information about the pathophysiology of earlier stages of disease, in contrast to other diagnostic techniques such as spirometry, which measures consequences of disease such as airflow limitation. The measurements from an airway tree can be summarised in a variety of ways with focus on different bronchial parameters such as wall thickening or loss of branches.

## Bronchial Parameters

Bronchial parameters are measurements of the airway tree that are taken at a specific location or summarised over a set of branches. Most bronchial parameters quantify the size of the airway lumen and wall. The airway changes due to pathology can thus be reflected in a changing bronchial parameter value.

Calculating bronchial parameters requires measuring the lumen and wall. Initial research into bronchial parameters was performed with predominantly manual measurements on axial CT slices at recognisable locations in the airway tree, such as RB1 (Figure 1.4).[15,16] More recently due to improvements in automated airway segmentation methods, measurements from multiple airways can be averaged by generation and location.

The most studied bronchial parameters are calculated from the measurements of the lumen radius (LR) and the radius of the total airway (TR). These are visualised in Figure 1.5A. The formulae to calculate commonly used bronchial parameters are:

1) Luminal area: $LA = \pi * LR^2$
2) Wall Thickness: $WT = TR - LR$
3) Wall Area Percent: $WAP=(TA-LA)/TA*100$,where $TA=\pi(TR)^2$

Another commonly reported bronchial parameter is the summary parameter Pi10, which stands for the square root of the wall area for a hypothetical airway with an internal perimeter of 10mm. It is obtained by calculating

the linear regression of the square root of the wall area against the internal perimeters of all or of a subset of branches from the airway tree, and finding the regression line intercept at an internal perimeter of 10mm (Figure 1.5B).[17]

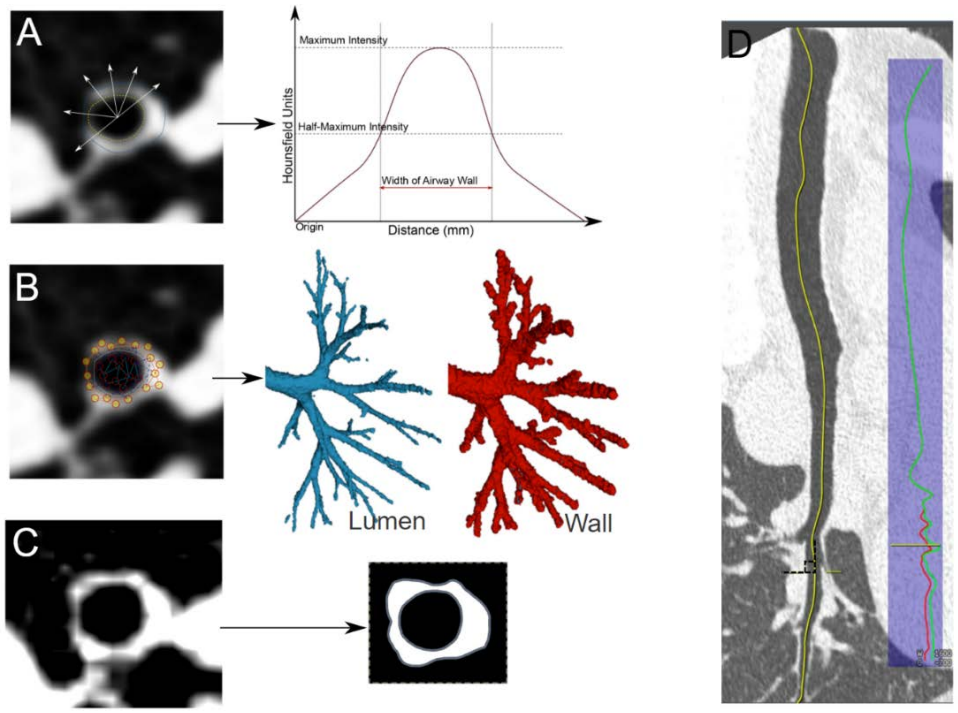


***Figure 1.3*** *– Examples of algorithms used for measuring airway walls. A) The Full-Width Half-Maximum approach measures intensity of voxels along a path that begins at the lumen centre and radiates out across the airway wall. The airway width is determined by measuring the distance between the points where the intensity is half of the maximum on both sides of the highest intensity point. B) The graph-cut approach represents the 2D image patch perpendicular to the airway centreline as a graph model. This model is then divided at the lumen-wall boundary and measurements of the lumen and wall are obtained by measuring the resulting segmentations. This approach can also be extended to the whole 3D image. C) Intensity-integration approach segments the airway wall using a thresholding technique followed by direct measurement of resulting segmentation. D) Multiplanar reconstruction approach involves reformatting the volumetric scan along the centreline of the airway to represent it as a straight branch. Measurements of airways are perpendicular to the centreline (highlighted in yellow).*

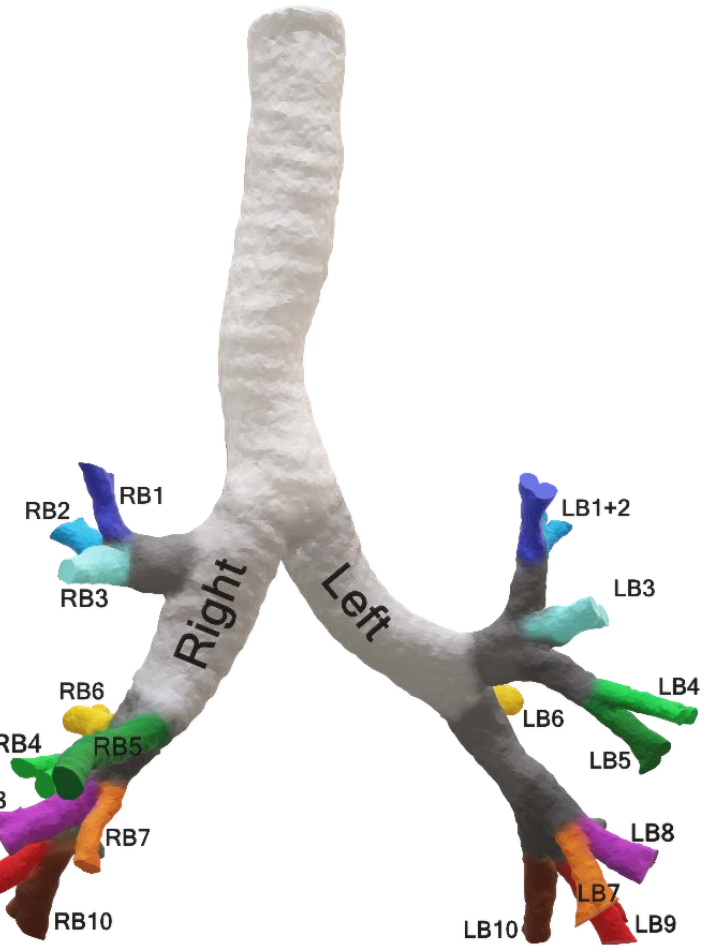


***Figure 1.4*** *- Airway tree segmentation with anatomical labels for segmental branches. RB – light branch, LB – left branch.*

Recently, the availability of high-quality 3D segmentations enabled the investigation of novel bronchial parameters, which aim to summarise the complexity and geometry of the airway tree. These parameters count the total number of airways, the rate at which the lumen tapers or the fractal dimension of the airway tree. Recent results from CT measurements illustrate parallels to results from micro-CT and histology, where a reduced airway segmentation complexity and airway count were seen in participants with disease.[18–20]

While spirometry is well-established in defining disease, emerging studies suggest a potential predictive relationship between bronchial parameters

and disease development and treatment response in asthma patients.[21–24] They may also have applications in exploring chronic obstructive pulmonary disease (COPD) phenotypes, and highlight differences in disease trajectories for men and women.[25–28] However, there are still gaps in our understanding of the influence of characteristics as age, height, weight and sex on bronchial parameters in the absence of disease.

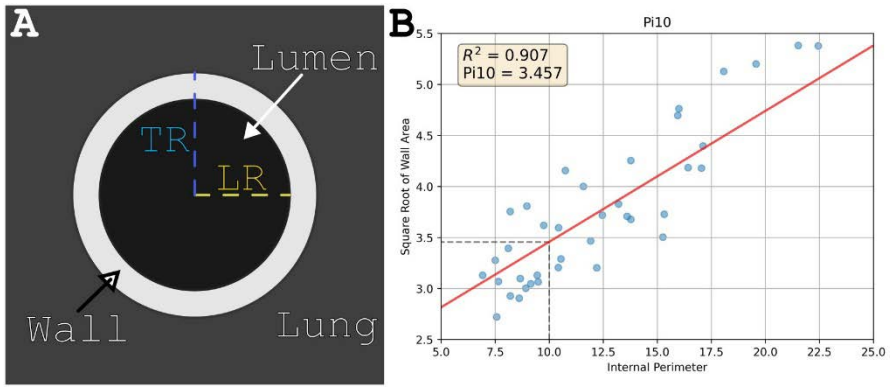


***Figure 1.5*** *- A) Simplified diagram of an airway cross-section perpendicular to the airway centreline. The total radius (TR, blue dashed line) and lumen radius (LR, yellow dashed line) are used to calculate bronchial parameters for an individual airway such as lumen area and wall thickness. B) Example of a Pi10 calculation based on multiple airway measurements from the same individual. The square root of the wall area is plotted against the internal perimeter for each airway and a linear regression performed. The square root of the wall area where the internal perimeter is 10mm is then identified and used as the summary bronchial parameter Pi10.*

## Bronchial Parameters in the General Population

Advances in medical imaging have facilitated early detection of diseases through techniques such as low-dose thoracic CT scanning. These developments offer improved sensitivity with lower-dose imaging, enhanced noise-removal algorithms, and automated methods for quantifying biomarkers. As a result, population-based screening programs are being implemented across the world, with a particular focus on lung cancer screening utilizing low-dose chest CT scans.[29–31]

CT scans provide quantitative data that can contribute to the development of measurable biomarkers. Moreover, they enable the measurement of both the airway tree and parenchyma within the lungs. Consequently, incorporating assessment of bronchial parameters into lung cancer screening protocols becomes feasible and holds promise for broader applications in population health.[32–34]

The significance of providing bronchial parameters lies in their relevance alongside emphysema evaluation to population screening efforts due to the substantial burden imposed by COPD on global populations. COPD ranks among the top ten causes of death worldwide.[35] To tackle this public health challenge effectively, a comprehensive approach is needed. This includes secondary prevention through early detection of disease and tertiary prevention by monitoring established disease and response to treatment. However, this requires establishing reference values for bronchial parameters. These benchmark values will aid comparing a screened individual's measurements against those of the general population and identifying deviations from normal ranges. To fully realize its potential, there is a need to address knowledge gaps regarding the measures of bronchial parameters in the general population.

## Aim of Thesis

### Automated Bronchial Parameter Calculation

The first goal of this thesis is to develop an efficient automated method for extracting and summarizing bronchial parameters in the general population. This challenging task is akin to counting and measuring the branches and bark of a tree without direct access to that tree. It has only become achievable with recent advancements in artificial intelligence and computing technology, particularly graphics processing unit enabled deep learning. The first step of this research is to integrate a novel airway tree segmentation AI method and a high-quality wall segmentation method to create a fully automatic pipeline for accurate measurement of airways.

### Reference Bronchial Parameters in the General Population

The field of CT-derived bronchial parameter research has been focused on the "unhealthy" airway, whether it is due to COPD, asthma, or other disease. On the other hand, it is crucial to understand how such parameters measure in the wider population, particularly in lung-healthy populations, to be able to use this research in efficient population health screening efforts, particularly in addressing COPD and early diagnosis. By understanding the range for normal measurements, we can gain deeper insights into pathological airway changes. Because of this rationale, in the second part of this thesis we focus on establishing reference bronchial parameters in the general population.

### Thesis Outline

Chapter 2 reviews current methods for obtaining bronchial wall parameters and compares them across different populations. It focuses particularly on populations of COPD and asthma patients, smoking individuals, and never smokers. This chapter also discusses the challenges that stem from the variety of measurement methods in bronchial parameter research.

Chapter 3 describes our approach for an efficient generation of accurate airway segmentations. This approach involves manual correction of initial airway segmentations obtained from a pre-trained deep-learning model architecture specialised for segmentation from volumetric CT images (U-Net).





Chapter 4 builds on our work to automate bronchial parameter calculation. We introduce and validate an automated pipeline for segmenting the lumen and wall surfaces of the bronchial tree. The pipeline combines a U-Net for airway extraction and an optimal-surface graph-cut method to segment the lumen and the wall surrounding the extracted airways.

Chapter 5 establishes reference values for bronchial parameters within a large, healthy cohort. This cohort comprises a lung-healthy group of participants from the Imaging in Lifelines study. The bronchial parameters are automatically obtained on low-dose chest CT scans using the approaches developed in Chapters 3-5.

Chapter 6 explores the relationship between the duration of smoking cessation and changes in bronchial parameters as measured by CT in a population-based cohort. This cohort encompasses lung-healthy and lung-unhealthy former-smokers. We postulate that the longer the period since smoking cessation, the more likely it is that bronchial measurements will approach normal values.

Chapter 7 investigates Total Airway Count (TAC) and its variability influenced by factors such as age, sex, height, weight, and smoking habits. Additionally, it assesses how TAC relates to variations in spirometry results and evaluates its effectiveness in predicting the spirometry-based categorization of participants.

Chapter 8 explores the measurements of lung lobe volumes in the general population and works on establishing reference equations for lung-healthy individuals based on sex, age, and height.

Chapter 9 presents a general discussion of the main findings achieved within the research presented in this thesis, alongside future directions for research.

# CHAPTER 2



## BRONCHIAL WALL PARAMETERS ON CT IN HEALTHY NEVER-SMOKING, SMOKING, COPD AND ASTHMA POPULATIONS: A SYSTEMATIC REVIEW AND META-ANALYSIS

I. Dudurych • S. Muiser • N. McVeigh • H.A.M. Kerstjens • M. van den Berge • M. de Bruijne • R. Vliegenthart

*European Radiology 2022*

## Abstract

**Objective** Research on computed tomography (CT) bronchial parameter measurements shows that there are conflicting results on the values for bronchial parameters in the never-smoking, smoking, asthma, and chronic obstructive pulmonary disease (COPD) populations. This review assesses the current CT methods for obtaining bronchial wall parameters and their comparison between populations.

**Methods** A systematic review of MEDLINE and Embase was conducted following PRISMA guidelines (last search date 25th October 2021). Methodology data was collected and summarised. Values of Percentage Wall Area (WA%), Wall Thickness (WT), summary airway measure (Pi10) and Luminal Area (Ai) were pooled and compared between populations.

**Results** 169 articles were included for methodologic review; 66 of these were included for meta-analysis. Most measurements were obtained from multiplanar reconstructions of segmented airways (93 of 169 articles), using various tools and algorithms; Third generation airways in the upper and lower lobes were most frequently studied. COPD (12,746) and smoking (15,092) populations were largest across studies and mostly consisted of men (median 64.4%, IQR 61.5%-66.1%). There were significant differences between populations; the largest WA% was found in COPD (mean SD 62.93±7.41%, n=6,045), the asthma population had the largest Pi10 (4.03±0.27mm, n=442). Ai normalised to Body Surface Area (Ai/BSA) (12.46±4mm², n=134) was largest in the never-smoking population.

**Conclusions** Studies on CT-derived bronchial parameter measurements are heterogenous in methodology and population, resulting in challenges to compare outcomes between studies. Significant differences between populations exist for several parameters, most notably in the wall area percentage; however, there is a large overlap in their ranges.




## Introduction



Smoking, chronic obstructive pulmonary disease (COPD), and asthma are some of the top non-infective pulmonary health burdens in developed countries[36–38]. Due to an aging population and global smoking rates among others, the number of adults affected with COPD is expected to rise in the future. Both asthma and COPD have a wide variety of phenotypes and presentations, and all have in common the presence of airway inflammation and remodelling[39,40].

Airway inflammation and remodelling can be measured on CT scans of the thorax. While progress in quantitative CT (QCT) has been made over the past couple of decades, there are many different parameters to evaluate airway disease[41]. Some recent advances have been made in the use of CT-derived bronchial parameters for monitoring disease trajectory, smoking cessation, genetic diversity, and treatment response[42–47]. These demonstrate the potential for quantification and characterisation of a diseased airway.

Current research in this field describes conflicting results for bronchial parameters. Some existing articles describe no differences between groups like lung cancer patients versus healthy individuals, smoking COPD patients versus smoking, and asthma patients versus controls[48–52], while others show significant differences between subgroups, such as COPD GOLD I-IV patients, that would enable further clinical applications like disease monitoring and identification of distinct groups within a population[14,53–56]. Additionally, some authors report that bronchial parameters vary by sex, age, and other characteristics[27,57–59], whereas this is not observed by others[60,61]. To explore this, we conducted a systematic review of bronchial parameter values in never-smoking, smoking, COPD and asthma populations and compared the resulting pooled values between these populations.

Studies assessing bronchial parameters use a wide range of CT scanning protocols, reconstruction algorithms, and post-processing tools. This may have an impact on radiologic measurements. To enable the possibility of comparing novel research to past studies, we aimed to identify a most used reference technique for bronchial parameter measurement; thus, this review also summarises the current methodologies in use for determining bronchial parameters on CT scans in the never-smoking, smoking, COPD, and asthma populations. We identified previous general reviews on the subject of method-

ology in bronchial parameter measurement [29], however to the best of our knowledge there are no previous systematic reviews of this subject involving review of the never-smoking population and pooling of never-smoking bronchial parameter data from multiple studies to enable comparison with other populations.

## Methods

This study was conducted following Preferred Reporting Items for Systematic Reviews and Meta-analyses (PRISMA)[62]. The entirety of the screening process was performed using Covidence[63].

### Search Strategy

Medline and EMBASE were systematically searched. The last search date was 25/10/2021. The search strings encompassed the key words and index/Mesh terms related to the Population: adult, smoking, never-smoking, COPD, asthma, the Intervention: computed tomography scan, and the Outcomes: bronchial wall measurements (e.g., wall measurement, lumen area, wall area etc.). The full search strings are provided in the supplemental material.

### Inclusion/Exclusion Criteria

The following criteria were required for an article to be included: 1. Original empirical research. 2. Study population: adults ≥ 18 years old and a focus on at least one of four target populations encompassing common respiratory states: never-smoking or smoking population (without pulmonary disease based on spirometry and GOLD criteria and no history of other pulmonary disease such as pulmonary fibrosis), COPD population, or asthma population. 3. Study includes inspiratory chest CT scan for bronchial measurements. 4. Research article must be: Peer-reviewed, English text available.

Exclusion criteria applied were: 1. Review article without new experimental data. 2. Outlier study population e.g., Coal Miners, World Trade Centre Firemen etc. 3. Article describing study on phantom/animal/histology specimen only. 4. <50 participants in the study. 5. Non-Volumetric CT scan. A scan was considered non-volumetric if the slice increment exceeded slice thickness and was >2 times larger than voxel size.

The results of the search were processed for eligibility in two steps. Titles and Abstracts were screened by one author for inclusion in full text screening. This



was followed by two of three researchers (I.D., S.M., N.McV.) screening the full text for eligibility in the review. Consensus between the two researchers was necessary for inclusion; if consensus could not be reached the conflict was resolved by the third author. All researchers were blinded to decisions made by one another to reduce bias in the selection process.



Studies included in the methodological systematic review were excluded from the meta-analysis if they had insufficient data for pooling of bronchial parameters.

### Data Extraction

Methodologic and study data were collected when available. We focused on tools and methods used in measuring the bronchial walls. These were: reconstruction used for measurement, whether bronchial parameters were normalised to other measurements e.g., body surface area (BSA), the studied airway branches and generations, and the algorithms and software used for measurement (Figure S2.1). Following the exclusion of studies with insufficient data for pooling, for each population we pooled bronchial parameters that were present in two or more of the included studies. These were: 3rd generation airway Wall Area Percentage (WA%), Wall Thickness (WT), Luminal Area (Ai), Ai normalised to BSA (Ai/BSA), and Square Root of the Wall Area of a theoretical airway with an internal perimeter of 10mm (Pi10) (Figure S2.2). When multiple articles related to the same bronchial parameters/participants, those articles were grouped by their study name. Per study, data from the article with the largest cohort was used for analysis.

Articles that were eligible for inclusion in pooling of parameters were assessed for bias using a modified Cochrane Risk of Bias tool (RoB 2)[64]. In short, articles were evaluated for Low/High or Some Concerns bias in the domains of: Sequence Generation, Allocation Concealment, Incomplete Outcome Data, Selective Outcome Reporting and Other Sources of Bias. A judgement of "High" in any of those domains marks a study as high risk of bias. Irrespective of bias, the reported mean and standard deviation of a bronchial parameter was extracted and included in pooled analysis.

### Statistical Analysis

Means and standard deviations from multiple studies were extracted and combined using the Cochrane formula for pooling groups[65]. The resulting pooled values were analysed using One-way ANOVA and Tukey-Kramer HSD Post-Hoc Test[66]. An additional meta-analysis of mean differences of COPD vs

controls (never-smokers or smokers) for 3rd generation WA% was performed using an inverse-variance with a random effects model, assuming heterogeneity[67]. To assess for publication bias, a funnel plot was graphed and Eggar's test performed[68]. A P value of <0.05 was considered statistically significant.

## Results

The search yielded 7,494 articles of which 2,719 were duplicates. Full-text screening was conducted on 375 articles resulting in 169 articles that were included for methodologic evaluation, a summary is provided in supplemental material Table S2.1. Of these, 66 were eligible for pooling of data, and for comparison of population groups (Figure 2.1). The most common source of bias was Low, with "Some Concerns" in the "Other" category due to study participants consisting mostly of men (Figure 2.2). The details of bias assessment are provided in the supplemental material Table S2.2.

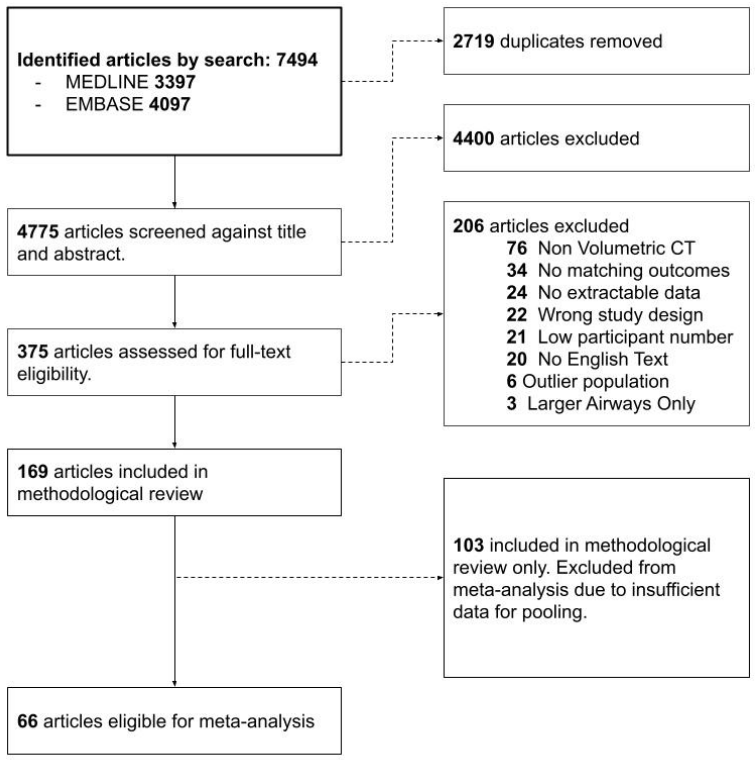


***Figure 2.1*** *- PRISMA Flowchart*



## Systematic Review - Population

We calculated the number of subjects in the four groups and per bronchial parameter measured (Figure 2.3). Among the reviewed studies, COPD and smoking populations had the largest number of participants: in WA% (n=11,839 COPD and 9,257 smoking) and Pi10 (n=12,746 COPD and 15,092 smoking). Across all measured parameters apart from Di, never-smoking had the lowest numbers of participants. Most of the COPD and smoking participants were men (64.41% male [61.5%-66.1%] median [IQR]), while the asthma and never-smoking populations had more women than men (56.44% female [54.7%-58.6%]) (Table 2.1).



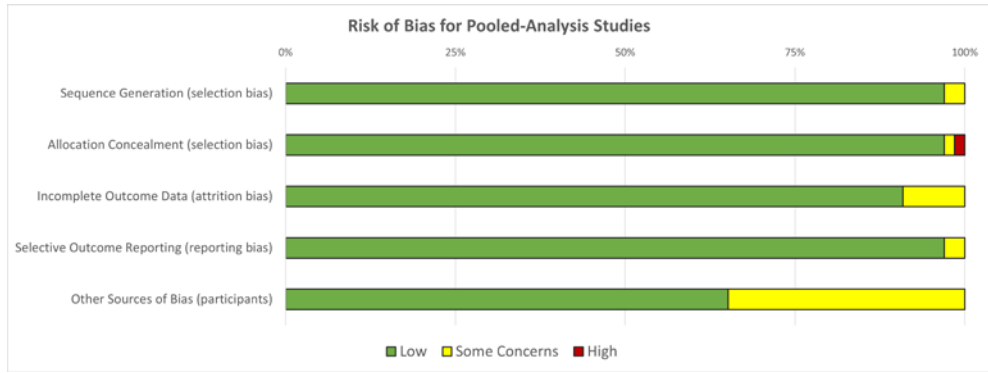


***Figure 2.2*** *- Risk of Bias summary for studies included in pooled-analysis (n=66)*

## Methodologic Review - Image Analysis Methods

We identified a wide range of methods used to obtain bronchial parameter measurements. 93 of the 169 articles obtained measurements from a reconstructed plane perpendicular to the centreline of the airway, 29/169 articles measured airways cut in cross section on axial slices. 36/169 articles normalised one or more bronchial parameters to Body Surface Area (BSA) or square root of BSA (√BSA).

| | WA% | WA | Pi10 | Ai | Di | WT |
|---|---|---|---|---|---|---|
| **COPD** | 11,839 (65.7) | 4,449 (64.9) | 12,746 (67.2) | 9,731 (62.3) | 3,020 (69.1) | 2,919 (75.3) |
| | n=41 | n=16 | n=25 | n=29 | n=10 | n=21 |
| **Asthma** | 1,856 (46.4) | 1,463 (40.8) | 1,604 (43.2) | 2,634 (45.4) | 712 (39.6) | 1,722 (41.5) |
| | n=27 | n=18 | n=9 | n=28 | n=6 | n=20 |
| **Smoking** | 9,257 (59.5) | 3,168 (60.8) | 15,092 (64.4) | 3,927 (64.5) | 5,207 (61.57) | 5,062 (61.3) |
| | n=23 | n=9 | n=24 | n=17 | n=9 | n=11 |
| **Never** | 965 (44.9) | 378 (43.9) | 898 (40) | 1,303 (49) | 742 (45.3) | 1,127 (41.7) |
| **Smoking** | n=22 | n=11 | n=9 | n=22 | n=7 | n=16 |

***Table 2.1*** *- Total number of participants across all studies reporting Wall Area Percentage (WA%), Wall Area (WA), Square root of the wall area of hypothetical airway with internal perimeter of 10mm (Pi10), Luminal Area (Ai), Luminal Diameter (Di), and Wall Thickness (WT). Percentage of participants that are men provided in parentheses. n = number of studies.*

To determine the airway lumen and wall outline, the Full-Width Half-Maximum (FWHM) algorithm was used in 48/169~ articles, and Graph-Cut segmentation was used in 49/169 articles. In 13/169 articles it was unclear which method was used. 43/169 articles used VIDA software, either based on the Apollo or Pulmonary Workstation. 28 articles used in-house software. The complete summary can be found in Table 2.2.

## Methodologic Review - Studied Airways and Generations

Of the articles that specified which Boyden Classification[69] airway branches were measured, Right Branch (RB)1 and RB10 were measured in 87/169~ and 66/169~ articles respectively, Left Branch (LB)1±2 and LB10 in 77/169~ and 42/169~ articles (Figure 2.4). Articles were not included when the airway generation was of a mathematical rather than anatomical distinction, i.e. according to Weibel's "A" Model of the Lung[2]. Out of the included articles, the 3rd generation airway was measured in 100/169 articles. 65/169 studies did not provide information on the airway generations that were measured and 4/169 papers measured airways beyond 4$^{th}$ generation and onward.



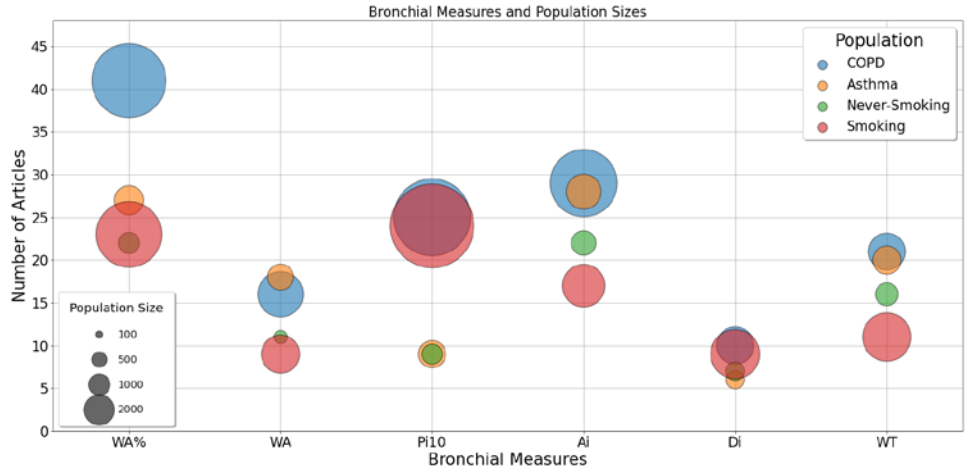


***Figure 2.3*** *- Number of articles investigating a bronchial parameter, with total number of participants per group and across studies indicated by bubble size.*

## Pooled Analysis - Measured Bronchial Parameters

Never-smoking populations had the smallest 3rd generation WA% (57.53±8.71% n=693) followed by smoking populations (61.2±6.43% n=3,228), and asthma populations (62.04±7.0% n=499), with COPD populations having the largest WA% (62.93±7% n=6,045) (Figure 2.5). One-way ANOVA analysis for WA% showed significant differences between all groups except for smoking versus asthma populations (p = 0.07, 95% CI [-0.05%, 1.7%]) (Table 2.3).

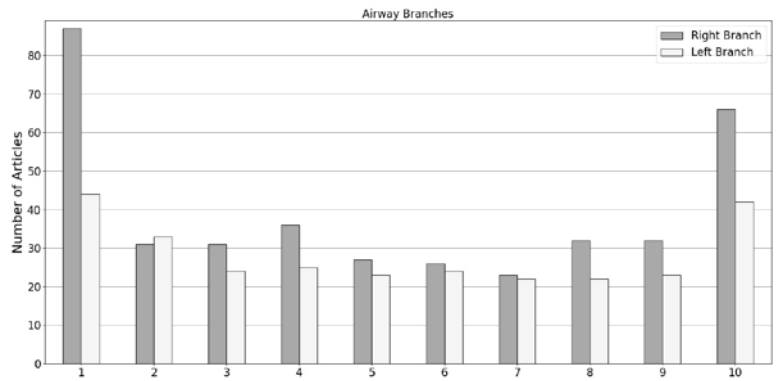


***Figure 2.4*** *- Studied Airway Branches, grey colour indicates right lung, white colour indicates left lung. Number on x axis indicates branch. Y axis indicates number of articles that include a measure of the specified branch.*

Pi10 pooled analysis indicates that never-smoking populations have a larger

Pi10 (3.81±0.7mm n=644) than smoking populations (3.23±0.83mm n=4,942) (p < 0.001, 95% CI [-0.5mm, -0.6mm]), but smaller than COPD populations (3.96±0.55mm n=6,887) (p < 0.001, 95% CI [0.1mm, 0.2mm]) (Figure 2.6) while asthma populations had the largest Pi10 (4.03±0.27 n=442)(p = < 0.001, 95%CI [0.1mm, 0.3mm]).

Third generation Ai normalised to BSA was largest in never-smoking populations (12.46±4mm² n=134), followed by asthma (10.09±3.21mm² n=336), smoking (9.89±3.96mm² n=108) and COPD populations (9.59±5.49mm² n=712). With non-normalised Ai, never-smoking had a smaller Ai (21.69±11.15mm² n=192) compared to smoking (24.09±12.8mm² n=2,358), and marginally larger than COPD (21.45±10.58mm² n=3,323) and asthma (19.45±6.77mm² n=161). WT pooled analysis revealed that never-smoking had the thickest 3rd generation walls (2.39±0.83mm n=460) compared to smoking (1.48±0.16 n=594), COPD (1.32±0.34 n=1,254) and asthma (1.36±0.4 n=163).

| Airway Generations | | Analysed by Lobe | | Wall Algorithm | | Software Used | |
|---|---|---|---|---|---|---|---|
| **3** | 100 | **RUL** | 21 | **Graph-Cut** | 49 | **In-house** | 28 |
| **4** | 77 | **LUL** | 16 | **FWHM** | 48 | **Apollo VIDA** | 25 |
| **5** | 68 | **RLL** | 14 | **Int-Int** | 17 | **Pulmonary Workstation VIDA** | 18 |
| **6** | 44 | **LLL** | 11 | **Unclear** | 13 | **Airway Inspector 3D Slicer** | 10 |
| **7** | 22 | **RML** | 10 | **Manual** | 6 | **Other** | 41 |
| **8+** | 17 | **Lingula** | 3 | **Other** | 8 | **Unclear** | 19 |

***Table 2.2*** *- Summary of methodology, indicating the number of articles investigating airway generations or lobes, and the algorithms, methods and software used for bronchial parameter measurement. N=169 articles. Most studies analysed more than one airway generation. FWHM = Full-Width Half Maximum. Int-Int = Intensity Integration.*





| WA% [%] | Smoking | COPD | Asthma |
|---|---|---|---|
| | [2.9, 4.5] | [4.7, 6.1] | [3.4, 5.6] |
| **Never-Smoking** | *<0.001* | *<0.001* | *<0.001* |
| | | [1.3, 2.1] | [-0.05, 1.7] |
| **Smoking** | | *<0.001* | *0.07* |
| | | | [-0.03, -1.7] |
| **COPD** | | | *<0.05* |

| Ai [mm²] | Smoking | COPD | Asthma |
|---|---|---|---|
| | [0.2, 4.6] | [-1.9, 2.4] | [-5.4, 0.9] |
| **Never-Smoking** | *0.03* | *0.98* | *0.26* |
| | | [-1.8, -3.4] | [-2.2, -7] |
| **Smoking** | | *<0.001* | *<0.001* |
| | | | [-4.4, 0.4] |
| **COPD** | | | *0.13* |

| Pi10 [mm] | Smoking | COPD | Asthma |
|---|---|---|---|
| | [-0.5, -0.6] | [0.1, 0.2] | [0.1, 0.3] |
| **Never-Smoking** | *<0.001* | *<0.001* | *<0.001* |
| | | [0.7, 0.8] | [0.7, 0.8] |
| **Smoking** | | *<0.001* | *<0.001* |
| | | | [-0.2, 0.02] |
| **COPD** | | | *0.16* |

| Ai/BSA [mm²] | Smoking | COPD | Asthma |
|---|---|---|---|
| | [0.9, 4.1] | [-1.7, -4] | [-1.1, -3.6] |
| **Never-Smoking** | *<0.001* | *<0.001* | *<0.001* |
| | | [-1.6, 0.9] | [-1.1, 1.5] |
| **Smoking** | | *0.92* | *0.98* |
| | | | [-0.3, 1.3] |
| **COPD** | | | *0.37* |

| WT [mm] | Smoking | COPD | Asthma |
|---|---|---|---|
| | [-0.9, -1] | [-1, -1.1] | [-0.9-1.1] |
| **Never-Smoking** | *<0.001* | *<0.001* | *<0.001* |
| | | [-0.1, -0.2] | [-0.01, -0.2] |
| **Smoking** | | *<0.001* | *0.02* |
| | | | [-0.06, 0.1] |
| **COPD** | | | *0.8* |

***Table 2.3*** *- 95% Confidence Interval (in parentheses) and p Values of One-way ANOVA with Tukey HSD Post-Hoc test comparing the difference between pooled values per population for Wall Area Percentage (WA%), Luminal Area (Ai), Ai normalised to Body Surface Area (BSA), Square root of the wall area of a hypothetical airway with internal perimeter of 10mm (Pi10) and Wall Thickness (WT).*

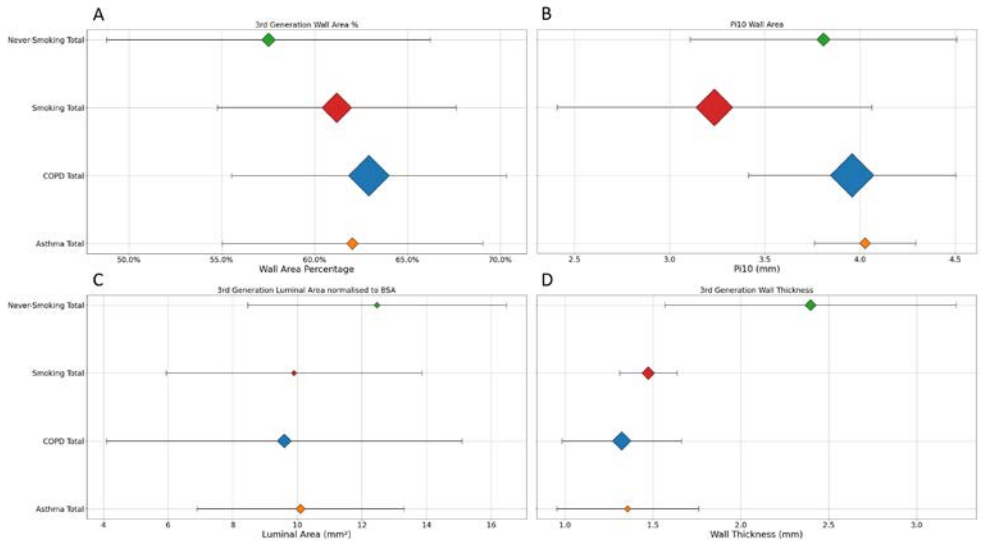


***Figure 2.5*** *- Pooled analysis of (a) Percentage Wall Area (WA%) of 3rd Generation Airways, (b) Square Root of the Wall Area of hypothetical airway of internal perimeter of 10mm (Pi10), (c) Luminal Area (Ai) normalised to Body Surface Area (BSA), (d) Wall Thickness (WT) of 3rd generation airways. Diamond location is the mean, size indicates relative number of included participants. Error-bars are standard deviation.*

## Meta-Analysis of 3rd Generation WA% for COPD vs Controls

16 studies were included in sub analysis of 3rd generation WA%, 6 with never-smokers as controls and 10 with smokers as controls. Overall, 3rd generation WA% was 2.78% larger in COPD compared to controls, p=<0.001, 95% CI [1.85, 3.71] (Figure S2.3). Sub-analysis between COPD and never-smokers shows a difference of 2.59% larger WA% for COPD, 95% CI [1.14, 4.05] and between COPD and smokers WA% was 2.90% larger in COPD, 95% CI [1.71, 4.09]. Egger's test shows an intercept of 0.35 and p=0.712. The $I^2$ ranged from 70.65% to 79.97% in the subgroups, and overall 87.71%.



## Discussion

This systematic review aimed to explore the field of bronchial parameter research in different specified populations. The results show that the study of CT bronchial parameters is biased towards the COPD population's larger airways. Exploration of airways in never-smokers is needed to solidify knowledge on the differences in bronchial parameters due to participant characteristics. Bronchial walls were most often measured using the full-width half-maximum or the graph-cut method on a plane perpendicular to the centreline of the airway, making full use of the utility of a volumetric CT scan. The 3rd generation right upper lobe apical segment branch was the most often measured bronchial parameter. From a subset of studies, we pooled and compared the reported bronchial parameter values for never-smoking, smoking, asthma, and COPD populations.

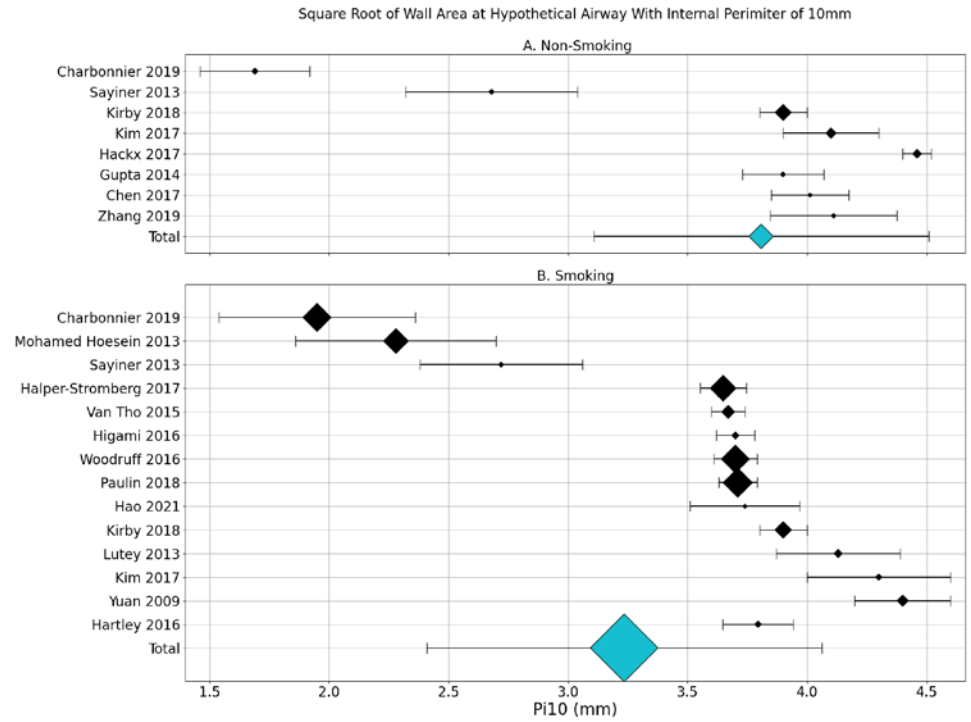


***Figure 2.6*** *- Pooled analysis of square root of wall area of hypothetical airway with internal perimeter of 10mm (Pi10) in Never-Smoking (A) and Smoking (B) populations. Values are Mean ± SD with diamond size indicating relative number of included participants.*

Bronchial parameter research is heavily focused on the COPD and smoking populations. Low numbers of never-smoking participants limit our baseline knowledge of the normal lung parenchyma and bronchial walls as assessed on CT. Our review showed that articles reporting on never-smoking and asthma populations tended to normalise parameters, while articles investigating smoking and COPD did not. Normalisation seeks to control for patient characteristics that affect bronchial wall parameters. The majority of normalisation is performed with body surface area or square root of body surface area due to the similarity of units[70]. Alternative methods of normalisation, such as normalisation to tracheal parameters, have been examined but may require further research to assess robustness[28,71,72]. Inclusion of more never-smokers in studies may allow for clearer understanding of the interplay between bronchial parameters and participant characteristics such as sex, height, and age, without the confounding factors of smoking and other disease states.

One of the challenges in conducting research in the field of quantitative CT bronchial parameters is determining the optimal CT methodology for bronchial wall measurement. Scanner model and protocol significantly influence the measurements[73,74], along with participant inspiration levels during the scan[75,76]. CT scanning is continually advancing, and much of the early research has been focused on individual slices where the airway is cut in cross section according to anatomical properties, e.g., the right upper lobe apical segment airway being almost perpendicular in the axial plane. However, volumetric scanning is increasingly more common and allows for segmentation of the airway tree, in turn allowing for more accurate measurement of the walls. Most articles using volumetric CT scanning employed multiplanar reconstruction when measuring airways, a method that unlocks more bronchial branches for measurement. Despite this, we identified that the larger airways in the upper and lower lobes of the lungs were most often studied, relying on a single location may not adequately capture the complex structural changes that the lungs undergo in disease (e.g. upper vs lower airways[77]). Access to cheap computing allows more complex segmentation and wall measuring tools; however, most articles use FWHM which has been shown by Gierada et. al and Washko et al. to over-estimate the wall thickness [50,78].

WA% was by far the most measured parameter within all populations and 3rd generation WA% was significantly different between all except smoking versus asthma populations. The meta-analysis focusing on the COPD population vs controls supports the results of the pooled analysis, showing significantly increased WA% in the COPD population. Egger's test and the funnel plot demonstrate no strong evidence for publication bias for this bronchial parameter. The analysis displayed heterogeneity which was not resolved when the sub-groups were analysed, this indicates that the heterogeneity does not stem from a difference in the populations. Overall 3rd generation WA% appears to be a robust parameter when used to differentiate COPD subjects to controls, despite considerable heterogeneity in the data which may stem from differences in methodology.

Pi10 was distinctly explored in COPD and smoking populations, and less so in asthma and the never-smoking populations. Pooled analysis of bronchial parameters shows significant differences between populations despite different measurement methodologies however with a considerable overlap between the ranges of populations. Pooled Ai normalised to BSA had a smaller range than non-normalised Ai and in both cases the numbers in pooled analyses were low. This may indicate that direct measures are not specific enough to discern between groups, as other participant/pathologic processes play a role in Ai, for example height and sex. Direct measures of bronchial parameters are important building blocks, however derived markers are more likely to be robust as they correct for confounding factors.

We noted that the pooled values of Pi10 and WT were larger in the never-smoking population compared to smokers, and smaller compared to COPD participants, due to differences of Pi10 measurements in some of the larger studies compared to the others. This was an unexpected finding as current literature indicates that never-smoking individuals have less airway inflammation than smoking, COPD, and asthma populations. The high Pi10 measurement in some studies may be due to several factors. First, Pi10 is calculated by plotting a regression line based on several airway measurements, the location and method of measurements may strongly influence the slope and intercept, leading to differing results[79,80]. Second, there were more Asian participants in the never-smoking pooled value of Pi10. Ethnicity may play a role and differences between Asian and Caucasian populations have been demonstrated in previous studies[81]. Thirdly, the smoking and COPD populations were predominantly older men with a larger number of participants, while never-smoking populations tended to be younger and included more women. As previous studies have shown, these characteristics play a role in bronchial parameters[82–86]. We were not able to identify suitable measurements to include in the pooled analysis for never-smoking from all studies; however, COPDGene noted a Pi10 of 1.69±0.23mm in 44 never-smoking individuals[87], which is much lower than the pooled analysis total. This suggests

that while Pi10 may be consistent within a study, differences in the methods used to calculate it may not allow for confident comparison between studies.

## Limitations

This study had several limitations. First, the pooled analysis could only include reported means and standard deviations, which assumes a normal distribution in the populations but may not reflect the true distribution. Second, due to the lack of a detailed breakdown of participants in most reviewed literature, it was not possible to perform pooled analysis of sub-groups, and so the pooled values include both men and women, and a wide range of ages, disease states (e.g. non-severe and severe asthma, or GOLD I-IV COPD) and backgrounds (Caucasian, Asian, African-American). Finally, while there are multiple novel potential bronchial parameters emerging due to advancing computation and automation, such as airway tapering and total airway count[23,88–91], we were able to focus only on the parameters that were available for data extraction. Lastly, of the papers included for meta-analysis, only one obtained post-bronchodilation CT measurements[88]. While post-bronchodilator pulmonary function testing was the norm for studies utilising this technique, it was not used during the CT scan, indicating a difference between the acquisition of spirometry and the CT.

## Conclusions

There are significant differences in bronchial parameters between populations, most notably in the wall area percentage of the 3rd generation airway; however, there is a large overlap in their ranges. While previous studies demonstrate that Pi10 can differentiate disease states within a study, our analysis indicates it may not be a robust parameter when comparing different studies. A paucity of never-smoking participants, along with heterogenous wall measurement methodology, may explain the diverging results from studies on the influence of participant characteristics in bronchial parameters.

# Part 2

## AUTOMATED BRONCHIAL PARAMETER EVALUATION

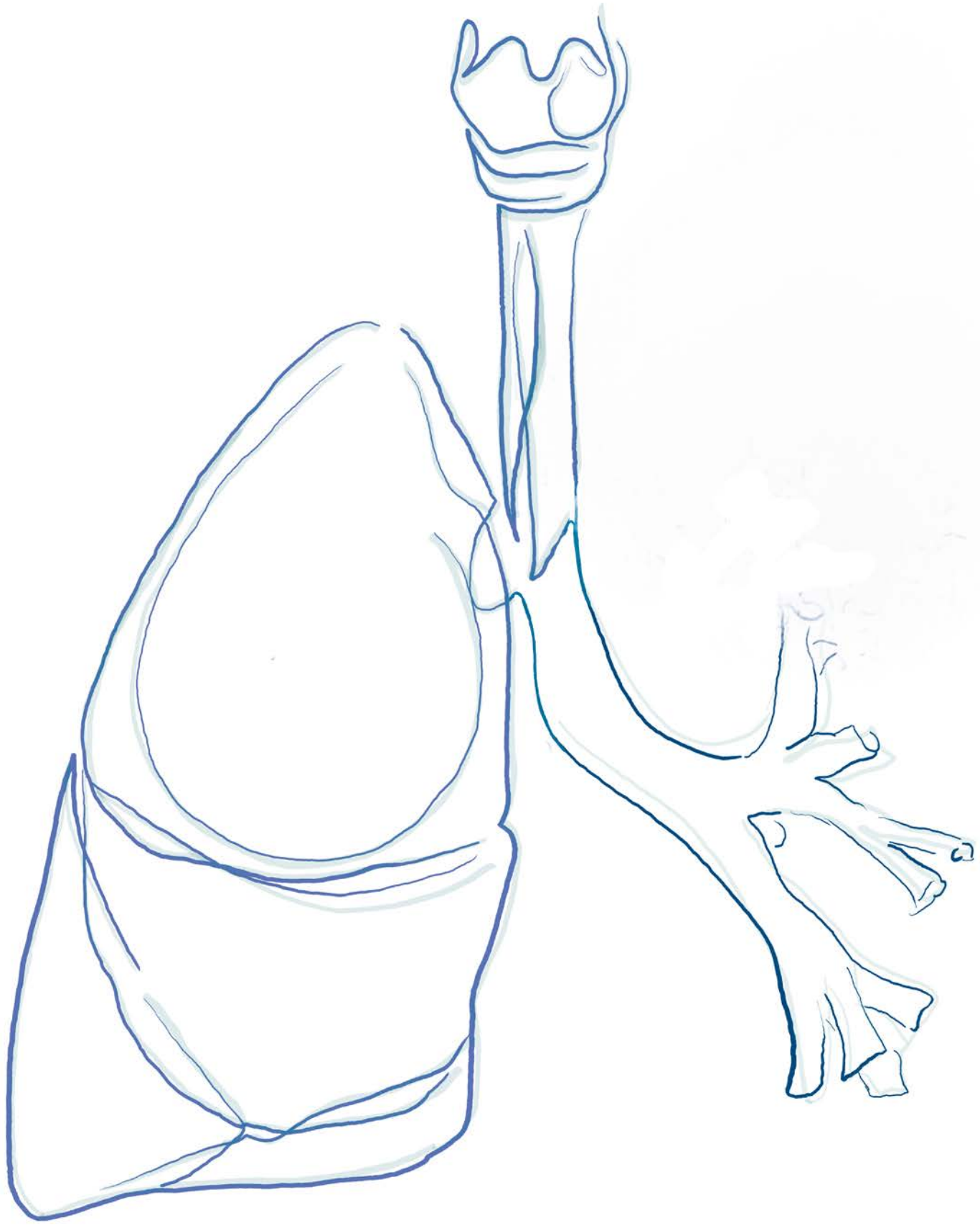

# CHAPTER 3

## CREATING A TRAINING SET FOR ARTIFICIAL INTELLIGENCE FROM INITIAL SEGMENTATIONS OF AIRWAYS



I. Dudurych • A. Garcia-Uceda • Z. Saghir • H. A.W.M. Tiddens

R. Vliegenthart • M. de Bruijne

*European Radiology Experimental 2021*

## Abstract

Airways segmentation is important for research about pulmonary disease but require a large amount of time by trained specialists. We used an openly available software to improve airways segmentations obtained from an artificial intelligence (AI) tool and retrained the tool to get a better performance. Fifteen initial airway segmentations from low-dose chest computed tomography scans were obtained with a 3D-Unet AI tool previously trained on Danish Lung Cancer Screening Trial and Erasmus-MC Sophia datasets. Segmentations were manually corrected in 3D Slicer. The corrected airway segmentations were used to retrain the 3D-Unet. Airway measurements were automatically obtained and included count, airway length and luminal diameter per generation from the segmentations. Correcting segmentations required 2–4 hours per scan. Manually corrected segmentations had more branches ($p < 0.001$), longer airways ($p < 0.001$) and smaller luminal diameters ($p = 0.004$) than initial segmentations. Segmentations from retrained 3D-Unets trended towards more branches and longer airways compared to the initial segmentations. The largest changes were seen in airways from 6th generation onwards. Manual correction results in significantly improved segmentations and is potentially a useful and time-efficient method to improve the AI tool performance on a specific hospital or research dataset.






## Background

Airway segmentation from computed tomography (CT) scans is important in the study of pulmonary disease such as chronic obstructive pulmonary disease (COPD)[14]. High-quality airway segmentation datasets are difficult to create, yet they are necessary for the training of artificial intelligence (AI) tools. Manually segmenting airways from noisy low-dose CT scans is time consuming and error prone, and methods that can provide adequate large airway segmentation via region growing may fail and require manual correction[92,93].

The volume of thoracic CT scans in clinical care will increase due to an increasing respiratory disease burden and the introduction of imaging-based cancer screening[37]. Computer assistance will become increasingly important in the radiology workflow. This should be supplemented with robust AI tools that can increase the accuracy and speed of diagnosis. Medical datasets used to train AI tools are typically small, due to the limited availability of imaging data and ground-truth annotations. In contrast, there is a wide range in possible CT scanning and population characteristics. Thus, pre-trained AI tools have issues generalizing when tested on new data, with typically different characteristics. In such a setting, the need for quickly adapting an existing AI model trained on different data may prove very useful.

AI segmentation tools are being widely studied for their potential in automation, accuracy, and reliability, however their use comes at the cost of flexibility inherent in AI systems. To achieve the highest accuracy, AI requires training on scans like those it will be used on. X-ray tube current, voltage, reconstruction methods and other parameters change the resulting CT image and may have an impact on segmentation performance[7].

So far, the methodology for obtaining high quality ground truth segmentations of airways using openly available tools is lacking. While many airway segmentation tools already exist, those that provide a highly detailed segmentation may be only available for sale, are run as a service or tied to specific CT scanner brands and hospital/research setup[94,95].

In this study we propose a solution to prepare good ground-truth segmentations by improving the airway segmentations that were obtained using openly available tools, and investigate the change in AI performance on our low-dose chest CT protocol following re-training using the corrected segmen-

tations[32].

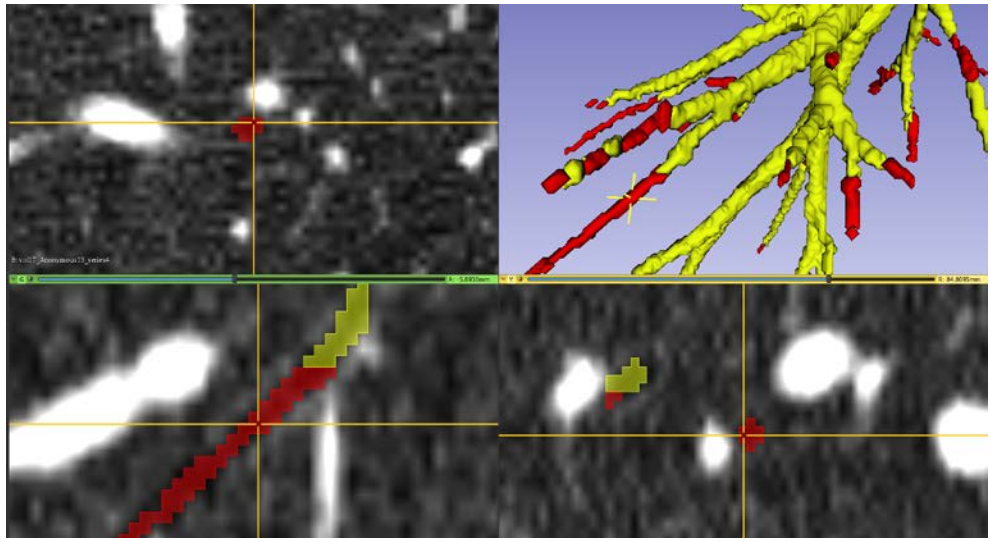

***Figure 3.1*** *- A 3D Slicer workspace for fast identification and correction of incomplete airways. Yellow: Incomplete airway segmentation of an ImaLife participant. Red: manual correction of the airway.*

## Methods

### Initial Segmentations

We used a 3D-Unet method[96,97] designed for automatic airway segmentation. The 3D-Unet is a deep-learning model for biomedical image segmentation, which classifies image voxels as airway/non-airway. The image filters in the convolution layers of the method were optimised automatically using training images and reference segmentations. For all our experiments, we used the same 3D-Unet model layout and hyperparameters as in[96], which were found to be well-suited for airway segmentation.

The current 3D-Unet was trained on Danish Lung Cancer Screening Trial (DLCST)[98] and Erasmus MC-Sophia data (paediatric cystic fibrosis patients)[9]. This model was used to obtain initial airway segmentations from scans of fifteen randomly selected participants from the ImaLife study[32]. The CT scans used were low-dose unenhanced, obtained using a 16-slice CT scanner (Somatom Sensation 16, Siemens Medical Solutions) with a pitch of 3 (with FOV 350) or 2.5 (with FOV 400) and 1mm increments at a tube voltage of 120kVp and reference current of 20mAs[99]. Images were reconstructed with overlapping 0.7-mm increments using the Qr59 kernel. The ImaLife study is part of the northern Netherlands' study and includes participants of at least 45 years of age from the general population. Complete details on ImaLife patient characteristics can be found in table S1 and the referenced material[32]. Differences in population and scanning parameters for DLCST and ErasmusMC datasets compared to ImaLife dataset contributed to incomplete initial segmentations. The prediction threshold of the 3D-Unet probability maps was set to 0.5, which resulted in a low number of false positive airways in the initial segmentations so that most corrections required addition of missing branches, rather than removal of false branches.



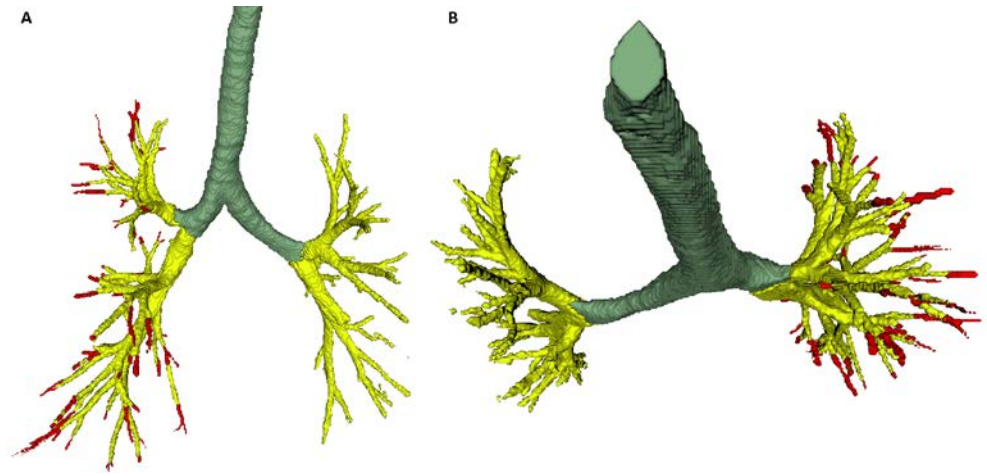


***Figure 3.2*** *- An example of an incomplete segmentation of an ImaLife participant's airway tree (in yellow) of the left lung, and a manually corrected segmentation (in red) of the right lung.*

### Manual Correction of Segmentations

Initial segmentations were imported into 3D Slicer 4.1 (http://www.slicer.org)[100]. Window settings were set to a width of 800 and a level of -625 to better visualise the airway lumen. One medical doctor with 6 months of work and training in pulmonology (I. D.) performed the manual corrections of segmentations.

The workflow screen displayed the coronal, sagittal, and transverse and three-dimensional (3D) views (Fig. 3.1). Corrections were performed using the segment editor tool in 3D Slicer[100]. The binary segmentation provided by the 3D-Unet was imported into the segment editor. Next, the airways segmentations were completed using the paint tool, with a spherical brush and brush size dynamically set to 1–3% of the active window size, based on the size of

the airway. 3D Slicer provides tools to follow along an incomplete airway in the 3D view and identify it on the three views. In this manner it was possible to quickly complete airway segmentations as they were identified on all three orientations simultaneously, with the results instantly visible on the 3D view.

The initial segmentation was combined with the corrections and exported as a set of DICOM slices. A standard operating procedure is provided in the supplemental materials, explaining the process in detail (S1 Manual Correction of Airways).

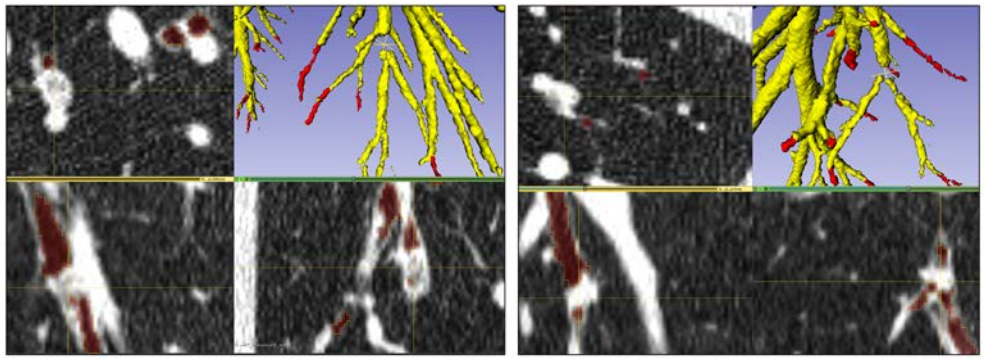

***Figure 3.3*** *- Two examples of large mucous plugging with total focal occlusion of the airway of an ImaLife participant. The 3D-Unet completed segmentation of branches distal to the occlusion without supervision.*

### 3D-Unet Evaluation

We used the 15 corrected ImaLife scan segmentations to train a new 3D-Unet, referred to as "retrained" model. For training and evaluation, we used a 5-fold cross-validation setting, splitting the dataset into 5 groups of equal size, and training 5 different models, assigning for each model one split group as testing set, and using the remaining 4 of the 5 data as training set. Within each training fold, 83% of data is used for model weight updating, and the remaining 17% for model selection. We evaluate each trained model on their corresponding independent testing set. Each training fold contains 12 scans. Despite the small number, the 3D-Unet[96] was validated with varying sizes of training sets and the learning curves show good performance with similar numbers of scans.

To assess the AI performance by introducing a larger set of heterogeneous data, we trained a second model with a combination of ImaLife, DLCST and ErasmusMC data, referred to as "combined" model. We used the same 5-fold cross-validation split of the ImaLife data as for the "retrained" model above, adding 20 scans each from DLCST and ErasmusMC to the training folds. Trained models were used to segment airways from ImaLife scans for comparison to the initial segmentations. The overall process is summarised in the flowchart shown in Fig. S3.1.





### Analysis of Segmentations and Statistical Analysis

From the segmentations obtained by the 3D-Unet, branches and their generation number were extracted automatically, similarly to methods used in the EXACT '09 paper[92]. The airway generation was defined as the number of branch bifurcations counted in the path linking the given branch and the first branch in the airway tree, i.e., the trachea. Thus, the trachea is generation 0, main bronchi generation 1, etc. Automatic measurements of lumen diameter were obtained every 1mm along the centreline of and averaged per branch. The branch length was calculated as the distance between bifurcations along the centreline of a branch.

Comparison was made between the initial segmentations and segmentations from the retrained and combined models trained with the manually corrected segmentations. Results were analysed using Python (Python Software Foundation, https://www.python.org/) and the SciPy package[101]. Wilcoxon Signed Rank test with Bonferroni correction was used for analysis. All comparisons were to the initial, incomplete segmentations. A p value lower than 0.05 was considered significant.

## Results

### Segmentations

Fifteen ImaLife scans were segmented by the initial 3DUnet and manually corrected (Fig. 3.2). In two cases of large mucous plugging, the 3D-Unet continued to segment the airways beyond the blockage without the need for manual interaction (Fig. 3.3). The time to complete a manual correction ranged from 2 to 4 hours.

### Airway Count

The initial, incomplete segmentations had the lowest median count of 151 airways (interquartile range [IQR] 131–169) followed by the retrained model

segmentation with 170 airways (IQR 161–197) (p = 0.098, initial vs retrained), the combined model segmentation with 174 airways (IQR 146-201) (p = 0.089, initial vs combined). The manually corrected segmentation had the highest median number of airways with 179 airways (IQR 167–215) (p < 0.001, initial vs manual) (Fig. 3.4a). The largest differences were seen in airways from 6th generation onwards (Fig. S3.2). The tabulated data is presented in Table S3.2.

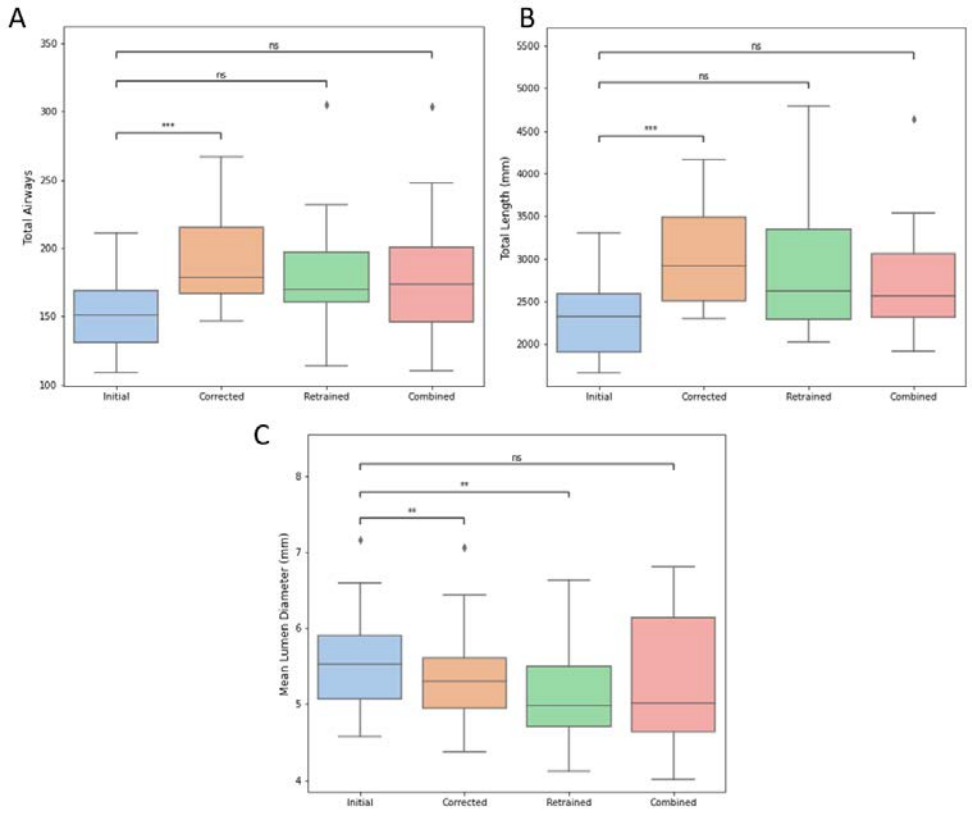


***Figure 3.4*** *- Boxplots for retrained and for combined retrained 3D-Unets. (a) Total airway count per segmentation; (b) total airway length per segmentation; (c) median luminal diameter per segmentation. ns Not significant, * p < 0.05, ** p < 0.01, ***p < 0.001.*

## Airway Length

Airway length increased with manual correction and retraining. The initial segmentation had a total airway length of 2,319.6 mm (IQR 1,905.4–2,588.7 mm) which was the lowest among all segmentations. This was followed by the combined model segmentation, retrained model segmentation and corrected segmentation, with airway lengths of 2,561mm (IQR 2,309.2–3,067.3 mm) (p = 0.079, initial vs combined), 2,622.2 mm (IQR 2,296.1–3,492.8 mm) (p = 0.051, initial vs retrained), and 2,917.3 mm (IQR 2508.8–3,492.8 mm) (p < 0.001, initial vs corrected), respectively (Fig. 3.4b). Airways from the 6th generation onwards showed the largest differences (Fig. S3.3).

## Airway Lumen

Relative to the initial segmentation airway lumen diameters of 5.5 mm (IQR 5.0–5.9 mm), the airway lumen diameters decreased with correction to 5.3 mm (IQR 4.9–5.6 mm) (p = 0.009, initial vs corrected) and the retrained model lumen diameters decreased to 4.9 mm (IQR 4.7–5.5 mm) (p = 0.004, initial vs retrained), however there was no significant difference between the initial segmentation diameters and the combined model segmentation diameters of 5.0 mm (IQR 4.6–6.1 mm) (p = 0.172, initial vs combined) (Fig. 3.4c). Detailed breakdown per generation is available in Fig. S3.4.

## Discussion

We outlined the process for correcting airway segmentations from initial, incomplete segmentations on low-dose CT scans for the purpose of training AI tools. Manual correction resulted into a significantly more complete airway segmentation, and retraining the 3D-Unet resulted into improved segmentations, with the greatest changes seen from the 6th generation onwards. Notably, small airways play an important role in lung diseases such as asthma, COPD, and cystic fibrosis and their accurate detection can be important for the accurate diagnosis and sensitive monitoring of respiratory illness[102,103]. A focus on improving the segmentation of smaller airways could therefore help in the research of bronchial parameters of early disease[104]. With our methods it is possible to quickly improve airway segmentations and retrain an AI model.

The research for robust bronchial parameters sometimes includes the evaluation of aggregate measures, such as total airway count and airway tapering[88,89]. If these measures are obtained from incomplete segmentations, the summary measure may be incorrect. This is illustrated in our study by the decrease in median lumen diameter after correction and retraining. The initial segmentation included too much of the lumen wall and did not include enough of the smaller airways that were visible on the CT scan. This resulted in a significantly larger median airway lumen aggregate measure.

One of the main challenges for AI training in radiology is that often only small,

specific datasets from a narrow range of scanning parameters and population characteristics are available for model training and current manual segmentation methods can take up to 15 hours to complete for one patient[9]. This makes the design of AI tools that generalize well to data from a broader range of scan parameters and population characteristics very difficult to be built. In turn, pretrained AI models tasked with segmentation may fail when used on data dissimilar to their training dataset. Several AI airway segmentation tools have been reported in the literature, which are typically trained and tested on their own in-house datasets and reference segmentation[105,106]. However, when deploying the trained AI methods on other data with different characteristics and scanning parameters, their performance may drop drastically[107]. Retraining with use-case specific data allows for the use of AI models in institutions with different scanning techniques.

The aim of DLCST and Erasmus MC-Sophia dataset addition was to improve the AI performance with heterogeneous data, as DLCST scanning protocol differs slightly, and Erasmus MC-Sophia includes paediatric Cystic Fibrosis patients. However, the combined model did not significantly improve AI performance for ImaLife scans.

To segment small airways in low-dose scans or airways beyond occlusions, typically requires manual intervention. A couple of the scans in our study contained mucous plugging, which prevents segmentation of the airways beyond it when using traditional methods. However, we observed the continuation of segmentation despite large blockages.

A strength of this paper is the use of openly available tools for the methodology. While this technical note focuses on airway segmentations, the same methods can be used to optimise potentially any other segmentation. Our methods are also much less time costly than preparing fully manual airway reference segmentations.

The limitations of this study are the investigation of just one dataset, with a small sample size, based on low-dose CT acquired at high-pitch in a general adult population. Despite the small data-set, previous investigations of 3D-Unet learning curves shows that models trained with small datasets of just 14 images had just slightly lower performance than the model with 28 images [9]. The manual corrections have been performed by one researcher; within the context of this project, we did not assess the impact of inter-observer variability on the completeness of segmentations.

In conclusion, we showed that openly available software can be used to manually correct initial, incomplete airway segmentations with significant improvement. The resulting segmentations can be used to retrain AI models to increase their efficacy for different scanning protocols and applications. This allows for the quick creation of datasets for AI training that match their use case.

# CHAPTER 4

## REPRODUCIBILITY OF A COMBINED ARTIFICIAL INTELLIGENCE AND OPTIMAL-SURFACE GRAPH-CUT METHOD TO AUTOMATE BRONCHIAL PARAMETER EXTRACTION

I. Dudurych • A. Garcia-Uceda • J. Petersen • Y. Du

R. Vliegenthart • M. de Bruijne

*European Radiology 2023*

## Abstract

**Objectives -** Computed Tomography (CT)-based bronchial parameters correlate with disease status. Segmentation and measurement of the bronchial lumen and walls usually requires significant manpower. We evaluate the reproducibility of a deep learning and optimal-surface graph-cut method to automatically segment the airway lumen and wall and calculate bronchial parameters.

**Methods –** A deep-learning airway segmentation model was newly trained on 24 Imaging in Lifelines (ImaLife) low-dose chest CT scans. This model was combined with an optimal-surface graph-cut for airway wall segmentation. These tools were used to calculate bronchial parameters in CT scans of 188 ImaLife participants who had two scans an average of 3 months apart. Bronchial parameters were compared for reproducibility assessment, assuming no change between scans.

**Results -** Of the total 376 CT scans, 374 CT scans (99%) were successfully measured. Segmented airway trees contained a mean of 10 generations and 250 branches. Coefficient of determination ($R^2$) for Luminal Area (LA) ranged from 0.93 at the trachea to 0.68 at the 6th generation, decreasing to 0.51 at the 8th generation. Corresponding values for Wall Area Percentage (WAP) were 0.86, 0.67 and 0.42, respectively. Bland-Altman analysis of LA and WAP per generation demonstrated mean differences close to 0; Limits of Agreement (LoA) were narrow for WAP and Pi10 (±3.7% of mean) and wider for LA (±16.4-22.8% for 2-6th generations). From the 7th generation onwards, there was a sharp decrease in reproducibility and a widening LoA.

**Conclusion -** The outlined approach for automatic bronchial parameter measurement on low-dose chest CT scans is a reliable way to assess the airway tree down to the 6th generation.




## Introduction

Bronchial parameters are increasingly being investigated for use in characterisation of pulmonary disease such as chronic obstructive pulmonary disease (COPD)[14]. A potential benefit of developing robust bronchial parameters is early detection of pulmonary disease. For example, screening for lung cancer with Computed Tomography (CT) may offer the opportunity for the evaluation of "off-target" organ systems such as the heart, bronchi, and vasculature[34]. While bronchial parameters could be used for evaluation of pulmonary disease, their use is limited by the man-hours necessary for (manual) measurements. This step is further complicated by the low dose of screening CT scans, which can result in a worse image quality with more noise. Due to this, the development of reliable automated methods for CT bronchial parameter measurement is a necessary step.

To calculate bronchial parameters, most methods require segmenting and measuring the airway lumen and wall from chest CT scans. Segmentation of the airway lumen is challenging, due to the complex structure of the airway tree and small size of most branches. Recently, deep learning methods for automatic segmentation of the airway lumen have achieved success[96,108–111]. Segmentation of the airway walls in the smaller branches is even more demanding, due to its small thickness and low contrast between the wall, lumen, and surrounding parenchyma. The thickness of the wall may fall below the scanner resolution, therefore lacking the stark contrast available in the larger airways. Airway wall segmentation has received less attention; currently there are no automatic methods to obtain this directly from the CT scan without an initial seed placement or lumen segmentation[7]. Instead, the airway wall can be obtained as an additional refinement step using, for example, full-width at half-maximum[112], phase congruency[113] or optimal-surface graph-cut methods[10].

To evaluate early biomarkers of respiratory disease on low-dose chest CT scans, we built an automated pipeline for segmenting and quantifying the airway lumen and wall. We did this by combining two validated, open-source methods, for obtaining the airway lumen and wall segmentations, respectively. While previous studies have evaluated AI on lumen segmentations, we could not identify studies that have assessed their reproducibility when also measuring the airway wall in a fully automated way. Further, this is the first combination of these 3D-Unet and 3D optimal-surface graph-cut methods

for fully-automated bronchial parameter evaluation. We aim to quantify the repeatability of this pipeline on low-dose chest CT. Subsequently, we computed the bronchial parameter measurements. We tuned this pipeline for the low-dose chest CT scan protocol and investigated its reproducibility using short-term repeated scanning.

## Methods

### CT Scans

Scans for this study were obtained from the Imaging in Lifelines (ImaLife) study, which was approved by the local medical ethics committee, and is registered with the Dutch Central Committee on Research Involving Human Subjects (https://www.toetsingonline.nl, Identifier: NL58592.042.16)

All scans were obtained using third generation dual source CT (Somatom Force, Siemens Healthineers). Imaging was performed with the participants in supine position and coached to hold their breath at maximum inspiration. The ImaLife scanning protocol for lung imaging was as follows: 120 kVp, 20mAs, pitch 3.0 (2.5 in large habitus), 1/0.7mm slice thickness/increment and Dose Length Product (DLP) of <100mGycm. Images were reconstructed with a quantitative-sharp reconstruction kernel (Qr59)[32].

### Lumen Segmentation

We used a deep learning airway segmentation method (Bronchinet)[96], based on a 3D U-Net model, to automatically obtain airway lumen segmentation from the CT scans. For training, we used a dataset of 24 ImaLife scans to train Bronchinet from scratch, with ground truth airway segmentations generated with a previously reported method[114]. From the full dataset, we used 22 scans for training (i.e., optimize the model weights) and the remaining 2 scans for validation (i.e., early stopping and model convergence). The Bronchinet method was validated in a previous paper with a training set of similar size showing good performance[96]. We assessed the model performance using 6-fold cross-validation.



| Variable | Number or mean±SD |
|---|---|
| **Participants** | 168 (100%) |
| **Male/Female** | 98 (58%) /70 (42%) |
| **Never-smoking** | 40 (24%) |
| **Smoking** | 76 (45%) |
| **COPD** | 39 (23%) |
| **No status** | 13 (8%) |
| **Age** (years) | 59.6±9.4 |
| **BMI** (kg/m2) | 26.46±3.78 |
| **Pack-Years*** | 14.7±8.1 |
| **TLV** (L) | 5.52±1.28 |
| **Pi10** (mm) | 3.92±0.12 |
| **WAP** (%) | 56.4±3.42 |
| **LA** ($mm^2$) | 42.0±2.31 |
| **TAC** (n) | 250±54 |

***Table 4.1*** *- Characteristics of participants. Data displayed as mean and standard deviation or number (percentage). Mean CT measurements were calculated from the first scan. BMI – Body Mass Index, N – Number, SD – Standard Deviation, TLV – Total Lung Volume, WAP – Wall Area Percentage, LA – Luminal Area, TAC – Total Airway Count. * Pack-years does not include never-smokers.*

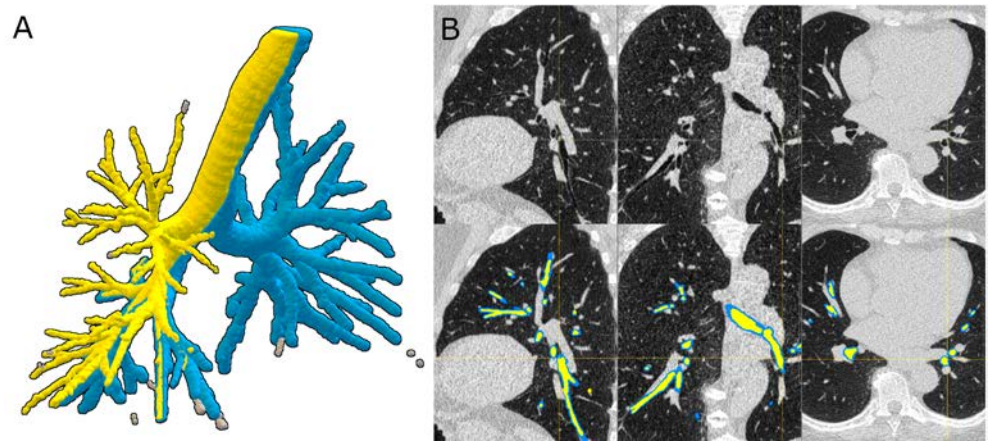


***Figure 4.1*** *- A) 3D rendering of the airway lumen (yellow) and wall (blue) of an ImaLife participant CT scan. Disconnected components (grey) were discarded prior to bronchial parameter measurement. Maximum generation - 8 B) 2D overlay of the airway lumen (yellow) and wall (blue) segmentations on sagittal, coronal, and axial planes respectively.*

### Wall Segmentation

An optimal-surface graph-cut method (Opfront)[10,115] was used to refine the Bronchinet airway lumen segmentations and obtain the wall segmentation. Opfront performance was tuned on several parameters, which depend on the scan resolution and protocol. We optimized the Opfront parameters using the COPDGene phantom, scanned using the ImaLife protocol[116]. The optimised parameters were inner and outer derivatives, smoothness penalties/ constraints and surface separation penalty. These parameters were focused on as they most strongly influence the resulting lumen and wall segmentation. For all other parameters we used the values suggested in Petersen 2015[10]. The lumen and total diameters of the Opfront segmentation for the phantom tubes were measured and compared to the known dimensions. To automatically search for the optimal parameter values, we used the Tree-structured Parzen Estimator algorithm[117], which modified parameters if the measurement error between phantom measurements and known dimensions was large[10]. Once phantom measurements were close to the known dimensions, Opfront was considered optimised.

### Measurement of Branches

From the airway lumen segmentations obtained by Bronchinet, discarding disconnected components. individual branches were extracted using a front-propagation method as described in the EXACT'09 challenge[92,118]. Branch generations were determined based on Weibel's airway model, which defines a new generation at each branching point[2]. Measurements of the airway lumen and wall radii were calculated for all branches, measured at regular intervals of 0.5 mm along the branch centreline and averaged. Terminal branches of less than 2mm in length were automatically discarded.

### Automated Pipeline

We combined the Bronchinet and Opfront methods in an automated pipeline to obtain the wall segmentation and bronchial parameter measurements directly from input CT scans. For this we built a docker image[119] to link both tools and manage software dependencies. This allows deploying the pipeline in any computing system featuring at least 16GB RAM and a CUDA-compatible graphics card with at least 8GB memory.



### Reproducibility Study

188 ImaLife participants with two scans an average of 3 months apart were included. None of these participants were included for the Bronchinet model training. For more information on the ImaLife study, please see prior publications[32,120]. Participants were invited for a short-term repeat scan for scientific purposes in case of an intermediate nodule (100–300mm³) on the first scan. All scans were automatically processed by the proposed pipeline. Inspiration levels were quantified based on the total lung volume (TLV), derived from automated lung segmentation[106]. Participants with a difference in inspiration defined by a TLV difference between first and second scans greater than 15% were excluded from analysis[75]. Bronchial parameters were automatically calculated from airway branch lumen and wall radii, namely luminal area (LA), wall area percentage (WAP), and square root of the wall area (SRWA) at a hypothetical airway with internal perimeter of 10mm (Pi10). Pi10 was calculated by linear regression of SRWA compared to the internal perimeter of the airway branch, excluding the trachea, and including branches up to and including the 6$^{th}$ generation (Fig. S4.1)[121].



### Statistical Analysis

To measure the reproducibility of the pipeline, the coefficient of determination ($R^2$) was calculated for bronchial parameters per airway generation by first and second CT scan comparison. An $R^2$ of >0.7 was considered good, 0.7-0.5 moderate, <0.5 poor[122]. Bland-Altman analysis was performed to calculate the Limits of Agreement (LoA) for each bronchial parameter per generation. The python package statsmodels (v 0.13.5) was used for statistical analysis[123].

## Results

### Bronchinet and Opfront Performance

On the cross-validation assessment of Bronchinet with the 24 ImaLife scans, the median Dice overlap coefficient for the obtained airway lumen segmentations was 0.92 (inter-quartile range (IQR), 0.83-0.93), the median centreline completeness was 85.2% (IQR 78.8-89.4%) and median centreline leakage (indicating predicted false-positive centrelines) was 7.1% (IQR, 3.5-10.8%) As the volume of the trachea and main bronchi dominate these values, they were excluded to focus on downstream segmentation performance.

| | Measurement Error (mm) | |
|---|---|---|
| **Tube** | **Lumen** | **Wall** |
| **1** | 0.09 | -0.15 |
| **2** | 0.09 | 0.03 |
| **3** | 0.09 | -0.22 |
| **4** | -0.00 | 0.21 |
| **5** | 0.05 | -0.01 |
| **6** | 0.04 | 0.24 |
| **7** | -0.05 | 0.33 |
| **8** | 0.14 | -0.22 |

***Table 4.2*** *- Opfront measurement error for phantom tube lumen and wall.*

Optimised Opfront segmentation of the COPDGene phantom resulted in sub-voxel accuracy. The lumen diameter was estimated within a mean unsigned error of 3.1% (0.13±0.07mm), and the total diameter with an average unsigned error of 5.8% (0.35±0.20mm) (Table 4.2). The airway segmentations were fully 3D and the extracted airways reached the 10th generation on average (Figure 4.1). Total execution time was 28±4min per scan.

## Reproducibility Study

Out of 376 scans, 374 (99%) were successfully segmented and measured. Twenty of 188 participants were excluded due to a difference in TLV of >15% between the first and second scan. The final group comprised 98 male and 70 female participants with a repeat scanning within 3 months (98±14 days). The mean age was 59.6±9.4 and body mass index (BMI) was 26.5±3.8. Of the 168 included participants, 40 were never-smokers, 76 were smokers, 39 had a COPD diagnosis and 13 participants had missing COPD disease status (Table 4.1). The mean pack-year history for smokers was 14.7±8.1 years. Mean CT measurements were 5.52±1.28L for TLV, 250±54 for total airway count (TAC), 42.0±2.3% for 3rd generation LA, 56.4±3.4% for 3rd generation WAP, and 3.92±0.12 for Pi10.

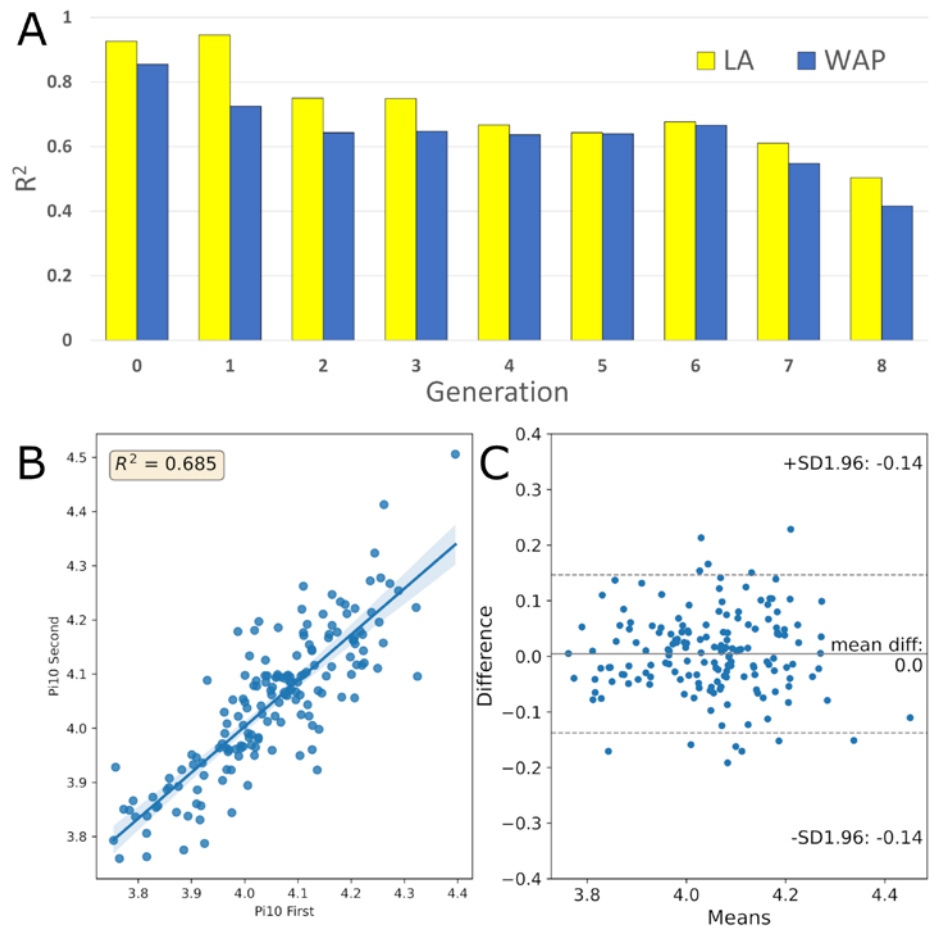


***Figure 4.2*** *- A) Reproducibility analysis. Comparison of bronchial parameter measurements between first and second scans per generation by coefficient of determination. B) Scatter plot and regression line of Pi10 measurement on first and second scans. C) Limits of Agreement for Pi10 between first and second scans. R² – Coefficient of Determination, SD – Standard Deviation.*

| | Luminal Area (mm²) | | | Wall Area Percent (%) | | |
|---|---|---|---|---|---|---|
| **Gen** | **MD** | **LoA** | **LoA%** | **MD** | **LoA** | **LoA%** |
| **0** | -1.10 | ±37 | ±7.4 | 0.05 | ±1.4 | ±5.9 |
| **1** | -0.19 | ±16 | ±6.8 | 0.02 | ±2.3 | ±6.1 |
| **2** | 0.37 | ±19 | ±16.4 | -0.14 | ±3.8 | ±6.1 |
| **3** | 0.19 | ±9.2 | ±12.6 | -0.01 | ±4.2 | ±9.1 |
| **4** | 0.25 | ±6.3 | ±20.6 | -0.13 | ±4.5 | ±8.5 |
| **5** | -0.09 | ±4.4 | ±22.5 | 0.12 | ±4.2 | ±7.5 |
| **6** | -0.10 | ±3.7 | ±22.8 | 0.14 | ±4.0 | ±6.8 |
| **7** | -0.04 | ±3.5 | ±28.9 | 0.12 | ±4.5 | ±7.4 |
| **8** | -0.15 | ±6.6 | ±36.3 | 0.25 | ±5.4 | ±9.3 |

***Table 4.3*** *- Mean Difference (MD) and Limits of Agreement (LoA) and LoA as a percentage of overall range (LoA%) between the first and second scan for luminal area and wall area percentage per airway generation. Gen – generation.*

Coefficient of determination ($R^2$) of LA ranged from 0.93 at the trachea to 0.68 at the 6th generation, decreasing to 0.51 at the 8th generation. Corresponding values for WAP were 0.86, 0.67 and 0.42, respectively (Figure 4.2A). For Pi10, $R^2$ was 0.69 (Figure 4.2B) and LoA was ±0.14mm (±3.7% of mean) with a mean difference (MD) of 0.00mm (Figure 4.2C). For LA, MD±LoA ranged from -0.1±37mm² at the trachea to -0.1±3.7mm² at 6th generation, and down to -0.15±6.6mm² at the 8th generation (Table 4.3). For WAP, MD±LoA ranged from 0.05±1.4% at the trachea to 0.14±4% at 6th generation and down to 0.25±5.4% at the 8th generation. LoA expressed as a percentage of mean (LoA%) was between ±5.9-9.3% for WAP. LoA% for LA was ±7.4-6.8% at 0-1st generations, widening to ±16.4-22.8% for 2nd to 6th generations and further increasing to ±28.9-36.3% at 7th to 8th generations (Table 4.3).

## Discussion

In this study we built an automated pipeline for low-dose chest CT scans to obtain segmentations of the airway lumen and wall by combining two open-source methods. The resulting segmentations yielded automated quantitative bronchial parameters. Repeated scans showed moderate to good reproducibility ($R^2$>0.6) of bronchial parameters down to the 6th generation. Bland-Altman analysis showed no systematic bias and narrow limits of agreement for Pi10 and WAP, but wider for LA, demonstrating a lower variability in summary parameters like Pi10 and WAP compared to the direct measurement of LA.

Use of low-dose CT scans for lung cancer screening provides the opportunity to screen for other early disease such as COPD, bronchiectasis, and cardiac disease, which may influence lung cancer risk and/or prognosis. Automated bronchial parameter measurement can enable screening of large cohorts in a reasonable timeframe with good reliability. Further, the fully 3D segmentation can be readily useful in clinical tasks such as virtual bronchoscopy or surgical planning. However, for bronchial parameters, it is hard to determine whether the airways are normal or abnormal. The number of never-smokers in bronchial parameter research is typically very small[124]. Combined with heterogenous bronchial parameter methodology, it is unclear what quantitatively defines "normal" airways on low-dose CT and by which bronchial parameter. This study demonstrated a wider variability in measurements for LA than Pi10 or WAP. While this could in part concern variability or error due to methodology, additional factors like seasonal changes, smoking or illness before a scan could result in true differences. Pi10 averages many branches, while WAP includes wall thickness in its calculation and so could be more resistant than LA to localised variations in measurements. Our pipeline provides similar reproducibility of LA and WAP as previous methods on similar datasets[10], but it also gives better reproducibility of Pi10[125]. Additionally, it offers fully automatic bronchial parameter measurement using low-dose noisy scans.

Various methods can be used as an initial step for lumen segmentation. We used Bronchinet due to its state-of-the-art performance[96], speed and open-source availability which enabled retraining on the low-dose scans in this study. Fully automated bronchial parameter calculation has been previously proposed using tools trained on manually traced borders alongside older algorithms such as FWHM, intensity-based and phase congruency[126,127]. However, previous research shows that manual and FWHM measurement overestimates the airway wall[128], which is also evident when used to measure the COPDGene phantom (Table S4.2). Compared to these approaches the advantage of our method is that Opfront was optimized on a phantom with precise physical measurements, eliminating the bias in wall measurements that comes with the previously mentioned approaches. The pipeline output is a ready-to-use 3D model of the airways, which has potential applications in tasks such as virtual bronchoscopy, airflow simulation, and 3D printing. Deploying the pipeline in a docker image provides the method as ready-to-use and implementable in clinical practice. For lumen segmentation good results could be readily achieved by using the publicly available trained model bundled with Bronchinet[96], which uses airway segmentations

for training from the Danish Lung Cancer Screening Trial[98] in combination with an Erasmus-MC Sophia (cystic fibrosis) dataset[9]. The ImaLife scan protocol has a lower radiation dose with a total DLP of <100mGycm, and more noise in the scans; retraining the tools resulted in better performance[114]. For maximum performance on different datasets, optimising the pipeline for the target CT protocol may be necessary. This was achieved by re-training the Bronchinet with efficiently generated ground-truths, and tuning Opfront using a physical phantom.

A limitation of this study is the lack of severe airway disease in the cohort as the ImaLife study comprises a general population. Evaluation of severe cases is important prior to adoption in a clinical setting, where scan protocol may also change. For the analysis we assumed that there are no short-term differences in bronchial parameters between the scans. However, factors such as illness or smoking before the scan could have an impact on the bronchial parameter results. This would tend to increase variability between scans, which could mean that the actual scan-rescan repeatability may be better than we currently report. The methods used do not perform anatomical airway labelling, and so we could not compare the repeat measurements of specific airway branches directly. Instead, we focused on average values per generation for participants. Lastly, Bronchinet does not guarantee a fully connected airway segmentation, some peripheral branches may be discarded during measurement. For cases with an occluded lumen, this could result in exclusion of segmented airways beyond the blockage.

In conclusion, we demonstrate a comprehensive and fully automatic pipeline for bronchial parameter measurement on low-dose CT using open-source tools. Based on results of short-term repeat CT scanning, the pipeline provides reliable bronchial parameters down to the 6$^{th}$ generation. Overall, these methods enable the exploration of bronchial parameters in large low-dose CT datasets after an initial investment in the training and optimisation of deep learning and optimal-surface graph-cut methods.

# PART 3

# AIRWAY AND LUNG MEASUREMENTS IN THE GENERAL POPULATION

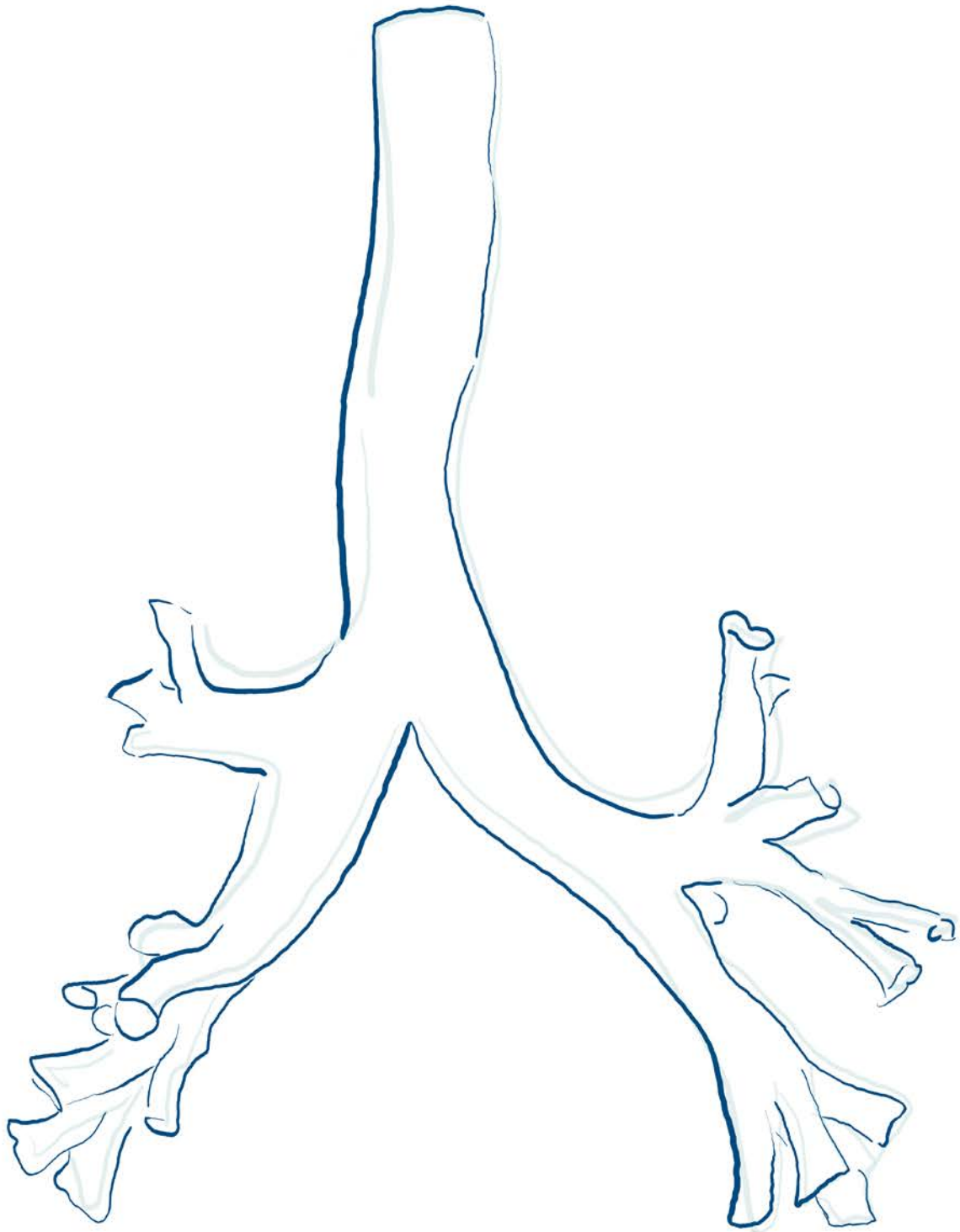

# CHAPTER 5

## LOW-DOSE CT–DERIVED BRONCHIAL PARAMETERS IN INDIVIDUALS WITH HEALTHY LUNGS

I. Dudurych • G.J. Pelgrim • G. Sidorenkov • A. Garcia-Uceda • J. Petersen • D.J. Slebos • G. H. de Bock • M. van den Berge

M. de Bruijne • R. Vliegenthart

*Radiology 2024*

## Abstract

**Background:** CT-derived bronchial parameters have been linked to chronic obstructive pulmonary disease and asthma severity, but little is known about these parameters in healthy individuals.

**Purpose:** To investigate the distribution of bronchial parameters at low-dose CT in individuals with healthy lungs from a Dutch general population.

**Materials and Methods:** In this prospective study, low-dose chest CT performed between May 2017 and October 2022 were obtained from participants who had completed the second-round assessment of the prospective, longitudinal Imaging in Lifelines study. Participants were aged at least 45 years, and those with abnormal spirometry, self-reported respiratory disease, or signs of lung disease at CT were excluded. Airway lumens and walls were segmented automatically. The square root of the bronchial wall area of a hypothetical airway with an internal perimeter of 10 mm (Pi10), luminal area (LA), wall thickness (WT), and wall area percentage were calculated. Associations between sex, age, height, weight, smoking status, and bronchial parameters were assessed using univariable and multivariable analyses.

**Results:** The study sample was composed of 8869 participants with healthy lungs (mean age, 60.9 years ± 10.4 [SD]; 4841 [54.6%] female participants), including 3672 (41.4%) never-smokers and 1197 (13.5%) individuals who currently smoke. Bronchial parameters for male participants were higher than those for female participants (Pi10, slope [β] range = 3.49–3.66 mm; LA, β range = 25.40–29.76 mm2; WT, β range = 0.98–1.03 mm; all $P < .001$). Increasing age correlated with higher Pi10, LA, and WT ($r^2$ range = 0.06–0.09, 0.02–0.01, and 0.02–0.07, respectively; all $P < .001$). Never-smoking individuals had the lowest Pi10 followed by formerly smoking and currently smoking individuals (3.62 mm ± 0.13, 3.68 mm ± 0.14, and 3.70 mm ± 0.14, respectively; all $P < .001$). In multivariable regression models, age, sex, height, weight, and smoking history explained up to 46% of the variation in bronchial parameters.

**Conclusion:** In healthy individuals, bronchial parameters differed by sex, height, weight, and smoking history; male sex and increasing age were associated with wider lumens and thicker walls.




## Introduction

Chronic respiratory diseases are among the top 10 causes of death worldwide[35]. Early diagnosis combined with proactive management of chronic obstructive pulmonary disease is being explored as one method to reduce the associated morbidity and mortality rates[129]. Although smoking cessation remains central to treatment of chronic obstructive pulmonary disease, other therapeutic interventions are aimed at reducing symptoms and improving quality of life. For both early detection with timely smoking cessation and monitoring of treatment response, CT-derived bronchial parameters could play a key role[14,33,130]. Bronchial parameters at CT have been linked to respiratory disease severity and progression in symptomatic patients across a variety of respiratory illnesses, including chronic obstructive pulmonary disease, asthma, and interstitial lung disease[11,87,91,131,132]. However, underlying physiologic differences with respect to sex and age may contribute to bronchial parameter variation[25,27]. For their potential use as a screening or diagnostic tool, it is important to consider the distribution and range of these parameters in the target population. Currently, most large-scale analyses of bronchial parameters have been conducted in individuals who smoke or patients with chronic obstructive pulmonary disease, with only limited data in individuals who do not currently smoke[124]. Most of the insights into bronchial parameters in healthy individuals originate from small groups of healthy control participants who, due to study design and requirements, may not represent the healthy general population, with conflicting results for normal values of bronchial parameters[124]. Furthermore, reference values for individuals with healthy lungs from general populations have not been well established. The aim of this study was to examine the distribution of low-dose CT–derived bronchial parameters in individuals with healthy lungs from a Dutch general population.

## Materials and Methods

In this prospective study, imaging analysis was performed on data from 12041 participants from the Imaging in Lifelines (ImaLife) study[120], which was approved by the local medical ethics committee (University Medical Centre Groningen) and is registered with the Dutch Central Committee on Research Involving Human Subjects (https://www.toetsingonline.nl; identifier: NL58592.042.16). All participants gave informed consent before participation.

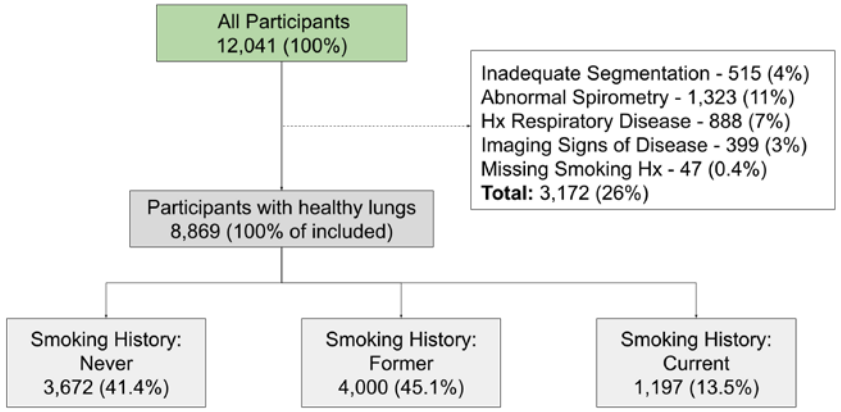


***Figure 5.1*** *- Flowchart of participant inclusion and exclusion and group division. Hx = history.*

## Study Design and Participants

ImaLife is part of the Lifelines multidisciplinary prospective population-based three-generation cohort study examining the health and health-related behaviours of 167729 persons living in the three northern provinces in the Netherlands[120]. The ImaLife study focuses on imaging biomarkers for the general population from low-dose CT scans. That study includes participants aged 45 years and older who completed a lung function test during the second-round assessment of the Lifelines study and who were invited to undergo low-dose chest CT between May 2017 and October 2022. The full study design was published previously[32] and includes participant recruitment and sample size estimation. Previous analyses of ImaLife participants are listed in Table S4.1. Because the focus of the current study was on individuals with healthy lungs, participants with self-reported history of pulmonary disease, medication use for respiratory disease, or abnormal spirometry according to the lower limit of normal for percent predicted forced expiratory volume in 1 second of expiration or forced expiratory volume in 1 second of expiration to forced vital capacity ratio were excluded (Appendix S1). Participants with CT features of respiratory disease, such as interstitial lung disease, emphysema, bronchiectasis, and infection, and those with inadequate airway segmentation were also excluded from the study. Details of lung findings at CT leading to exclusion are described in Appendix S1.





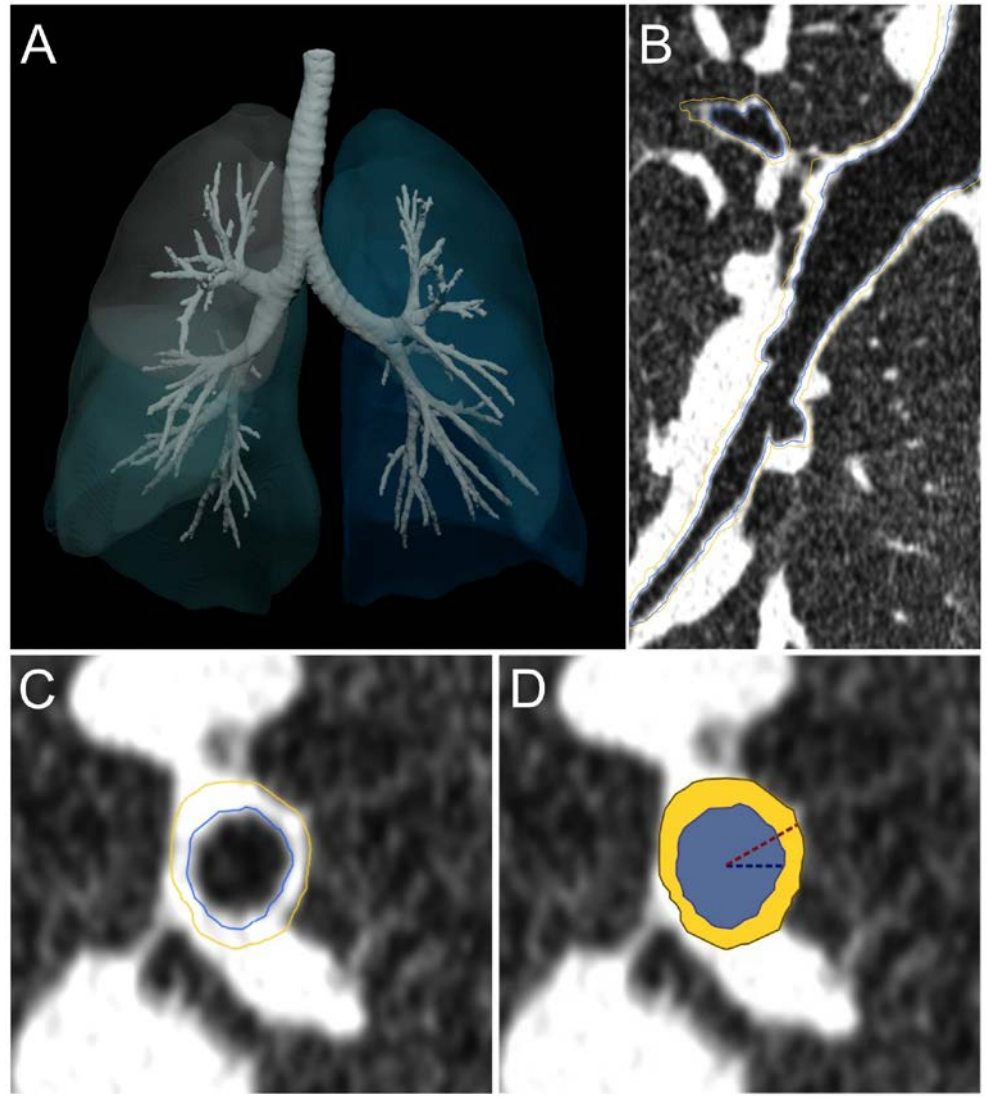


***Figure 5.2*** *- (A) Three-dimensional rendering of an exemplary airway segmentation. (B) Coronal view of a low-dose CT example of airway lumen and wall segmentation along the length of an airway (yellow outline). (C) Multiplanar reconstructed low-dose CT section perpendicular to the airway centre line demonstrates the airway lumen (blue outline) and wall (yellow outline) segmentation boundaries. (D) Example measurements of lumen radius (blue dashed line) and total radius (red dashed line). These measurements are obtained every 0.5 mm along the centre line of the airway. They are used to calculate the rest of the bronchial parameters: the luminal area (blue region) and wall area (yellow region).*

Participants were split into groups based on their smoking history (i.e., never, former, and current), and their bronchial parameters were measured and

analysed, consisting of the square root of the bronchial wall area of a hypothetical airway with an internal perimeter of 10 mm (Pi10), luminal area (LA), wall thickness (WT), and wall area percentage.

## Definitions of Terms

Never smoking was defined as a 0 pack-years history, former smoking as self-reported quitting smoking without restarting smoking, and current smoking as self-reported smoking within the last month of answering the questionnaire and not reporting having quit smoking.

## Image Acquisition and Reconstruction

Each participant underwent a supine inspiratory chest CT examination based on a low-dose non-contrast volumetric scan protocol, using a third-generation dual-source CT scanner (Somatom Force; Siemens Healthineers). For scan reconstruction, a hard Qr59 kernel that was designed for quantitative purposes was used with section thickness of 1 mm and section increment of 0.7 mm.

## Image Analysis

Scans were automatically processed to calculate bronchial parameters. The airway lumen was extracted using a three-dimensional U-Net as previously described[96]. Next, the airway lumen was refined, and the outer wall segmented using an optimal-surface graph-cut method[115]. This in-house pipeline (https://github.com/id-b3/AirFlow-ImaLife) was validated previously in a representative sample of the ImaLife data set with good reproducibility[133]. Segmentations were automatically flagged for review when unusually low or high lung volume, airway volume, airway count, or rapid radius changes indicated potential segmentation errors. The segmentations flagged for review were combined with a random sample of nonflagged segmentations for a total of 2000 segmentations reviewed by a medical doctor (I.D., with 3 years of experience in airway segmentation research and evaluation and experience in radiology and pulmonology departments) who was blinded to participant characteristics. A three-point Likert scale was used to evaluate quality for leaks, segmentation completeness, and segmentation extent (Appendix S2). Several bronchial parameters were calculated from measurements of the lumen and total radii taken every 0.5 mm along the centreline of the airway segmentation. The average of these measurements per branch was used to calculate the lumen radius (LR) and total radius (TR). LR and TR were used to calculate the following parameters: LA = $\pi(LR)^2$; WT = TR – LR; and WAP = [(TA – LA)/TA]100, where WAP is wall area percentage and TA is total area, calculated as $\pi(TR)^2$. Pi10 was calculated using airways from generation zero (trachea) through six. The sixth airway generation was chosen as a threshold based on the robustness of airway measurements[17]. The square root of the bronchial wall area was plotted against the internal perimeter per branch, and a robust regression line was calculated[17]. Pi10 was measured at the intercept for an internal perimeter of 10 mm (Fig. S5.1). LA, WT, and wall area percentage were averaged across airway generations three through five[10].

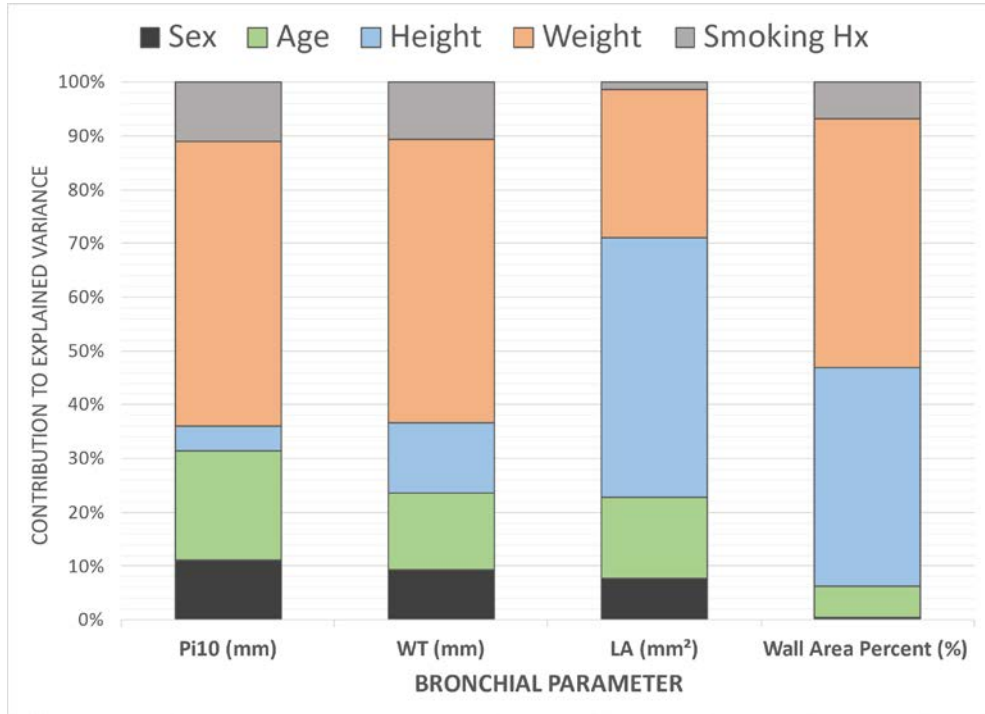


***Figure 5.3*** *- Stacked bar plot shows the feature importance of independent variables for each bronchial parameter. Feature importance was calculated using the coefficients of the independent variables sex, age, height, weight, and combined smoking history from normalized multivariable linear regression models for each of the bronchial parameters. Hx = history, LA = luminal area, Pi10 = square root of the wall area of a hypothetical airway with an internal perimeter of 10 mm, WT = wall thickness.*

## Statistical Analyses

The Student t-test was used to compare group means by sex with Bonferroni correction for multiple comparisons. One-way analysis of variance with the Tukey honest significant difference post hoc test was used to assess means

across groups based on smoking history. Percentiles ($10^{th}$–$90^{th}$) for each bronchial parameter were determined for sex and smoking status using 5-year age categories. To examine the strength and direction of relationships between age, height, weight, and bronchial parameters, univariable linear regression was performed, and the slope (β) and coefficient of determination ($r^2$) were calculated. Additionally, multivariable linear regression models were created for each bronchial parameter incorporating the independent variables sex, age, height, weight, smoking status, and pack-years. The adjusted $R^2$ was used to investigate explained variance for each multivariable model. To assess feature importance, independent variables were normalized, and the absolute value of the resulting coefficients was visualized for each model. Last, equations for calculating reference bronchial parameters were derived and adjusted for sex, age, height, weight, smoking status, and pack-years. The threshold for significance (α) was indicated by .05. When Bonferroni correction was used, the threshold for significance was indicated by .0038. Statistical analyses were performed (I.D.) using SciPy and Statsmodels (Python, version 3.10; Python Software Foundation).

## Results

### Participant Characteristics

Of 12041 participants, 1323 were excluded for abnormal spirometry, 888 for history of respiratory disease, 399 for imaging features of respiratory illness, 47 for missing smoking data, and 515 for inadequate bronchial segmentation (Fig. 5.1). A total of 8869 participants (mean age, 60.9 years ± 10.4 [SD]; 4841 [54.6%] female participants, 4028 [45.4%] male participants) were included; 3672 (41.4%), 4000 (45.1%), and 1197 (13.5%) were never smoking, formerly smoking, and currently smoking, respectively (Table 5.1). The mean pack-years were 16.9 pack-years ± 11.5 for individuals who currently smoked and 10.4 pack-years ± 9.7 for individuals who formerly smoked. Height (mean, 1.81 m ± 0.07 vs 1.68 m ± 0.06; $P < .001$), weight (mean, 86.8 kg ± 12.4 vs 73.7 kg ± 12.5; $P < .001$), smoking pack-years (mean, 13.9 pack-years ± 11.9 vs 9.8 pack-years ± 9.2; $P < .001$), and total lung volume (mean, 6.1 L ± 1.2 vs 4.7 L ± 0.8; $P < .001$) were greater in male participants than in female participants, respectively. Exemplary segmentation of airway tree, lumen, and wall borders is shown in Figure 5.2. Visual scoring of the random sample of scans from the included participants showed a mean quality of 2.86 ± 0.43 for leaks, 2.86 ± 0.44 for completion, and 2.63 ± 0.59 for extent (Fig. S5.2).



### Bronchial Parameter Distribution and Percentile Values

Pi10, LA, and WT were larger and wall area percentage was smaller in male participants compared with female participants ($P < .001$; Table 5.1). These sex differences were still observed when stratified by smoking status (Table S5.2). Bronchial parameters are provided as percentile values per age category in Table 5.2 for men and Table 5.3 for women. Generally, it was observed that with increasing age, Pi10 and WT increased, and the LA widened. Furthermore, it was observed that wall area percentage decreased until age 65–70 years, when it began to increase again. These observations were also observed when male participants and female participants were categorized as individuals who never smoked (Table S5.3) and individuals who currently smoke (Table S5.4).



### Univariable Analysis Assessing Relationships Between Participant Characteristics and Bronchial Parameters

For both sexes, univariable linear regression analysis showed a positive but weak correlation of age, weight, and body mass index (calculated as weight in kilograms divided by height in meters squared) with Pi10 (β range, 0.01–0.04; $r^2$ range, 0.06–0.13; $P < .001$) (Table 5.4). Although a small change in Pi10 for a unit increase in height was shown, there was no evidence that one variable explained the other for male and female participants (β = 0.08, −0.08; $r^2 = 0$; $P = .02$, .004, respectively). There was a weak positive correlation of age, weight, and body mass index with WT for both sexes (β = 0.01; $r^2$ range = 0.02–0.16). For both sexes, age and height displayed a weak positive correlation with LA (β range = 0.56–11.5; $r^2$ range = 0.01–0.02), while weight and body mass index were negatively correlated (β range = −0.37 to −0.16; $r^2$ range = 0.0–0.03). This result was reversed for wall area percentage (β range = −6.56 to −0.1, $r^2$ range = 0.0–0.02 for age and height; β range = 0.2–0.58, $r^2$ range = 0.03–0.09 for weight and body mass index). Comparing bronchial parameters between participants stratified by smoking history, individuals who never smoked had lower values for Pi10 versus former and current smokers (Pi10: 3.62 mm ± 0.13, 3.68 mm ± 0.14, and 3.70 mm ± 0.14 for never, former, and current smoking male participants, respectively; 3.47 mm ± 0.13, 3.49 mm ± 0.13, and 3.53 mm ± 0.14 for never, former, and current smoking female participants, respectively; $P < .001$ for all comparisons; Table S5.2). In male participants who formerly smoked, the LA value was larger than that in current smokers (LA mean difference, 0.863 mm2; $P = .004$; Table S5.5).

| Characteristics | Total | Male | Female | *P*-value |
|---|---|---|---|---|
| **Participants** | 8869 (100%) | 4028 (45.4%) | 4841 (54.6%) | |
| **Age (Years)** | 60.9±10.4 | 61.7±10.8 | 60.2±10.1 | <.001 |
| **Height (m)** | 1.74±0.09 | 1.81±0.07 | 1.68±0.06 | < .001 |
| **Weight (kg)** | 79.7±14.1 | 86.8±12.4 | 73.7±12.5 | < .001 |
| **BMI (kg/m²)** | 26.18±3.81 | 26.37±3.27 | 26.02±4.19 | < .001 |
| **Smoking history:** | | | | |
| **Never** | 3672 (41.4%) | 1562 (42.5%) | 2110 (57.5%) | |
| **Former** | 4000 (45.1%) | 1852 (46.3%) | 2148 (53.7%) | |
| **Current** | 1197 (13.5%) | 614 (51.3%) | 583 (48.7%) | |
| **Pack Years* - Total** | 11.8±10.8 | 13.9±11.9 | 9.8±9.2 | < .001 |
| **Pack-years - Former** | 10.4±9.7 | 12.7±11.3 | 8.1±8.1 | < .001 |
| **Pack-years - Current** | 16.9±11.5 | 17.8±12.6 | 16.1±10.3 | .012 |
| **$FEV_1$ (L)** | 3.30±0.78 | 3.89±0.68 | 2.83±0.48 | < .001 |
| **$FEV_1$ PP (%)** | 100±12 | 100±13 | 100±12 | .77 |
| **FVC (L)** | 4.34±1.01 | 5.13±0.85 | 3.69±0.61 | < .001 |
| **$FEV_1$/FVC** | 0.76±0.05 | 0.76±0.05 | 0.77±0.05 | < .001 |
| **TLV (L)** | 5.4±1.2 | 6.1±1.2 | 4.7±0.8 | < .001 |
| **Pi10 (mm)** | 3.57±0.16 | 3.66±0.14 | 3.49±0.13 | < .001 |
| **Wall area percent (%)** | 47.25±3.36 | 46.96±3.42 | 47.50±3.29 | < .001 |
| **LA (mm²)** | 27.38±5.64 | 29.76±5.79 | 25.40±4.66 | < .001 |
| **WT (mm)** | 1.00±0.05 | 1.03±0.05 | 0.98±0.05 | < .001 |

***Table 5.1*** *- Except where indicated, data are means ± SDs. Data in parentheses are percentages. P values are for t test comparisons between male and female participants. BMI = body mass index (calculated as weight in kilograms divided by height in meters squared), $FEV_1$ = forced expiratory volume in 1 second, FVC = forced vital capacity, LA = luminal area, Pi10 = square root of the wall area of a hypothetical airway with an internal perimeter of 10 mm, PP = percent predicted, TLV = total lung volume, WT = wall thickness. * Individuals who never smoked were not included in calculating the mean pack-years. a = .0038 for significance after Bonferroni correction.*



| Age | | 45-50 | 50-55 | 55-60 | 60-65 | 65-70 | 70-75 | 75-80 | 80+ |
|---|---|---|---|---|---|---|---|---|---|
| **Male n** | **Percentile** | 547 | 648 | 743 | 664 | 436 | 378 | 450 | 346 |
| | 10th | 3.45 | 3.48 | 3.47 | 3.48 | 3.51 | 3.50 | 3.54 | 3.54 |
| | 25th | 3.52 | 3.55 | 3.56 | 3.56 | 3.59 | 3.59 | 3.62 | 3.64 |
| **Pi10** | 50th | 3.60 | 3.64 | 3.64 | 3.65 | 3.69 | 3.70 | 3.70 | 3.73 |
| | 75th | 3.70 | 3.72 | 3.74 | 3.75 | 3.79 | 3.80 | 3.82 | 3.83 |
| | 90th | 3.77 | 3.81 | 3.83 | 3.83 | 3.87 | 3.88 | 3.90 | 3.91 |
| | 10th | 0.96 | 0.98 | 0.97 | 0.97 | 0.98 | 0.97 | 0.98 | 0.98 |
| | 25th | 0.99 | 1.00 | 1.00 | 1.00 | 1.01 | 1.00 | 1.01 | 1.02 |
| **WT** | 50th | 1.02 | 1.03 | 1.03 | 1.03 | 1.04 | 1.04 | 1.04 | 1.05 |
| | 75th | 1.05 | 1.05 | 1.06 | 1.06 | 1.07 | 1.07 | 1.07 | 1.08 |
| | 90th | 1.08 | 1.08 | 1.09 | 1.09 | 1.09 | 1.10 | 1.10 | 1.10 |
| | 10th | 21.95 | 21.86 | 22.66 | 22.88 | 23.04 | 23.48 | 23.27 | 22.97 |
| | 25th | 25.03 | 25.02 | 25.90 | 25.87 | 26.47 | 26.68 | 26.58 | 25.87 |
| **LA** | 50th | 28.13 | 28.44 | 29.19 | 30.03 | 30.00 | 30.08 | 30.55 | 29.90 |
| | 75th | 31.52 | 32.46 | 33.33 | 33.61 | 34.29 | 34.06 | 34.70 | 34.91 |
| | 90th | 35.32 | 36.52 | 37.01 | 37.67 | 38.17 | 37.31 | 38.87 | 39.21 |
| | 10th | 43.24 | 43.12 | 42.87 | 42.22 | 42.34 | 42.67 | 41.87 | 41.87 |
| | 25th | 45.26 | 45.24 | 44.59 | 44.30 | 44.25 | 44.41 | 43.91 | 44.29 |
| **WAP** | 50th | 47.53 | 47.26 | 46.86 | 46.47 | 46.73 | 46.67 | 46.40 | 46.85 |
| | 75th | 49.60 | 49.65 | 48.97 | 48.97 | 48.86 | 48.96 | 49.02 | 49.58 |
| | 90th | 51.58 | 51.82 | 51.49 | 51.17 | 50.99 | 51.00 | 51.23 | 51.95 |

***Table 5.2*** *- Reference bronchial parameter percentiles split by age for men. Data are percentile values. LA = luminal area, Pi10 = square root of the wall area of a hypothetical airway with an internal perimeter of 10 mm, WT = wall thickness.*

| Age | | 45-50 | 50-55 | 55-60 | 60-65 | 65-70 | 70-75 | 75-80 | 80+ |
|---|---|---|---|---|---|---|---|---|---|
| Female n | Percentile | 766 | 851 | 964 | 765 | 580 | 438 | 454 | 238 |
| | 10th | 3.32 | 3.31 | 3.32 | 3.31 | 3.33 | 3.35 | 3.39 | 3.41 |
| | 25th | 3.37 | 3.38 | 3.38 | 3.38 | 3.40 | 3.43 | 3.47 | 3.52 |
| Pi10 | 50th | 3.45 | 3.45 | 3.47 | 3.47 | 3.49 | 3.52 | 3.57 | 3.62 |
| | 75th | 3.52 | 3.53 | 3.56 | 3.56 | 3.59 | 3.61 | 3.66 | 3.71 |
| | 90th | 3.59 | 3.61 | 3.65 | 3.65 | 3.67 | 3.70 | 3.73 | 3.76 |
| | 10th | 0.92 | 0.91 | 0.92 | 0.92 | 0.93 | 0.93 | 0.95 | 0.95 |
| | 25th | 0.94 | 0.94 | 0.94 | 0.94 | 0.95 | 0.96 | 0.97 | 0.98 |
| WT | 50th | 0.97 | 0.97 | 0.97 | 0.97 | 0.98 | 0.99 | 1.01 | 1.02 |
| | 75th | 1.00 | 1.00 | 1.01 | 1.01 | 1.01 | 1.02 | 1.03 | 1.05 |
| | 90th | 1.02 | 1.02 | 1.04 | 1.04 | 1.04 | 1.05 | 1.06 | 1.07 |
| | 10th | 18.84 | 19.53 | 19.99 | 19.86 | 20.25 | 20.29 | 20.15 | 19.44 |
| | 25th | 20.94 | 21.89 | 22.29 | 22.65 | 23.01 | 22.81 | 22.62 | 22.18 |
| LA | 50th | 23.90 | 24.73 | 25.29 | 25.56 | 26.05 | 25.71 | 25.96 | 25.45 |
| | 75th | 26.93 | 27.90 | 28.30 | 28.80 | 29.29 | 28.93 | 29.36 | 28.51 |
| | 90th | 29.69 | 30.92 | 31.31 | 32.16 | 32.98 | 32.12 | 32.52 | 32.16 |
| | 10th | 44.15 | 43.52 | 43.43 | 43.00 | 42.57 | 42.87 | 43.18 | 43.81 |
| | 25th | 46.00 | 45.26 | 45.10 | 44.72 | 44.61 | 44.97 | 45.46 | 46.18 |
| WAP | 50th | 48.05 | 47.46 | 47.19 | 46.71 | 46.82 | 47.05 | 47.49 | 48.01 |
| | 75th | 50.26 | 49.64 | 49.58 | 49.42 | 49.14 | 49.55 | 49.81 | 50.75 |
| | 90th | 52.20 | 51.40 | 51.69 | 51.71 | 51.17 | 51.83 | 51.82 | 52.93 |

***Table 5.3*** *- Reference bronchial parameter percentiles split by age for women. Data are percentile values. LA = luminal area, Pi10 = square root of the wall area of a hypothetical airway with an internal perimeter of 10 mm, WT = wall thickness.*



| Male | | | | | | | | | | | |
|---|---|---|---|---|---|---|---|---|---|---|---|
| | Age* | | | Height | | | Weight* | | | BMI | |
| β | $R^2$ | p-val | β | $R^2$ | p-val | β | $R^2$ | p-val | β | $R^2$ | p-val |
| 0.03 | 0.07 | <0.001 | 0.08 | 0 | 0.02 | 0.04 | 0.12 | <0.001 | 0.02 | 0.14 | <0.001 |
| 0.01 | 0.03 | <0.001 | -0 | 0 | 0.7 | 0.01 | 0.12 | <0.001 | 0.01 | 0.16 | <0.001 |
| 0.68 | 0.02 | <0.001 | 11.5 | 0.02 | <0.001 | -0.37 | 0.01 | <0.001 | -0.31 | 0.03 | <0.001 |
| -0.22 | 0.01 | <0.001 | -4.92 | 0.01 | <0.001 | 0.58 | 0.04 | <0.001 | 0.32 | 0.09 | <0.001 |
| **Female** | | | | | | | | | | | |
| | Age* | | | Height | | | Weight* | | | BMI | |
| β | $R^2$ | p-val | β | $R^2$ | p-val | β | $R^2$ | p-val | β | $R^2$ | p-val |
| 0.04 | 0.09 | <0.001 | -0.08 | 0 | 0.004 | 0.03 | 0.07 | <0.001 | 0.01 | 0.1 | <0.001 |
| 0.01 | 0.07 | <0.001 | -0.04 | 0 | <0.001 | 0.01 | 0.09 | <0.001 | 0.01 | 0.12 | <0.001 |
| 0.56 | 0.01 | <0.001 | 10.7 | 0.02 | <0.001 | -0.26 | 0 | <0.001 | -0.16 | 0.02 | <0.001 |
| -0.1 | 0 | 0.03 | -6.56 | 0.02 | <0.001 | 0.49 | 0.03 | <0.001 | 0.2 | 0.07 | <0.001 |

***Table 5.4*** *- Univariable linear regression and correlation analysis for bronchial parameters with participant characteristics. β = slope, BMI = body mass index (calculated as weight in kilograms divided by height in meters squared), LA = luminal area, Pi10 = square root of the wall area of a hypothetical airway with an internal perimeter of 10 mm, WT = wall thickness. * Per 10-unit increase.*



## Multivariable Analysis and Reference Bronchial Parameter Equations

The multivariable linear regression model for each bronchial parameter showed a good fit based on the overall F statistic (P < .001). Multivariable linear models for Pi10 and WT achieved an adjusted $R^2$ of 0.465 and 0.412, respectively, whereas those for LA and wall area percentage achieved an adjusted $R^2$ of 0.207 and 0.104, respectively (Table 5.5Sex was correlated with a change in Pi10 (β1 = 0.12; P < .001), LA (β1 = 2.38; P < .001), and WT (β1 = 0.037; P < .001), but no evidence of a correlation with a change in wall area percentage was observed (β1 = 0.08; P = .41). All parameters increased with age except for wall area percentage, which decreased (β1 = −0.27% per 10 years; P < .001). Height was related to increased Pi10 and LA and decreased WT and wall area percentage (β1 = 0.008 mm, 20.23 mm2, −0.07 mm, and −12.46%, respectively; P = .002 for Pi10; P < .001 for LA, WT, and wall area percentage). Weight correlated with increased Pi10, WT, and wall area percentage and decreased LA (β1 = 0.04, 0.015, 0.73, and −0.59, respectively; all P < .001). Current smoking was related to increased Pi10 (β1 = 0.041;

P < .001), WT (β1 = 0.015; P < .001), and wall area percentage (β1 = 0.49; P < .001), but no evidence of a relationship with LA was observed (β1 = −0.11; P = .55). A history of more than 10 pack-years was related to increased Pi10, WT, and wall area percentage but had no evidence of an effect on LA. Based on feature importance analysis, it was observed that age, height, and weight together accounted for 80% or more of the explained variance for each bronchial parameter, and smoking history had an overall influence of less than 20% (Figure 5.3). For each bronchial parameter, the model coefficients were used to derive a normalized reference parameter equation, accessible as an online calculator at https://www.b3care.nl/bp_calc/ and in Figure S5.3 and Appendix S5.3.

| | Pi10 (mm) | | WT (mm) | | LA (mm²) | | Wall area percent (%) | |
|---|---|---|---|---|---|---|---|---|
| | $R^2$ 0.465, *P* <.001 | | $R^2$ 0.412, *P* <.001 | | $R^2$ 0.207, *P* <.001 | | | |
| | $\beta_1$ | *P* | $\beta_1$ | *P* | $\beta_1$ | *P* | $\beta_1$ | *P* |
| Sex | 0.12 | <.001 | 0.037 | <.001 | 2.38 | <.001 | 0.08 | .41 |
| Age* (years) | 0.043 | <.001 | 0.01 | <.001 | 0.91 | <.001 | -0.27 | <.001 |
| Height (m) | 0.008 | .002 | -0.07 | <.001 | 20.23 | <.001 | -12.46 | <.001 |
| Weight* (kg) | 0.04 | <.001 | 0.015 | <.001 | -0.59 | <.001 | 0.73 | <.001 |
| Current smoker | 0.041 | <.001 | 0.015 | <.001 | -0.11 | .55 | 0.49 | <.001 |
| Pack-Years 1-10 | 0 | .56 | 0 | .75 | 0.09 | .48 | -0.04 | .63 |
| Pack-Years 10-20 | 0.017 | <.001 | 0.007 | <.001 | 0.13 | .43 | 0.21 | .045 |
| Pack-Years 20+ | 0.059 | <.001 | 0.021 | <.001 | -0.12 | .57 | 0.79 | <.001 |

***Table 5.5*** *- Multivariable linear regression for bronchial parameters. The adjusted $R^2$ values and F statistic P values are shown for the overall model. For each independent variable, the coefficients are shown with their corresponding P values. β = slope, LA = luminal area, Pi10 = square root of the wall area of a hypothetical airway with an internal perimeter of 10 mm, WT = wall thickness. * Per 10-unit increase.*

## Discussion

To determine the distribution and influencing factors of bronchial parameters in individuals with normal lung function, we measured the airways of 8869 participants of the Imaging in Lifelines study. We found that male participants had thicker bronchial walls and wider bronchial lumens than female participants (wall thickness [WT]: 1.03 mm ± 0.05 vs 0.98 mm ± 0.05, P < .001; luminal area [LA]: 29.76 mm2 ± 5.79 vs 25.40 mm2 ± 4.66, P < .001), and this difference remained after accounting for age, height, weight, and smoking status. With aging, there was a small but steady increase in WT (β = 0.01 mm per 10 years; P < .001) and LA (β = 0.91 mm2 per 10 years; P < .001), which was also reflected in a higher square root of the bronchial wall area of a hypothetical airway with an internal perimeter of 10 mm (β = 0.043 mm per 10 years; P < .001). Previous studies that investigated CT-derived bronchial parameters in a healthy group have included healthy individuals primarily as a control group for respiratory disease cohorts[124]. These studies report inconsistent findings regarding bronchial parameters, with some suggesting thinner airway walls in male participants[27] and others showing thicker walls[25,85,134] or no difference[135]. However, our study in a much larger cohort of 8869 individuals with healthy lungs from the general population now provides evidence that men have higher wall thickness compared with women, even when accounting for age, height, weight, and smoking history. The discrepancies observed in previous studies may be attributed to the variation in method, scale, and differential impact of physical characteristics on different bronchial parameters[124]. Our analysis revealed that sex, age, height, weight, and smoking history explain some of the variation in wall area percentage and LA ($R^2$ range = 0.104–0.207; P < .001) and accounted for almost half of the explained variation of the WT and Pi10 distributions ($R^2$ range = 0.412–0.465; P < .001). Aging was related to small increases in LA and WT, resulting in an increased Pi10, but showed no evidence of an influence on wall area percentage. The increase in LA could be due to parenchymal changes of the aging lung, namely loss of elasticity[136,137] and reduction in density[138,139]. This change in increased airspace has been noted on histology and micro-CT of donor lungs[140]. The findings are similar to a recent investigation[26] of the aging airway morphologic structure in 431 participants who never smoked, which found an LA increasing with aging in male participants. Although the authors did not find the same association in female participants, our findings in a larger study sample support that age-related changes are present in both sexes. This result has also been observed in a past study; however, the study sample was primarily heavy smokers recruited for a lung cancer screening trial[75]. Moreover, we found that height and weight exerted an influence on bronchial parameters. Height demonstrated a positive correlation with Pi10 and LA. Meanwhile, weight exhibited positive associations with Pi10, WT, and wall area percentage but showed a negative correlation with LA. The results reinforce the importance of considering sex, age, and height in the evaluation of bronchial parameters. This study had several limitations. First, the study sample examined in the ImaLife study represents a specific population from the northern provinces of the Netherlands, primarily composed of White individuals who were taller compared with most countries. Second, the segmentation methods and scan protocols used may influence bron-

chial parameters, which may have contributed to potential inconsistencies in comparisons between studies. Last, the non-systematic nature of the image review beyond lung nodules and emphysema may have resulted in the retention of a small number of participants with undiagnosed or subtle respiratory conditions, particularly if findings at CT were not extensive. This factor should be considered when interpreting the findings. Bronchial parameters not only provide insights into airway morphologic structure in the context of screening and diagnosis but also have potential therapeutic applications, as shown by their capacity to gauge treatment response in respiratory illnesses after intervention[45,141,142]. Previous research also highlighted bronchial parameters as measures of improvement after smoking cessation in individuals with chronic obstructive pulmonary disease[18,143]. However, confounding factors such as sex, age, and height have sometimes been overlooked in studies measuring bronchial parameters. Our findings emphasize the importance of these factors, suggesting their integration could enhance bronchial parameter sensitivity in clinical applications. Overall, this study examined the distribution of CT-derived bronchial parameters in a large healthy Dutch cohort. In healthy individuals, bronchial parameters differed by sex, height, weight, and smoking history. Male sex and increasing age were associated with wider lumens and thicker walls. The reference equations and percentile values provided in this study could be used as a benchmark for assessing the bronchial parameter for an individual stemming from a population similar to our study sample and identify deviations from normal values. Future research of bronchial parameters is needed in diverse populations in other countries as well as standardization of bronchial parameter calculation methods.

# CHAPTER 6

## CT-DERIVED TOTAL AIRWAY COUNT IN LUNG-HEALTHY AND UNHEALTHY INDIVIDUALS FROM A GENERAL POPULATION: INSIGHTS FROM THE IMAGING IN LIFELINES STUDY

I. Dudurych • M. van Tuinen • A. Garcia-Uceda • G. Sidorenkov

M. van den Berge • M. de Bruijne • R. Vliegenthart

*Submitted*

## Abstract

### Purpose

Total airway count (TAC) is a CT-based metric for evaluating respiratory anatomy, but its association with age, sex, anthropometric factors, and spirometry results is unclear. We investigated these relationships in a general population sample comprising lung-healthy and unhealthy individuals.

### Materials and Methods

We included 11,056 low-dose CT scans from the ImaLife study. Participants were stratified into lung-healthy/-unhealthy based on spirometry, imaging, and history of respiratory disease. TAC, wall area percent (WAP), luminal area (LA) and Pi10 were automatically calculated. We used multivariate linear regression and area under receiver operator characteristic curve (AUC) analysis. Spirometry thresholds for AUC analysis were defined as forced expiratory volume in the first second ($FEV_1$)/forced vital capacity (FVC) ratio<0.7 and/or $FEV_1$ percent predicted<80%.

### Results

Among participants, 8,561 (77%) were lung-healthy (mean age 60.4±10 years, 44.9% men) and 2,495 (23%) were lung-unhealthy (61.7±10.4 years, 42.6% men). TAC averaged 172±33 in lung-healthy and 161±36 in lung-unhealthy individuals (p<0.001). Age, male sex, and height were associated with higher TAC values, explaining 19% of its variance in those with normal and 10% in those with impaired lung-health. The discriminatory ability of TAC for spirometry outcomes (AUC 0.73 for $FEV_1$/FVC% and 0.75 for $FEV_1$% predicted) was comparable to WAP and LA.

### Conclusions

Higher age, larger height and male sex are associated with increased total airway count, both in individuals with normal and impaired lung health. Lower TAC values are associated with reduced lung function similarly to WAP and LA, whereas TAC is easier to obtain.




## Introduction

Respiratory diseases such as chronic obstructive pulmonary disease (COPD) often involve airway abnormalities. Clinically, these respiratory diseases are characterized by lung function impairment, which for decades has been measured by spirometry. While invaluable towards measuring the severity of airflow obstruction, spirometry does not provide insights into regional airway anatomy and remodelling at early stages of disease. Recent research exploring the initiation and progression of COPD shows abnormalities and pruning of smaller airways, even before the onset of symptoms or airflow obstruction at spirometry [20,140]. Given these findings, an objective assessment through CT imaging may enhance our understanding of early-stage airway changes, which are crucial for timely intervention.



Thoracic CT scans provide volumetric imaging of the lungs that enables the evaluation of the parenchyma and airways. The scans can be processed to segment the airway lumen and walls from which bronchial parameters can be calculated. Bronchial parameters such as luminal area (LA), wall area percent (WAP) and wall thickness have previously been shown to correlate with spirometry results, and show promise for the assessment of early disease, monitoring of treatment response and differentiation of disease phenotypes [87,90,91,131]. In addition to direct measurements of airway lumen and wall, other information can be extracted from the airway segmentations, for example the count of the total number of airway branches segmented – also called total airway count (TAC). Recent studies have linked a decline in TAC to lung function impairment and respiratory symptoms in smokers and COPD patients [18] with lower values predicting development of COPD [130] and asthma severity [144]. The extent to which factors like age, sex, height, and weight impact TAC in the general population is yet unexplored. Since these are standard factors that should be taken into account for a proper interpretation of lung function measurements [145], we would anticipate them to also influence TAC measurements derived from thoracic CT.

Our study aims to expand current knowledge on TAC by evaluating measurements in a general population, assessing its relationship with general characteristics, and comparing its efficacy with established CT-based bron-

chial parameters in predicting lung function impairment. We investigate the relationship of TAC with age, sex, height, weight, and smoking status - both in those with normal and impaired lung-health. In addition, we assess the discriminatory ability of TAC for reduced lung function compared to established CT-based bronchial parameters.

## Methods

### Study and Participants

Analysis was performed on scans from the prospective Imaging in Lifelines (ImaLife) study, which was approved by the local medical ethics committee, and registered with the Dutch Central Committee on Research Involving Human Subjects (https://www.toetsingonline.nl, Identifier: NL58592.042.16). All participants gave informed consent for participation.

ImaLife is part of Lifelines. Lifelines is a multi-disciplinary prospective population-based cohort study examining in a unique three-generation design the health and health-related behaviours of 167,729 persons living in the North of the Netherlands. It employs a broad range of investigative procedures in assessing the biomedical, socio-demographic, behavioural, physical and psychological factors which contribute to the health and disease of the general population, with a special focus on multi-morbidity and complex genetics [120]. In ImaLife, we included individuals participating in Lifelines when they met the following criteria: age 45 years and older and available spirometry data from the second Lifelines round. These individuals were invited to undergo low-dose thoracic CT scanning, which was performed between May 2017 and October 2022 in 12,041 participants. The full study design including population details has been previously published [32].



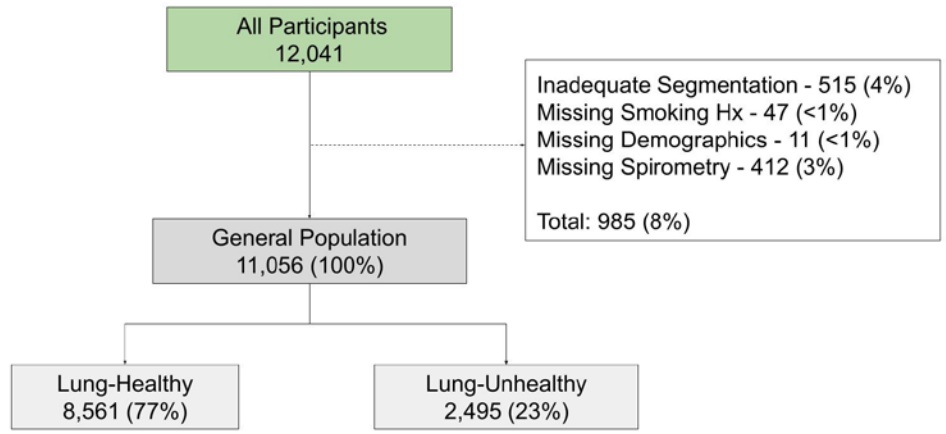


***Figure 6.1*** *- Flowchart for participant inclusion, exclusion, and group division for this study. Hx – History.*



We split the participants into "lung-healthy" and "lung-unhealthy" subgroups. Individuals with imaging signs of pulmonary illness, a self-reported history of pulmonary disease, medication use for respiratory issues or abnormal spirometry according to the lower-limit of normal for Forced Expiratory Volume in the first second of expiration ($FEV_1$) percent predicted (PP) or $FEV_1$/Forced Vital Capacity (FVC) were assigned to the "lung-unhealthy" group. The full details of criteria for study inclusion/exclusion and subgroup stratification are provided in Supplemental Document 6.1.

### Image Acquisition and Analysis

The ImaLife scan protocol included a low-dose non-contrast volumetric CT scan of the thorax at full inspiration with the participants in supine position, using a third-generation dual-source CT scanner (SOMATOM Force, Siemens Healthineers, Germany). For bronchial segmentations, images were reconstructed using Qr59 (hard-quantitative) kernel. Reconstructed voxel size was 0.68x0.68mm and slice increment was 0.7mm.

| | Lung-Healthy | Lung-Unhealthy | p-value |
|---|---|---|---|
| **Participants** | 8,561 (77.4%) | 2,495 (22.6%) | |
| **Age (years)** | 60.4±10.0 | 61.7±10.6 | 0.14 |
| **Height (m)** | 1.74±0.09 | 1.74±0.09 | 0.7 |
| **Weight (kg)** | 79.7±14.1 | 79.2±14.7 | 0.41 |
| **Smoking status†** | | | <0.001 |
| **Never-smoker** | 3,560 (41.6%) | 849 (34.0%) | |
| **Ex-Smoker** | 3,828 (44.7%) | 1,129 (45.3%) | |
| **Current-Smoker** | 1,173 (13.7%) | 517 (20.7%) | |
| **Pack-Years*** | 11.7±10.7 | 14.9±12.9 | <0.001 |
| **$FEV_1$ PP (%)** | 100.1±12.4 | 89.9±14.9 | <0.001 |
| **$FEV_1$/FVC** | 0.76±0.05 | 0.67±0.08 | <0.001 |
| **TLV (L)** | 5.36±1.21 | 5.62±1.24 | <0.001 |
| **Pi10 (mm)** | 3.56±0.16 | 3.61±0.17 | <0.001 |
| **WAP (%)** | 47.26±3.36 | 48.91±3.55 | <0.001 |
| **LA ($mm^2$)** | 27.3±5.6 | 25.8±5.7 | <0.001 |
| **TAC (N)** | 172±33 | 161±36 | <0.001 |

***Table 6.1 -*** *Population demographics by lung health status. $FEV_1$ - Forced Expiratory Volume in the first second, FVC – Forced Expiratory Volume, $FEV_1$ PP – $FEV_1$ Percent Predicted, TLV – Total Lung Volume, Pi10 – Square root of the wall area of a hypothetical airway with an internal perimeter of 10mm, WAP – Wall Area Percent, TAC – Total Airway Count. † p-value for overall chi-squared test for smoking status groups. * pack-years for ever-smokers.*

Scans were automatically processed to calculate TAC. The airway lumen was extracted using a 3D-Unet , which was refined and validated on ImaLife data as previously described [96,115,133]. Participants with inadequate airway segmentation based on automated measures of airway completeness and visual assessment were excluded. Individual airway branches were automatically identified by detecting branching points along the airway tree, similarly to the previously published methods in the EXACT'09 challenge [92]. TAC was calculated by counting all separate branches that were >2mm in length within an airway tree.



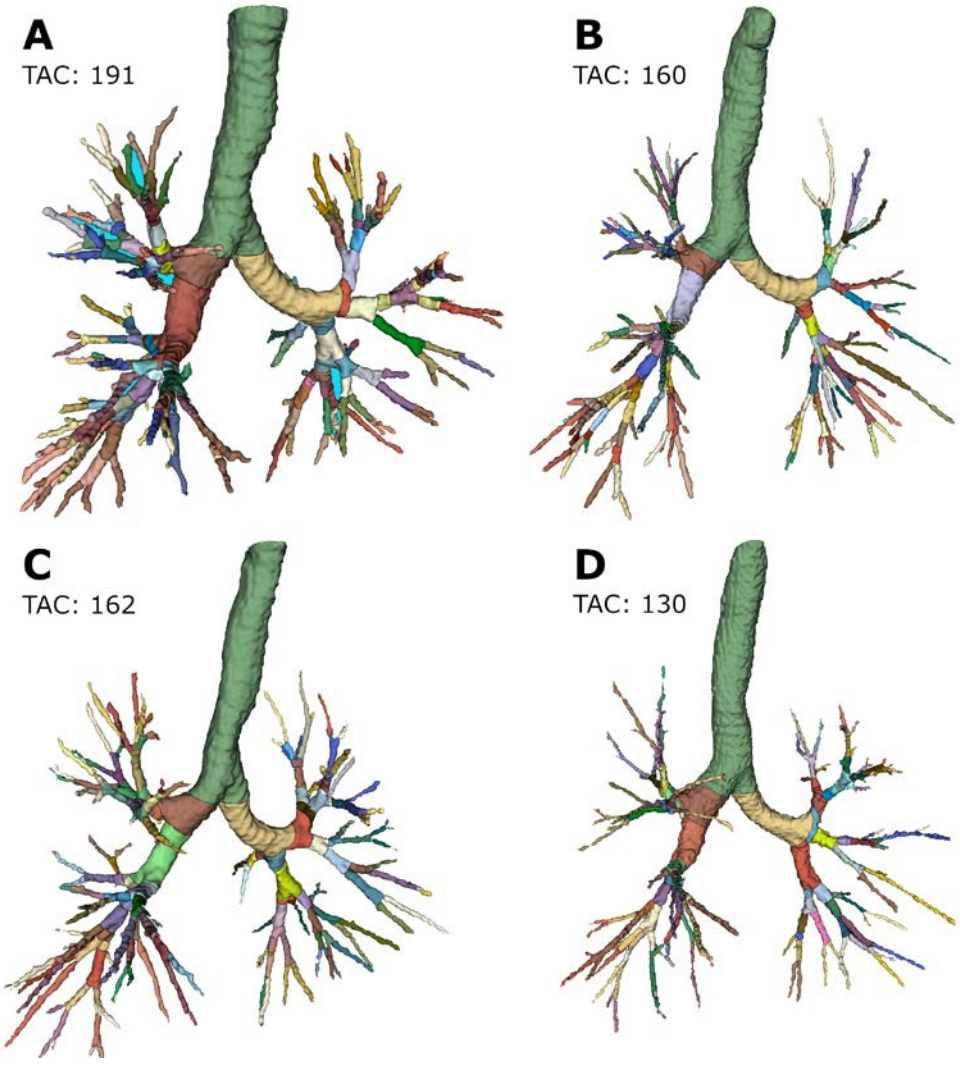


***Figure 6.2*** *Rendering of a segmented airway tree. Each branch is separately indexed and randomly coloured. Branches of less than 2mm in length were excluded from the total airway count. A) Healthy man with average TAC. B) Average unhealthy man. C) Average healthy woman. D) Average unhealthy woman. TAC – Total airway count.*

Wall area percentage (WAP) was determined by calculating the ratio of the wall area to the total cross-sectional area of the airway. Similarly, luminal area (LA) was defined as the cross-sectional area within the lumen. These calculations were averaged for branches within the 3rd to 6th generations to ensure consistency [133]. Pi10, which represents a summary index of airway wall thickness, was determined through regression analysis. Specifically, we plotted the square root of the airway wall area (WA) against the internal

perimeter (Pi) of airway branches, spanning from 0-6th generation. This linear regression provided an intercept that corresponds to the square root of WA when Pi is 10 mm. This is referred to as Pi10 [17].

## Statistical Analyses

Student's independent t-test was used to compare the group means of bronchial parameters by lung health status and by sex. Differences in smoking status between lung-healthy and was tested using the Chi-squared test. To assess the strength and direction of association of age, sex, height, weight, smoking status and smoking pack-year history with TAC we used univariable linear regression and calculated the slope (β), significance (p-value) and Coefficient of Determination ($r^2$). Multivariate linear regression was used to assess the associations between independent variables and TAC. Initially, we selected these independent variables based on their significance in univariable analyses and subsequently refined the model using a forward stepwise approach, which eliminated nonsignificant variables ($p>0.05$). The $r^2$ reflects the proportion of variance in the dependent variable predicted from the independent variable. It indicates the tightness of data around the regression line; low $r^2$ suggests considerable spread in the data. The slope (β) from the regression, despite significant scatter, provides insight into the association between variables, which, even if slight, can contribute meaningfully when combined with other predictors in multivariate models.

We applied multivariate linear regression to elucidate the associations of age, sex, height, weight, pack-years, and bronchial parameters with spirometry outcomes, namely $FEV_1$/FVC and $FEV_1$ PP. These analyses were performed separately for the lung-healthy and unhealthy groups. Beginning with a forward stepwise regression model incorporating age, sex, height, weight, and pack-years, we established a base model for testing the associations with the continuous spirometry results. Subsequently, in separate models, we individually added each bronchial parameter—WAP, LA, Pi10, or TAC—to this base model to assess their additional explanatory value. We assessed the model explanatory value by examining the adjusted $R^2$ values and model fit by comparing the Bayesian Information Criterion (BIC) between the addition of TAC to the base model versus other bronchial parameters added to the base model. Significance of the overall model was evaluated by the F-statistic and associated p-value. The F-statistic determines the significance of the variables combined impact in explaining variance. Alpha was set to 0.05 for significance.

To evaluate how well TAC, WAP, LA, and Pi10 discriminate between participants with or without an $FEV_1$/FVC ratio <0.7 or $FEV_1$ PP <80%, we evaluated two multivariate logistic regression models using a stratified 5-fold cross-validation approach. The dataset was segmented into five equal-sized folds, ensuring a representative distribution of outcome classes in each with implementation of data balancing techniques. In each successive iteration, four folds served as the training set, while the remaining fold was used as the validation set. Initially, we included age, sex, height, weight, and pack-years in the base model, followed by the inclusion of one of the bronchial parameters. For each model, we calculated the area under the curve (AUC) of the receiver operating characteristic (ROC) plots to quantify their discriminatory ability. Optimal thresholds for sensitivity/specificity were obtained from the ROC results using Youden's J statistic.

| | Lung-Healthy $R^2$ 0.187 | | | Lung-Unhealthy $R^2$ 0.096 | | |
|---|---|---|---|---|---|---|
| | $\beta_1$ | $\beta_1$-norm | p-val | $\beta_1$ | $\beta_1$-norm | p-val |
| **Sex** | 8.42 | 0.031 | <0.001 | 9.27 | 0.035 | <0.001 |
| **Age*** | 10.04 | 0.190 | <0.001 | 7.77 | 0.132 | <0.001 |
| **Height** | 95.64 | 0.263 | <0.001 | 55.67 | 0.141 | <0.001 |
| **Weight*** | -2.18 | -0.116 | 0.04 | -0.07 | -0.036 | 0.26 |
| **Pack-Years** | | | | | | |
| **1-10** | 0.63 | 0.002 | 0.42 | -3.88 | -0.011 | 0.35 |
| **10-20** | 2.09 | 0.008 | 0.04 | -1.15 | -0.005 | 0.62 |
| **20+** | 6.77 | 0.022 | <0.001 | -0.06 | -0.001 | 0.97 |

***Table 6.2 -*** *Multivariable model for total airway count (TAC) with the independent variables sex (0 if woman, 1 if man), age, height, weight, and pack-years (categorised). $\beta_1$ - variable coefficient (normalised). * - per 10-unit increase.*

# Results

## Participants

Of 12,041 processed scans, 985 were excluded due to inadequate segmentation or missing data (Figure 6.1). From the remaining 11,056 participants 8,561 (77%) were lung-healthy, and 2,495 (23%) lung-unhealthy. For the overall population, means and standard deviations for age, height and weight were 61.3±10.5 years, 1.74±0.09m and 79.5±14.1kg respectively (Table 6.1). Spirometry measures for lung-healthy and unhealthy groups were $FEV_1$/FVC of 0.76±0.05 and 0.67±0.08 and $FEV_1$ PP 100.1±12.4 ($p<0.001$) and 89.9±14.9 ($p<0.001$) respectively. Significant differences existed between men and women in both lung-healthy and lung-unhealthy groups for mean age, height, weight, pack-years, $FEV_1$, FVC and CT-derived total lung volume and bronchial parameters ($p<0.001$) (Table S6.1).

## Participant Characteristics and TAC

Exemplary airway segmentations for male and female participants is shown in Figure 6.2. Mean TAC was 172±33 in the lung-healthy and 161±36 in the unhealthy subgroup ($p<0.001$). Male sex was associated with higher TAC values, both in lung-healthy (183±34 vs 163±30, $p<0.001$) and lung-unhealthy subjects (167±38 vs 155±31, $p<0.001$). In univariable analysis, higher age, height, and number of pack-years were associated with increased TAC values in lung-healthy men and women (Table S6.2). In the lung-unhealthy group, similar significant associations were observed for age and pack-years in both sexes, with larger height additionally showing a significant association with higher TAC in women, but not in men. Multivariate analyses demonstrated that demographic factors together explained 18.7% and 9.6% of the variation in TAC in lung-healthy and lung-unhealthy subjects respectively (Table 6.2). In both subgroups, sex, age, and height significantly contributed to the explained variance of TAC ($p<0.001$), with height being the most influential factor (norm-$\beta_1$ 0.263, 0.141 for lung-healthy and unhealthy individuals respectively). Although a higher number of pack-years was associated with increased TAC in lung healthy individuals, it only explained a small part



| | A: $FEV_1$ PP Prediction | | | | |
|---|---|---|---|---|---|
| | **Base** | **WAP** | **LA** | **Pi10** | **TAC** |
| | | | **Healthy** | | |
| **Adj-$R^2$** | 0.055 | 0.158 | 0.161 | 0.055 | 0.142 |
| **ΔBIC** | 0 | -1023.2 | -1063.1 | -4.2 | -868.3 |
| **F-Stat** | 75.42 | 239.2 | 245.8 | 87.4 | 185.0 |
| | | | **Unhealthy** | | |
| **Adj-$R^2$** | 0.071 | 0.189 | 0.155 | 0.081 | 0.196 |
| **ΔBIC** | 0 | -285.7 | -196.5 | -14.1 | -295.9 |
| **F-Stat** | 24.2 | 100.3 | 66.4 | 32.2 | 74.3 |

| | B: $FEV_1$/FVC Prediction | | | | |
|---|---|---|---|---|---|
| | | | **Healthy** | | |
| **Adj-$R^2$** | 0.140 | 0.225 | 0.214 | 0.141 | 0.196 |
| **ΔBIC** | 0 | -935.9 | -935.9 | -13.5 | -611.8 |
| **F-Stat** | 207 | 325.4 | 346.9 | 184 | 273.5 |
| | | | **Unhealthy** | | |
| **Adj-$R^2$** | 0.219 | 0.304 | 0.273 | 0.227 | 0.309 |
| **ΔBIC** | 0 | -247.8 | -154.8 | -23.2 | -254.0 |
| **F-Stat** | 85.2 | 117.7 | 101.4 | 90.8 | 118.8 |

***Table 6.3 -*** *A) Comparison of multivariable models to examine factors explaining variance in Forced Expiratory Volume in 1 second ($FEV_1$) Percent Predicted (PP). B) Comparison of multivariable models to examine factors explaining variance in Forced Expiratory Volume in 1 second ($FEV_1$) / Forced Vital Capacity (FVC). Adjusted $R^2$ indicates the effectiveness of the model by quantifying the variance it explains, the difference in Bayesian Information Criteria (ΔBIC) assesses model fit, with lower values indicating a better fit. The F-statistic determines the significance of the variables combined impact in explaining variance, where all models in this study demonstrated significance with p-values <0.001. Base model: sex, age, height, weight, pack-years. WAP - Wall Area Percent, LA - Luminal Area, Pi10 - Square Root of the Wall Area of a hypothetical airway with an internal perimeter of 10mm, TAC - Total Airway Count.*

of its variance (Figure 6.3). While ex-smokers and current-smokers had slightly higher values of TAC in both lung-healthy and lung-unhealthy groups (Table S6.2) smoking status did not contribute to explained variance in the multivariable models. For unhealthy participants weight and pack-years no longer contributed significantly to TAC's explained variance.

| Model | $FEV_1$/FVC < 0.7 | | | | $FEV_1$ PP < 80% | | | |
|---|---|---|---|---|---|---|---|---|
| | *AUC* | *95% CI* | *Sens.* | *Spec.* | *AUC* | *95% CI* | *Sens.* | *Spec.* |
| **Base** | 0.67 | [0.65-0.70] | 0.58 | 0.69 | 0.63 | [0.61-0.64] | 0.47 | 0.75 |
| **TAC** | 0.73 | [0.72-0.75] | 0.64 | 0.72 | 0.75 | [0.73-0.78] | 0.70 | 0.70 |
| **WAP** | 0.72 | [0.71-0.74] | 0.67 | 0.67 | 0.74 | [0.73-0.77] | 0.73 | 0.66 |
| **LA** | 0.73 | [0.72-0.74] | 0.66 | 0.69 | 0.73 | [0.72-0.75] | 0.73 | 0.63 |
| **Pi10** | 0.68 | [0.67-0.71] | 0.65 | 0.63 | 0.64 | [0.63-0.66] | 0.42 | 0.80 |
| **All BPs** | 0.75 | [0.74-0.76] | 0.66 | 0.71 | 0.77 | [0.75-0.79] | 0.71 | 0.71 |

***Table 6.4 -*** *Multivariable logistic regression models for discriminating reduced spirometry outcomes. Base model incorporates age, height, weight, sex and pack-years. AUC – receiver operator characteristic area under the curve, BPs – bronchial parameters, $FEV_1$ - forced expiratory volume in the 1st second of expiration, FVC – forced vital capacity, $FEV_1$ PP – $FEV_1$ percent predicted, LA – luminal area, TAC – total airway count, WAP – wall area percent.*

## TAC and Spirometry Relationships

In the lung-healthy group, LA was most strongly associated with $FEV_1$ PP, explaining 16% of the variance. Addition of LA to the model demonstrated a substantial improvement in fit compared to the base model (decrease in Bayesian Information Criterion [ΔBIC], -1063), surpassing the improvement seen with the addition of TAC to the base model (ΔBIC, -868) (Table 6.3A). The strongest association for $FEV_1$/FVC in the lung-healthy group was seen with WAP ($R^2$ = 0.225). In the unhealthy subgroup, TAC has a strong association with $FEV_1$ PP, explaining 19% of the variance, and the greatest association to $FEV_1$/FVC ratio among the bronchial parameters, explaining 31% of the variance (Table 6.3B). In the lung-unhealthy subgroup, TAC was more strongly associated to $FEV_1$/FVC than both Luminal Area (LA) and Wall Area Percent (WAP). A TAC increase of 100 was associated with absolute increases in $FEV_1$ PP of 12% in the lung-healthy subgroup and 15% in the unhealthy subgroup ($p<0.001$), and 0.04-point and 0.08-point increase in the $FEV_1$/FVC ratio, respectively ($p<0.001$) (Table S6.3).

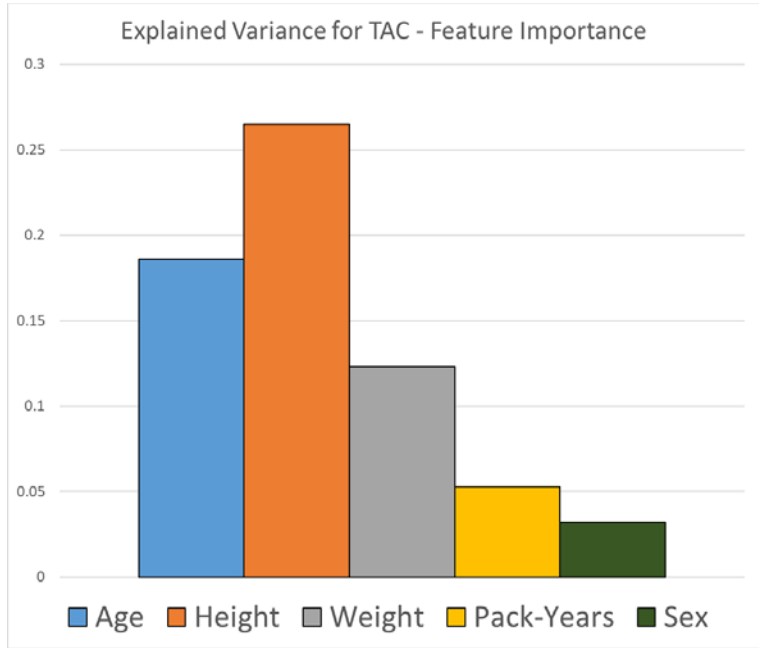


***Figure 6.3 -*** *Feature importance of each independent variable in contributing to the explained variance of TAC in the lung-healthy group.*

In ROC analysis, models including WAP, LA, or TAC had better discriminatory ability for abnormal spirometry result than the base model and Pi10 model (Figure 6.4). The model incorporating TAC achieved an AUC of 0.73 (95% CI [0.72-0.75], sensitivity=0.64, specificity=0.72) for reduced $FEV_1$/FVC, compared to AUC of 0.67 for the base model (95% CI [0.66-0.70], sensitivity=0.58, specificity=0.69) (Table 6.4). The model that included all bronchial parameters had AUC of 0.75 (95% CI [0.74-0.76]). For reduced $FEV_1$ PP, the TAC model showed similar discriminatory performance with an AUC of 0.75 (95% CI [0.73-0.78]), again higher than the base model (AUC 0.63, 95% CI [0.61-0.64]) (Figure 6.4A). For reduced $FEV_1$ PP, all models except base and Pi10 had higher sensitivity (range, 0.70-0.73) than for $FEV_1$/FVC prediction, at comparable specificity (range, 0.63-0.80).

## Discussion

This study investigates automatic Total Airway Count (TAC) from low-dose chest CT scans and demonstrates how TAC correlates with other bronchial parameters and lung function impairment. We demonstrate that age, weight, pack-years and sex are factors that affect TAC measures in the general population, and should be taken into account for proper interpretation, similar to other, established, lung function measurements. Our findings demonstrate the clinical relevance of chest CT-based TAC as lower TAC values were associated with reduced lung function. TAC outperformed Pi10 and showed similar discriminative ability compared to other CT-based bronchial parameters, that are more difficult to measure, such as luminal area (LA) and wall area percent (WAP).

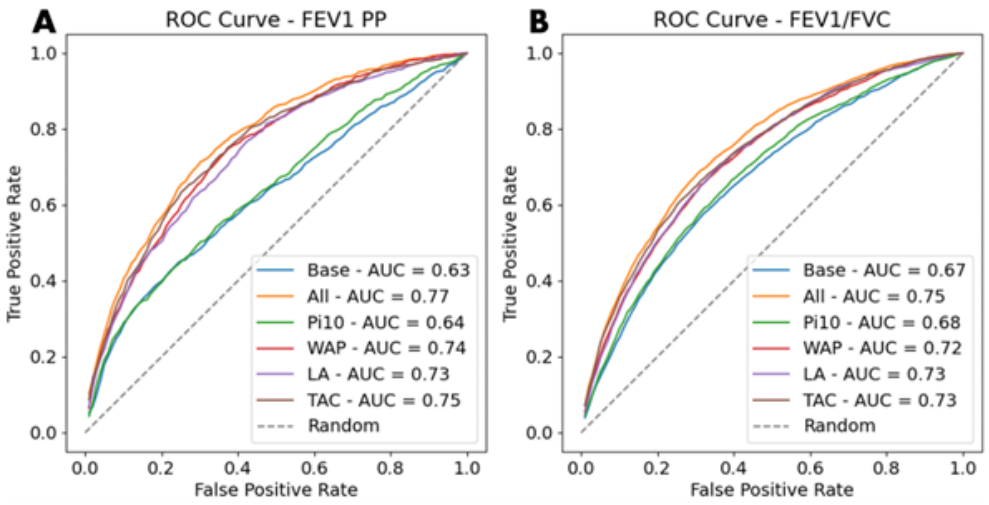


***Figure 6.4 -*** *Receiver Operating Characteristic (ROC) curves for spirometry threshold prediction using multivariable logistic regression with calculated area under the curve (AUC) for the base model (age, height, weight, sex, pack-years), base model with all bronchial parameters (All) and for the base model with the addition of each bronchial parameter separately, namely Pi10, wall area percent (WAP), luminal area (LA) and total airway count (TAC). A) ROC for predicting an $FEV_1$ PP of less than 80%. B) ROC for predicting an $FEV_1$/FVC of less than 0.7.*

TAC has been studied in several smaller cohorts [25,26,146]. Bhatt et al. observed higher TAC in men compared to women within those groups [25] similarly as observed in our study. A difference in TAC by sex was also observed in 431 healthy never-smokers by Terada et al. [26]. The actual TAC values diverge among studies, with an overall mean TAC of 264±128 in the former and 190-210 in the latter study, compared to 172±33 in ours. This difference could be due to several factors. Different scanning protocols, inspiration levels, and software tools can yield varying TAC even on identical scans or with identical patients [146]. As the method to obtain TAC has influence over the final value, clear and standardized methodology is essential when reporting TAC. Studies using AI models for TAC need to reference the training and validation studies or provide comprehensive model cards.

Despite the differences in absolute TAC values between studies, there is consistency in the relationship between TAC and spirometry results. We found that both lung-healthy and lung-unhealthy groups exhibited increased $FEV_1$/FVC ratios with higher TAC (0.04 per 100 TAC increase for lung-healthy and 0.08 per 100 TAC increase for lung-unhealthy). These increments are in line with findings from the COPDGene and CanCOLD studies, which showed a 0.025-0.028 increase in $FEV_1$/FVC and a similar increase in ever-smokers, respectively [25,147]. Furthermore, in our study we demonstrated similar positive increments in $FEV_1$ PP related to higher TAC in both lung-healthy (12.2% per 100 TAC increase) and unhealthy groups (15.0% per 100 TAC increase).

TAC, added to the base model, was strongly associated with spirometry results in the lung-unhealthy subgroup, similar to WAP, and better than LA and Pi10 (providing 30.9% explained variance vs 30.4%, 27.3%, 22.7% respectively). In the lung-healthy group, TAC outperformed Pi10 but WAP and LA provided slightly better insights in this case (explained variance of 19.6% vs 14.1%, 22.5%, 21.4% respectively). In addition, among bronchial parameters, TAC provided discriminative ability for reduced $FEV_1$/FVC and $FEV_1$ PP (AUC 0.73 and 0.75 respectively), similar to WAP (AUC of 0.72 and 0.74 respectively), and better than LA and Pi10. The increased association of TAC with spirometry values in the unhealthy group likely stems from disease-related variation, such as emphysema, fibrosis, and mucus build-up [148], which causes both genuine airway loss and complexities in segmentation. For example, a decrease in LA is associated with reduced TAC in COPD patients [90]. This decrease signifies a narrower airway, the typical segmentation target, making accurate CT-based evaluation of small airways more difficult [149]. Notably, a decrease in detectable airway branches may occur without actual physical loss. TAC reflects the number of branches segmentable by CT, not their true quantity [150]. Additionally, TAC tends to rise with age in healthy individuals, possibly due to increasing LA and other age-related changes in bronchi [26,135–137]. Interest-

ingly, high pack-years slightly elevated TAC in lung-healthy people, a trend also noted in smokers from the Bhatt et al. study [25]. Smoking-related damage, initially to the smallest airways not visible on CT, may cause airway enlargements that become detectable, offering a potential explanation for this rise in TAC [151]. Future research should further illuminate these phenomena through longitudinal TAC analysis.

Using CT-based measures of the airways for diagnosis or monitoring of respiratory health has been of interest for several years. For the most part, this has involved manual or semi-automated measures of the airway lumen and occasionally the airway wall, from which bronchial parameters such as WAP, LA, and Pi10 can be calculated [124]. This process demands comprehensive segmentation of the airway tree, with precise demarcation of the airway lumen, wall, and adjacent parenchyma. Low-dose scans complicate matters as noise and partial volume effects can obscure the interfaces in smaller branches. TAC sidesteps the need for detailed measurements of lumen and wall, requiring only an overall segmentation of the airway tree. TAC offers ease of calculation, particularly when traditional measurement methods are not suited for specific datasets or protocols, leading to imprecise lumen and wall definitions. Additionally, TAC values can be readily visualized with airway tree renderings, providing a clearer representation compared to subtle variations in airway dimensions. Yet, the utility of TAC is hindered by its varying measurement methods across studies, influenced by differences in scanning and segmentation techniques. Moreover, TAC visualizations, while clear, do not readily explain the origins of airway loss. To overcome these limitations, a unified methodology across studies should be encouraged, which might encompass the use of an imaging phantom designed explicitly for airway counting methods. Establishing standardized protocols would enhance TAC's comparability and interpretability, thereby strengthening its role in respiratory health assessment.

This study has several strengths. Encompassing a large and representative sample size of 11,055 participants, it offers an extensive analysis of bronchial parameters within the lung-healthy and lung-unhealthy general population. The inclusion of a large sample, including 77% healthy individuals, allows for a detailed examination of TAC, with adjustments for potential confounders such as sex, age, height, weight, and pack years. This adjustment enables the assessment of the pure role of TAC and a relative exploratory values comparison between WAP, LA, Pi, and TAC in explaining spirometry outcomes. Automated image analysis techniques were adopted in our methodology to ensure efficient measurements across the substantial study sample. This approach minimizes potential variance and bias that could originate from manual reader measurements.

There are a few limitations for consideration regarding the findings of this study. Firstly, the generalizability of the findings may be limited to populations like those included in the ImaLife cohort (i.e., Caucasian individuals from the North of the Netherlands) for example the Dutch population is the tallest in the world [152] and our findings strongly link height with TAC. Studies focusing on heterogenous population cohorts and patient groups would be beneficial in exploring potential differences and similarities in TAC. Second, the airway segmentation method does not guarantee complete airway segmentation, as some peripheral branches may be discarded during measurement leading to lower total airway counts than reported in other studies. For cases with an occluded lumen, this could result in exclusion of segmented airways beyond the blockage.

In conclusion, in this general population sample, higher age, larger height and male sex are associated with increased TAC, both in individuals with normal and impaired lung health. Lower TAC values are associated with reduced lung function similarly to WAP and LA, whereas TAC is easier to obtain.

# CHAPTER 7

## CT-BASED AIRWAY CHANGES AFTER SMOKING CESSATION IN THE GENERAL POPULATION

I. Dudurych • G. Sidorenkov • Marcel van Tuinen • D.J. Slebos

G. H. de Bock • M. van den Berge • M. de Bruijne • R. Vliegenthart

*Submitted*

## Abstract

### Purpose

Previous research has demonstrated improvements in CT-derived bronchial parameters in the first years after smoking cessation. This study investigates the association between longer smoking cessation duration and bronchial parameters in lung-healthy and lung-unhealthy ex-smokers from the general population.

### Materials and Methods

We conducted a cross-sectional analysis using low-dose CT scans of ex-smokers with at least 10 pack-years from the Imaging in Lifelines study. We divided them into lung-healthy and lung-unhealthy based on spirometry, self-reported diagnosis or imaging signs of respiratory disease. Bronchial parameters Pi10, wall thickness, luminal area and wall area percent (WAP) were obtained using a previously validated method. Multivariable linear regression adjusted for sex, age, height, weight, and pack-years was performed to assess the independent association of smoking cessation duration with bronchial parameters.

### Results

The study included 1,869 ex-smokers; 1,421 (76%) were classified as lung-healthy (58% men, mean age 64.2±9.8 years, pack-years 16.5 [12.5-23.3], smoking cessation duration 20.0 [14.0-29.0] years) and 448 (24%) as unhealthy (56% men, mean age 66.1±10.5 years, pack-years 18.2 [13.4-25.2], smoking cessation duration 20.0 [13.8-29.0] years). Longer smoking cessation duration was associated with a decrease in WAP for the lung-unhealthy group (-0.528% per 10 years, p=0.005). No significant associations were observed with other bronchial parameters or in the healthy group.

### Conclusions

In individuals with respiratory conditions, longer smoking cessation duration is related to a decrease in wall area percent of the bronchial walls. The results suggest the potential for improvements in airway health when people quit smoking, warranting further investigation with longitudinal studies.




## Introduction

Smoking is widely recognized as the primary cause of chronic obstructive pulmonary disease (COPD), responsible for over 80% of all cases [153]. Prolonged exposure to tobacco smoke leads to persistent irritation and inflammation of the airways, resulting in progressive damage to lung tissue and constriction of the airway passages [154]. The risk of developing COPD is closely associated with the duration and intensity of smoking, with heavier smokers more likely to develop severe forms of COPD [155]. A higher smoking burden results in airway changes, noted on micro-CT and histological analysis of airway remodelling [20]. These airway changes have been found to contribute to worsening symptoms and exacerbations in COPD [147].

Computed tomography (CT) can be used to measure the airways and calculate bronchial parameters to summarise their condition. Deviations from normal values in CT-derived bronchial parameters are often observed in COPD, and correlate with airway obstruction and impaired lung function [87]. Such airway changes can be airway wall thickening and lumen narrowing, reflected by increased wall area percent (WAP) and decreased luminal area (LA) as bronchial parameters in CT. This deviation from normal is also seen in smokers at risk of developing respiratory illness, before the onset of spirometry-evident COPD [24].

In COPD, smoking cessation stands out as an effective intervention to slow down the progression of COPD and improve overall lung health [156]. Quitting smoking has been shown to significantly reduce symptoms, decrease the frequency and severity of exacerbations, and enhance lung function [157]. Notably, ex-smokers experience a slower decline in lung function compared to those who continue smoking. Recent studies investigating changes in airway morphology after smoking cessation show measurable improvements already in a time-span of 1-3 years [18,158], but changes to CT based airway measurements over a longer time after stopping smoking are currently unexplored. Leveraging data from our population-based study, we can capture a valuable cross-sectional snapshot that allows for the identification of associations between smoking cessation duration and CT-derived bronchial parameters.

Our study aims to address the cross-sectional relationship between smoking cessation duration and CT-derived bronchial parameters in ex-smokers from the general population with and without respiratory diseases. We hypothesize that over longer time after smoking cessation, bronchial parameters become less abnormal. By investigating these questions, we hope to gain a

better understanding of the long-term benefits of quitting smoking in relation to airway morphology.

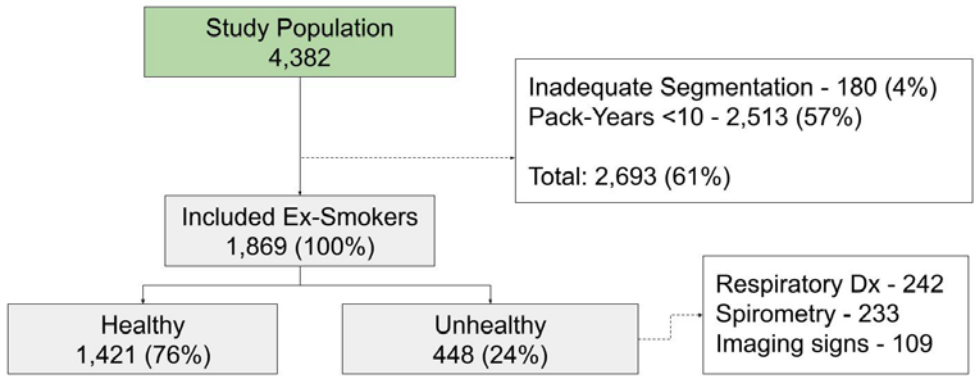


***Figure 7.1 -*** *Participant inclusion flowchart for the study. Dx – diagnosis. Participants in the unhealthy group had one or more of self-reported respiratory diagnosis, abnormal spirometry, or imaging signs of respiratory illness.*

| | Healthy | Unhealthy | p-value |
|---|---|---|---|
| **Participants** | 1,421 (76%) | 448 (24%) | |
| **Sex (M/F)** | 822/599 | 250/198 | |
| **Age (years)** | 64.3±9.9 | 66.1±10.5 | <0.001 |
| **Height (m)** | 1.75±0.09 | 1.75±0.09 | 0.57 |
| **Weight (kg)** | 83.6±13.7 | 81.6±13.6 | 0.008 |
| **Pack-Years** | 16.5 [12.5-23.3] | 18.2 [13.4-25.2] | 0.023 |
| **SCD (years)** | 20.0 [14.0-29.0] | 20.0 [13.8-29.0] | 0.76 |
| **$FEV_1$ PP (%)** | 99.0±12.4 | 88.4±14.3 | <0.001 |
| **$FEV_1$/FVC** | 0.75±0.05 | 0.67±0.09 | <0.001 |
| **TLV (L)** | 5.57±1.19 | 5.74±1.2 | 0.009 |
| **Pi10** | 3.63±0.16 | 3.67±0.17 | <0.001 |
| **WT (mm)** | 0.99±0.05 | 1.01±0.06 | <0.001 |
| **LA ($mm^2$)** | 23.7±4.7 | 22.5±4.6 | <0.001 |
| **WAP (%)** | 49.8±3.3 | 51.3±3.4 | <0.001 |

***Table 7.1*** *- Population demographics split by health status. SCD – Smoking Cessation Duration, $FEV_1$ - Forced Expiratory Volume in the first second, FVC – Forced Expiratory Volume, $FEV_1$ PP – $FEV_1$ Percent Predicted, TLV – Total Lung Volume, Pi10 – Square root of the wall area of a hypothetical airway with an internal perimeter of 10mm, WT – Wall Thickness, LA – Luminal Area, WAP – Wall Area Percent.*



# Methods

## Study and Participants

Participants were included from the Imaging in Lifelines (ImaLife) study, which was approved by the local medical ethics committee, and is registered with the Dutch Central Committee on Research Involving Human Subjects (https://www.toetsingonline.nl, Identifier: NL58592.042.16). Informed consent was obtained from all participants.

The ImaLife study is a part of Lifelines. Lifelines is a multi-disciplinary prospective population-based cohort study examining in a unique three-generation design the health and health-related behaviours of 167,729 persons living in the North of the Netherlands. It employs a broad range of investigative procedures in assessing the biomedical, socio-demographic, behavioural, physical and psychological factors which contribute to the health and disease of the general population, with a special focus on multi-morbidity and complex genetics. [120].

In ImaLife, participants aged 45 years and older who had completed a lung function test during the second round Lifelines assessment were invited to undergo low-dose thoracic CT scanning between May 2017 and October 2022. The complete study design and relevant population details have been previously published [32]. For this sub-study we included ex-smokers with a smoking history of at least 10 pack-years. The 10 pack-year cut-off aligns with epidemiological studies like COPDGene, DLCST and MESA, facilitating comparison of findings [98,159,160]. All ImaLife individuals had undergone spirometry, and spirometry results were compared against the lower-limit of normal for Forced Expiratory Volume in the first second of expiration ($FEV_1$) percent predicted or $FEV_1$/Forced Vital Capacity (FVC). Ex-smoking status was determined from self-reported smoking questionnaires completed closest to the CT scan (on average 2 years prior to CT). The time difference between questionnaire and CT scan results in our dataset consisting of ex-smokers with at least two years of smoking cessation. Participants having scans with inadequate airway segmentation or with incomplete data were excluded. The participants were split into lung-healthy and lung-unhealthy groups, based on self-reported history of pulmonary disease, medication use for respiratory issues and/or abnormal spirometry and/or presence of imaging signs of potential respiratory illness. Spirometry for pulmonary function testing was performed in adherence with American Thoracic Society guidelines, employing the Wellch Allyn SpiroPerfect apparatus (Wellch Allyn version

1.6.0.489, a computer-based SpiroPerfect™ system coupled with CardioPerfect® Workstation software)[161]. The duration of smoking cessation was calculated as the time in years between the age at which they quit smoking, and the age at which the scan was obtained. Detailed inclusion, exclusion criteria and health status assignment are provided in Supplementary Document 7.1.

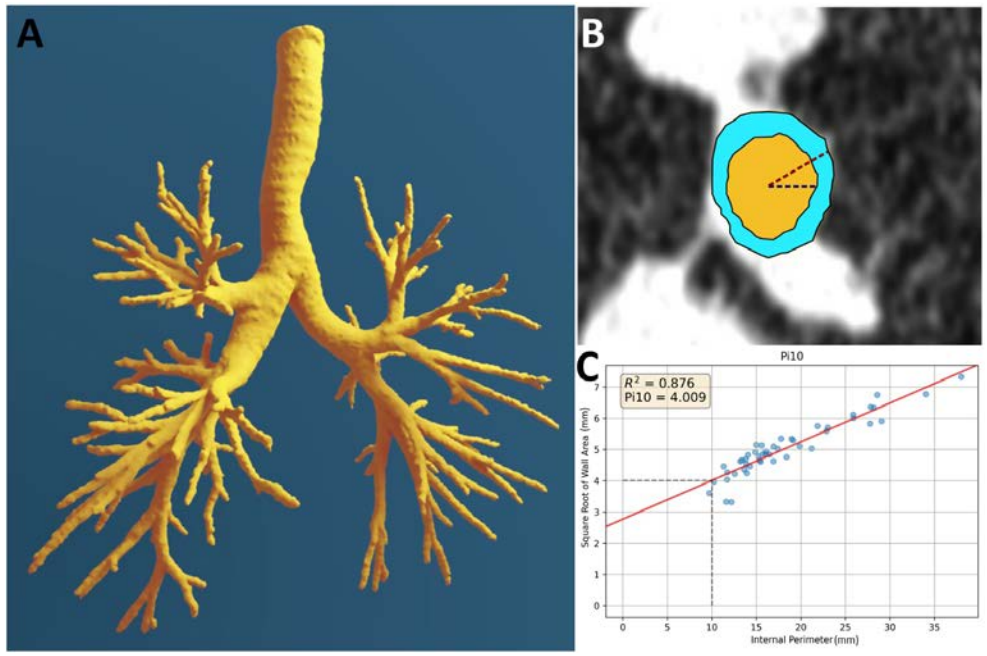


***Figure 7.2 -*** *A) Rendering of an airway segmentation from a 60 y/o lung-healthy male participant. B) Example measurements of lumen radius (blue dashed line) and total radius (red dashed line). C) Graph visualising the calculation of Pi10 for a participant. For all branch measurements between generation 0-6 the square root of the wall area (SRWA) is plotted against the internal perimeter, and linear regression performed. Then, the SRWA is identified at a point where the internal perimeter is 10mm.*

## Image Acquisition

Each participant received a chest CT scan using a low-dose non-contrast volumetric scan protocol, using a third-generation dual-source CT scanner (SOMATOM Force, Siemens Healthineers, Germany). The scans were reconstructed using a kernel (Qr59) designed for quantitative analysis, with a slice thickness of 1mm and a slice increment of 0.7mm.

## Outcomes Definition

The primary outcomes of interest in this study were CT-derived bronchial parameters. The bronchial parameters were calculated through automated processing of the scans. Initially, a 3D-Unet was used to extract the airway lumen [96]. Then, an optimal-surface graph-cut method was employed to segment and refine the airway wall [115]. The reliability of this pipeline was previously validated on a subset of the ImaLife dataset, demonstrating good reproducibility [133].

Airway measurements were taken at intervals of 0.5mm along the centreline of the airway segmentation. The average measurements per branch were used to determine the lumen radius (LR) and total radius (TR). LR and TR were then utilized to calculate additional parameters:

1. Luminal area (LA): $\pi(LR)^2$
2. Wall Thickness (WT): TR – LR
3. Wall Area Percent (WAP): [(TA – LA)/TA]*100, where TA is total area, calculated as $\pi(TR)^2$
4. The square root of the wall area for a hypothetical airway with an internal perimeter of 10mm (Pi10) was calculated using airways from generation 0 (trachea)-6. The 6$^{th}$ generation was chosen as a threshold based on the robustness of airway measurements [133]. The square root of the wall area was plotted against the internal perimeter (Pi) per branch and a robust regression line calculated [17]. Pi10 was measured at the intercept for a Pi of 10mm.

LA, WT and WAP were averaged across airway generations 3-6 [10].

## Statistical Analyses

Independent t-testing was performed to discern differences in demographic and bronchial parameter group means by health status. The Wilcoxon rank-sum test was used to compare differences for pack-years and smoking cessation duration. Univariable linear regression was used to test the association between demographic variables and bronchial parameters. The variables significantly associated with bronchial parameters were selected for multivariate modelling. The multivariable linear regression models utilized a forward stepwise approach, incorporating sex, age, height, weight, and pack-years. The inclusion of smoking cessation duration as final variable in the model provided a measure of its contribution to the variance explained in bronchial parameters; this was quantified through changes in the model's adjusted-$R^2$. Bayesian Information Criterion (BIC) was used to evaluate the fit of each model. Models were built separately for the lung healthy and lung unhealthy groups. Marginal effects plots were generated for all models by

fixing the variables sex, age, height, weight and pack-years to their mean value, then plotting the effect of the bronchial parameter of interest on the fitted model. For each model, residual plots were made by plotting the differences between observed values and predicted values. The significance of variables in the model was gauged using a standard significance level ($\alpha<0.05$).

| Multivariate Regression Models | | | | |
|---|---|---|---|---|
| **Healthy** | | | | |
| | ***Pi10*** | ***WT*** | ***LA*** | ***WAP*** |
| **Adj $R^2$** | 0.48 | 0.416 | 0.163 | 0.069 |
| **$\Delta R^2$** | 0.001 | 0.001 | 0.002 | -0.001 |
| **ΔBIC** | 1.00 | 0.92 | -0.25 | 1.27 |
| **$\beta_1$** | -0.004 | -0.003 | -0.031 | -0.093 |
| **$\beta_1$ CI** | [-0.01, 0.00] | [-0.01, 0.00] | [-0.32, 0.26] | [-0.31, 0.12] |
| **p** | 0.30 | 0.05 | 0.84 | 0.39 |
| **Unhealthy** | | | | |
| | ***Pi10*** | ***WT*** | ***LA*** | ***WAP*** |
| **Adj $R^2$** | 0.482 | 0.384 | 0.234 | 0.110 |
| **$\Delta R^2$** | 0.001 | 0.001 | 0.003 | 0.014 |
| **ΔBIC** | 1.01 | 0.93 | -0.28 | -5.89 |
| **$\beta_1$** | -0.007 | -0.003 | 0.36 | -0.528 |
| **$\beta_1$ CI** | [-0.02, 0.01] | [-0.01, 0.00] | [-0.11, 0.83] | [-0.90, -0.16] |
| **p** | 0.32 | 0.30 | 0.14 | 0.005 |

***Table 7.2*** *- Differences in multivariable linear regression models with the addition of smoking cessation duration for the prediction of bronchial parameters and spirometry measurements. Model differences expressed as change in Adjusted $R^2$ ($\Delta R^2$), Bayesian Information Criterion (ΔBIC). Strength of association and significance shown by $\beta_1$ - Smoking cessation duration coefficient (per 10 years) and corresponding p-value (p). Pi10 – Square root of the wall area of a hypothetical airway with an internal perimeter of 10mm, WT – Wall Thickness, LA – Luminal Area, WAP – Wall Area Percent.*

# Results

## Participants and Image Analysis

Of 4,382 ex-smokers in ImaLife, 2,693 participants were excluded due to inadequate segmentation results (180, 4%) or a pack-year history below 10 (2,513, 57%) (Figure 7.1). An example of airway lumen segmentation is visualised in Figure 7.2. Of the 1,869 included ex-smokers, 1,421 (76%) were assigned to the healthy group and 448 (24%) were assigned to the unhealthy group due to the presence of one or more of self-reported history of respiratory disease (N=242), abnormal spirometry (N=233) or imaging signs of respiratory illness (N=109).

## Population Demographics

The demographic characteristics of our study population (1,869 participants) are presented in Table 7.1. The study population comprised 1072 (57.4%) men and 797 (42.6%) women. The mean age was 64.3±9.9 years for lung-healthy and 66.1±10.5 years for unhealthy participants. The median and interquartile range (IQR) for pack-years was 16.5 [12.5-23.3] and 18.2 [13.4-25.3] for healthy and unhealthy groups respectively. The median and IQR for smoking cessation duration was 20.0 [14.0-29.0] and 20.0 [13.8-29.0] years for the healthy and unhealthy groups respectively. Weight, lung function measures and bronchial parameters differed significantly between the lung-healthy and unhealthy groups.

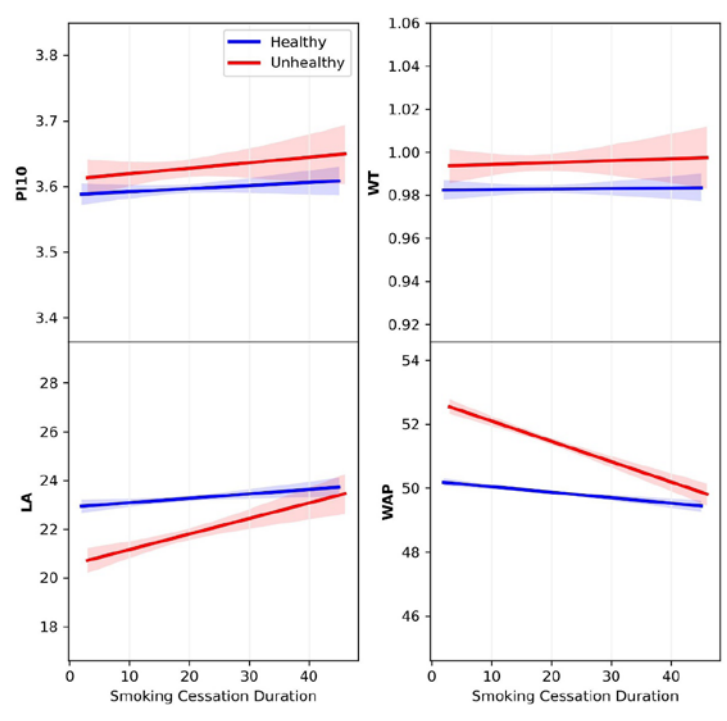


***Figure 7.3*** *- Marginal effect plots for Pi10, Wall Thickness (WT), Luminal Area (LA) and*

*Wall Area Percent (WAP) with respect to an increasing duration of smoking cessation. In this plot, the independent variables of sex, age, height, weight, and pack-years were fixed at their mean for each fitted multivariable model, allowing to isolate the relationship of smoking cessation duration to each bronchial parameter. Red line – lung-unhealthy cohort, blue line – lung-healthy cohort. Shaded area – 95% confidence intervals.*

## Smoking Cessation Duration and Bronchial Parameters

In both groups, univariable linear regression models showed a modest but significant association between smoking cessation duration and all bronchial parameters (Figure S7.2). In general, longer smoking cessation duration was related to higher WT, Pi10 and LA. Conversely, there was an inverse association of smoking cessation duration with WAP that was stronger in the lung-unhealthy group ($\beta_1$ -0.66% per year, $r^2$ 0.04, p<0.001) compared to the lung-healthy group ($\beta_1$ -0.19% per year, $r^2$ 0.0, p=0.028)

In multivariable regression models, the duration of smoking cessation was found to have a varied association with bronchial parameters in the lung-healthy and lung-unhealthy groups. Overall, there was no significant association between smoking cessation duration and bronchial parameters in the lung-healthy group (Table 7.2). For the lung-unhealthy group, WAP was significantly lower for those with longer smoking cessation duration ($\Delta R^2$ 0.014, $\beta_1$ -0.53% per year, p=0.005), while there were no significant associations for other bronchial parameters (Figure 7.3). Residual plots for each bronchial parameter demonstrated the model's goodness-of-fit. The plots show residuals scattered randomly around the horizontal zero line without any discernible pattern, suggesting that the models are appropriate. Additionally, the lack of fanning or patterning in the residual points indicates constant residual variance (Supplemental Figure 7.1).

## Discussion

In this cross-sectional study we addressed the association between smoking cessation duration and CT-derived bronchial parameters in lung-healthy and unhealthy individuals from a general population. Our findings suggest a dynamic nature of airway morphology in response to smoking cessation over time. In both groups, univariable linear regression models showed modest but significant associations between smoking cessation duration and all bronchial parameters (wall thickness, lumen area, Pi10 and wall area percent). In multivariable models adjusted for age, height, weight, sex and pack-year history, only the association of smoking cessation duration with wall area percent in the lung-unhealthy remained significant; wall area percent was lower with longer smoking cessation duration, towards the values present in the lung-healthy group. In the lung-healthy cohort, no such trend was visible, with bronchial parameters closer to those that have been reported in never smokers[162]. These findings add insight into the potential for airway remodelling in response to time since smoking cessation and highlight differences in the potential sensitivity to change for the evaluated bronchial parameters.

Previous research has shown differences in bronchial parameters in the short-term after smoking cessation. Wyszkiewicz et al. demonstrated in 90 ex-smokers that at a repeat CT scan after 3 years, ex-smokers had significantly decreased WAP and increased LA compared to their initial scan [18]. Similarly, at a repeat CT scan at 2 years of follow-up, 48 ex-smokers had a decrease in WAP compared to persisting smokers [163]. In a 4-year longitudinal study 31 recent quitters were compared to 405 continuing smokers, and past smokers who had already stopped smoking longer ago. Recent-quitters demonstrated a decrease in WAP and increase in LA that trended towards the measurements from the ex-smokers who had stopped for a longer time; the latter showed much less changes in bronchial parameters. While Li et al observed a steady state of bronchial parameters in ex-smokers who quit longer ago where there was no significant difference in WAP and luminal diameter in longer-term ex-smokers after a one-year follow-up period [46], our findings suggest a different trend. Our analysis indicates that the decrease in WAP not only persists but continues to improve with extended smoking cessation beyond the one-year mark. Analysis of current and ex-smokers in the COPDGene study showed a significant decrease in Pi10 only for those individuals who quit smoking after their first visit, i.e. within 5 years [87]. Taken together, these studies demonstrate measurable changes in airway morphology in the short-term after smoking cessation, however it is unclear from those results whether positive changes continue for many years after smoking cessation. As participant characteristics like age, sex, height, and weight could be covariates affecting the bronchial parameter measurement, accounting for these variables in the analysis is also of importance [162], as we noted in our univariable and multivariable regression models.

While previous studies have highlighted the benefits of smoking cessation by demonstrating immediate improvements in airway morphology as measured on CT, our study contributes by providing evidence for continued improvement in airway morphology over decades for ex-smokers, particularly evident in the lung-unhealthy group, with a gradual decrease in WAP towards the values in the healthy ex-smoker group. Contrarily, surprising results from

univariable analyses showed an increase in WT and Pi10 with longer smoking cessation duration, which may be attributed to the effects of ageing on airway wall and luminal areas [26]. When accounting for this in the multivariable models including age, sex and smoking pack-years, we no longer found significant changes in WT or Pi10. This suggests that the findings from univariable models are likely influenced by age amongst other factors, as longer duration of smoking cessation relate to older age. There was a consistent association showing that those with longer smoking cessation duration had lower WAP in both univariate and multivariate models, indicating that WAP is less dependent on age compared to wall thickness, luminal area, or Pi10. This may be due to the way WAP responds to changes in the airway; when both the airway lumen and wall increase at a steady rate (as may be observed with ageing) WAP does not change much (Supplemental Media 1). In cases where there is an imbalance to airway remodelling, the ratio at which airway wall and lumen change is mismatched and so WAP changes too (Supplemental Media 2). Due to this, WAP appears to be more sensitive as a bronchial parameter in comparison to WT, Pi10 or LA alone, and in addition has the benefit of being ubiquitous in this research field with the ability to differentiate between disease groups across various studies [124].

The decrease in WAP with increasing smoking cessation duration was not observed in the lung-healthy population. This could be in part due to the lung-healthy group having a healthier starting point with more normal airways, and so less room for improvement. The lung-unhealthy cohort may also be more predisposed to airway changes brought on by cigarette exposure, and so they could both be more likely to be ill, and more responsive to smoking cessation.

This study has several key strengths. Firstly, it utilises a large, well-established general population sample derived from the Imaging in Lifelines cohort, adding to the generalizability of the findings. This study includes both lung-healthy and unhealthy individuals allowing for comparisons between these groups. The automated and validated approach to bronchial parameter measurement that we used minimizes the potential bias that could stem from semi-automated and manual measurement.

There are some limitations regarding the findings within this study. Firstly, this study is a cross-sectional analysis of the general population, and we did not observe the values of bronchial parameters in the same individual over time, therefore, future long-term longitudinal studies would strengthen the confidence in the observations found here. Second, the generalizability of the findings may be limited to populations like those included in the ImaLife cohort (i.e., predominantly White individuals from the North of Netherlands), exploration of this subject in other diverse populations would be beneficial in exploring potential differences and similarities in airway morphology changes with increased duration of smoking cessation. Further, due to the time gap between the patient questionnaire determining smoking status and the scan acquisition date, we do not capture the early airway changes that happen in the first 2 years after smoking cessation in this data.

In conclusion, this study reinforces the evidence supporting the extensive advantages tied to prolonged smoking cessation among individuals with compromised lung health. While there were no significant associations with bronchial parameters and time since smoking cessation in the lung-healthy group, in lung-unhealthy ex-smokers the duration of smoking cessation was related to a decrease in wall area percent of the bronchial walls after adjusting for factors like age and height. The results suggest the potential for improvements in airway health with longer smoking cessation, warranting further investigation with longitudinal studies. Our results support the need for interventions aimed at promoting smoking cessation for long-term public health improvement.

# CHAPTER 8

## REFERENCE FORMULAS FOR CHEST CT-DERIVED LOBAR VOLUMES N THE LUNG-HEALTHY GENERAL POPULATION

J. T. Bakker • I. Dudurych • S. A. Roodenburg • J. M. Vonk • K. Klooster • M. de Bruijne • M. van den Berge • D.J. Slebos • R. Vliegenthart

*European Radiology 2024*

## Abstract

**Background** Lung hyperinflation, a key contributor to dyspnoea in Chronic Obstructive Pulmonary Disease (COPD), can be quantified via volumetric chest Computed Tomography (CT) analysis. However, the absence of reference values poses a challenge. Establishing reference equations for lobar volumes and total lung volume (TLV) can aid in evaluating lobar hyperinflation, especially for targeted lung volume reduction therapies.

**Methods** The Imaging in Lifelines study (ImaLife) comprises 11,729 participants aged 45 and above with analysed inspiratory low-dose thoracic CT scans. Lung and lobar volumes were measured using an automatic AI-based segmentation algorithm (LungSeg). Participants were excluded if they had self-reported COPD/asthma, lung disease on CT, airflow obstruction on lung function testing, were currently smoking, aged over 80 years, or had height outside the 99% confidence interval. Reference equations for TLV and lobar volumes were determined using linear regression considering age and height, stratified by sex.

**Results** The study included 7,306 lung-healthy participants, 97.5% Caucasian, 43.6% men, with mean age of 60.3±9.5 years. Lung and lobar volumes generally increased with age and height. Men consistently had higher volumes than women when adjusted for height. R2 values ranged from 7.8% to 19.9%. In smokers and those with airway obstruction, volumes were larger than in lung-healthy groups, with the largest increases measured in the upper lobes.

**Conclusion** The established reference equations for CT-derived TLV and lobar volumes provide a standardized interpretation for individuals aged 45 to 80 of Northern European descent.




## Introduction

Chronic Obstructive Pulmonary Disease (COPD) is a debilitating condition characterized by inability to effectively exhale. This can result in a state of hyperinflation where more air is retained in the lungs compared to individuals without disease. In clinical practice, body plethysmography is used to quantify the severity of total hyperinflation through the measurement of static lung volumes, especially total lung capacity (TLC) and residual volume (RV). To aid the interpretation of these measurements, the absolute volumes are standardized using reference values that are based on individuals without lung disease and are similar in terms of height, age, and sex, the most recent being established by the Global Lung Initiative (GLI)[164,165].

Accurate assessment of lung volumes is crucial to select appropriate patients for interventions targeting hyperinflation like endobronchial valve (EBV) treatment. This treatment aims to reduce lung volume by inducing a lobar atelectasis. Selecting the correct target lobe is essential because an inaccurate selection may exacerbate the patient's condition rather than providing relief from symptoms. Generally, the lobe of interest is the one most severely affected by emphysematous destruction which therefore contributes little to gas exchange[166]. Additional considerations include fissure completeness to prevent collateral ventilation and balancing the target lobe volume with the ipsilateral lobar volume(s)[167]. For these reasons, Computed Tomography (CT) scanning and quantitative CT analysis by lobar segmentation are essential for patient selection for EBV treatment, as no other modality can provide accurate lobar-based information. However, unlike plethysmography-derived volumes, standardized reference values for lobar volumes have not been universally established. Only one study has derived such equations, albeit in a relatively small cohort[168]. This kind of information could be valuable for assessing the feasibility of EBV treatment, determining, for example, whether hyperinflation is confined to a specific lobe.

Several studies have demonstrated that lung volumes can be established by CT, with strong correlation to their plethysmography counterparts[130,169–175]. We will refer to the CT-derived equivalent of TLC as total lung volume (TLV). One study highlighted that the repeatability of CT-derived volumes surpasses that of plethysmography-derived volumes[173]. We have recently demonstrated that lung volumes compare well to plethysmography counterparts in COPD patients as well, especially when spirometry-gating is used[176], highlighting the

potential utility in EBV treatment assessment. Relying on GLI predicted reference values for TLC is inadequate as the GLI equations significantly overestimate actual TLV values in a lung-healthy population[177].

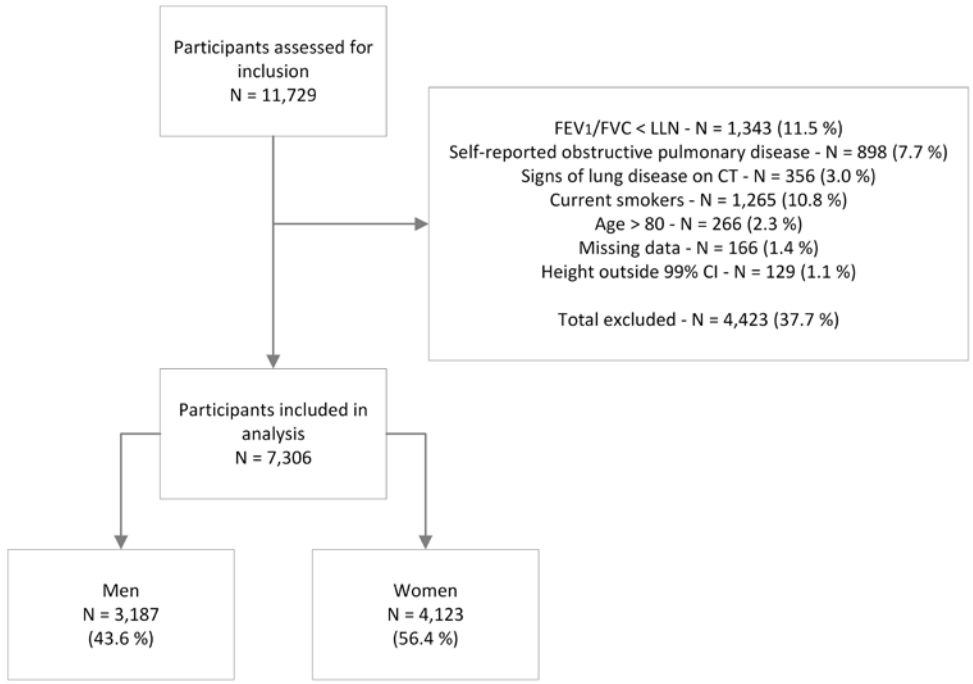


***Figure 8.1*** *- Flowchart of patient selection. CI = confidence interval, LLN = Lower Limit of Normal, N = number of individuals.*

Thus, while lung volumes can be accurately measured using CT, proper reference equations for normal values are lacking. We aim to establish reference equations, using age, sex and height in a similar fashion to the GLI model, for CT-derived lobar volumes and TLV in a lung-healthy cohort, representative of the Northern European general population.

## Methods

### Population

The Imaging in Lifelines study (ImaLife) comprises of 11,762 participants aged 45 and above with an assessable inspiratory low-dose thoracic CT scan. ImaLife is part of the larger Lifelines cohort study. Lifelines is a multi-disciplinary prospective population-based cohort study examining, in a unique three-generation design, the health and health-related behaviours of 167,729 persons living in the north of the Netherlands, with 97.5% of them having Caucasian origin. It employs a broad range of investigative procedures in assessing the biomedical, socio-demographic, behavioural, physical and psychological factors which contribute to the health and disease of the general population, with a special focus on multi-morbidity and complex genetics[120]. As a part of this, ImaLife is focused on imaging biomarkers that are gathered from low-dose chest CT scans. Lifelines participants aged 45 or older who had lung function test data available for the second visit in the Lifelines study were invited to undergo low-dose inspiratory chest CT scanning. The study design has been described in a previous publication[32].

The focus of the current study was on the lung-healthy population. We excluded participants with airflow obstruction as indicated by a Forced Expiratory Volume in one second (FEV) to Forced Vital Capacity (FVC) ratio below the lower limit of normal in spirometry, current smoking, self-reported history of obstructive pulmonary diseases (COPD/asthma), signs of lung disease on CT, individuals with a height outside the 99% confidence interval (CI) to address extreme outliers, and finally, participants aged over 80 years due to insufficient sample size. Specifics on exclusion criteria can be found in the Supplement. However, the participants with airflow obstruction and with current smoking were included in a sub analysis, described below. This study has been approved by the medical ethics committee in the University Medical Centre Groningen, the Netherlands and has been registered with the Dutch Central Committee on Research involving Human Subjects (https://www.toetsingonline.nl, Identifier: NL58592.042.16). All participants provided written informed consent.

### Image Acquisition, Reconstruction and Analysis

Each participant underwent a supine, breath-coached to inspiration, low-dose chest CT scan using a third-generation dual-source CT scanner (SOMATOM Force, Siemens Healthineers, Germany). The scans were performed between August 2017 and October 2022. The scan was reconstructed using a sharp Qr59 kernel specifically designed for quantitative analysis, and a slice thickness of 1mm and a slice increment of 0.7mm. All scans were automatically processed using an automatic AI-based lung and lobe segmentation algorithm called LungSeg (https://github.com/jtabalon/LungQuant)[178]. These segmentations were used to calculate the total inspiratory lung volume (TLV) and lobar volumes. Volume was calculated by multiplying the number of voxels in each segmentation by the volume of an individual voxel. Segmentations with a TLV greater than 8L or less than 3L were flagged for visual inspec-

tion. Abnormal segmentations were subsequently removed from the dataset.

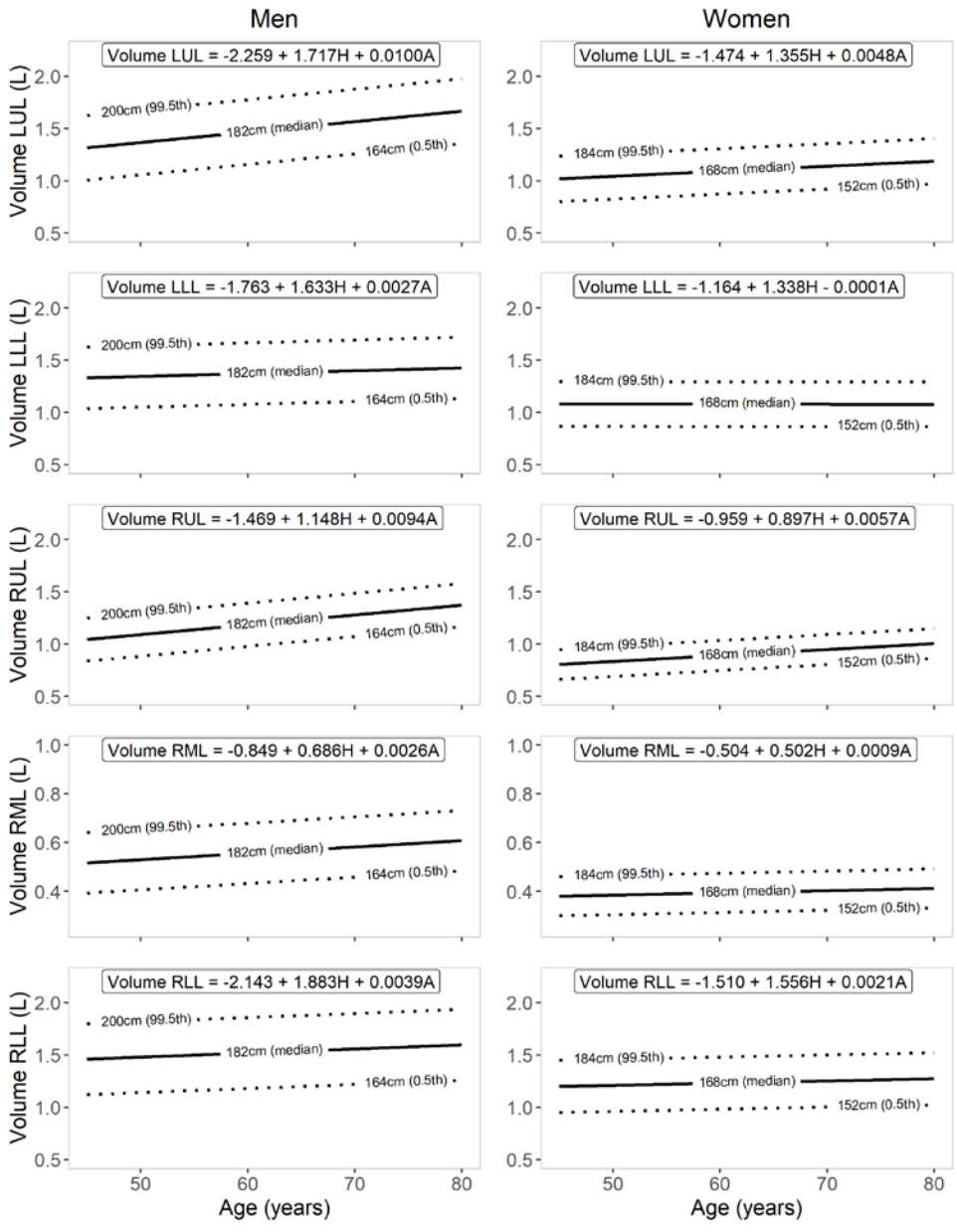


***Figure 8.2*** *- Reference equations for lobar volumes at all included ages for men and women for median, 0.5 percentile and 99.5 percentile heights. LUL = Left Upper Lobe, LLL = Left Lower Lobe, RUL = Right Upper Lobe, RLL = Right Lower Lobe, RML = Right Middle Lobe.*

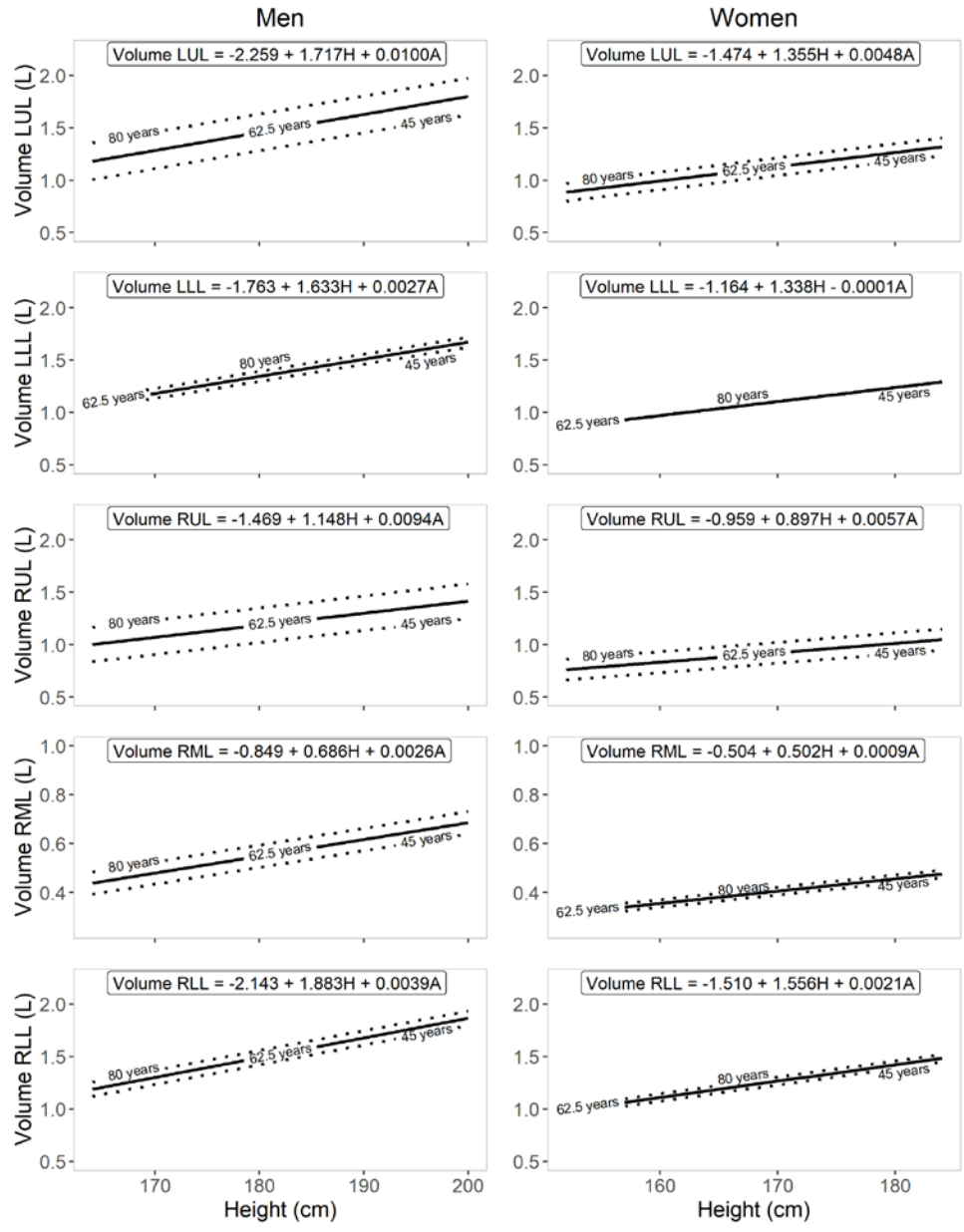


***Figure 8.3*** *- Reference equations for lobar volumes from the minimum included height to the maximum included height for men and women for the minimum age, around the median age and the maximum age. LUL = Left Upper Lobe, LLL = Left Lower Lobe, RUL = Right Upper Lobe, RLL = Right Lower Lobe, RML = Right Middle Lobe.*

## Statistical Analysis

The TLV and lobar volumes were visually assessed for a normal distribution. The reference equations were obtained by linear regression. Analogously to the reference equations established by GLI, this regression was stratified for sex, and the independent variables were age and height[165]. Statistical analyses and visualizations were conducted using R version 4.2.2 (R Core Team, Vienna, Austria). P values below 0.05 were considered significant.

## Sub-analysis of Subgroups with Lung Health Impairment

To investigate if the volumes in current smokers and people with airway obstruction ($FEV_1$/FVC ratio below the lower limit of normal) are indeed larger than in the lung-healthy group, we applied the calculated reference equations to current smokers and people with airway obstruction and compared the percentage predicted values in these groups to the values in the lung-healthy group. The current smokers and individuals with airway obstruction groups were made up of participants that were excluded from the lung-healthy group and were screened for all other exclusion criteria (including current smoking for airway obstruction group, and airway obstruction for current smoking group). We conducted independent two-sided t-tests, with Bonferroni correction applied to mitigate the effects of multiple comparisons, to compare the lung and lobar volumes of both these groups against those of the lung-healthy population.

# Results

## Population

The participant selection process is illustrated in Figure 8.1. For all participants (N=11,729) the inspiratory CT scan was analysed using LungSeg. A total of 1,343 (11.5%) patients exhibited a $FEV_1$/FVC ratio below the lower limit of normal, 1,265 (10.8%) were identified as current smokers, 898 (7.7%) reported a history of pulmonary disease (COPD or asthma), 356 (3.0%) displayed signs of lung disease on CT, 266 (2.3%) participants were over the age of 80, 166 (1.4%) had missing data, and 129 (1.1%) had a height outside the 99% confidence interval. Ultimately, 7,306 participants were included and stratified by sex. Among them, 3,183 (43.6%) were men and 4,123 (56.4%) were women. Men had a mean age of 61.0 ± 9.6 years and a height of 1.82 ± 0.07 m, while women had a mean age of 59.7 ± 9.4 years, and a height of 1.68 ± 0.06 m. Men and women demonstrated a significant difference for all considered parameters according to independent two-sided t-tests. Further demographic details of the included participants are presented in Table 8.1.

| | Men (n = 3,183) | Women (n = 4,123) | p-value |
|---|---|---|---|
| **Characteristics** | | | |
| Age, years | 61.0 ± 9.6 | 59.7 ± 9.4 | <0.001 |
| Height, m | 1.82 ± 0.07 | 1.68 ± 0.06 | <0.001 |
| Weight, kg | 86.9 ± 12.4 | 73.8 ± 12.6 | <0.001 |
| **Spirometry** | | | |
| $FEV_1$, L | 3.92 ± 0.65 | 2.84 ± 0.47 | <0.001 |
| $FEV_1$ %-predicted, % | 103.6 ± 13.5 | 105.6 ± 13.7 | <0.001 |
| FVC, L | 5.17 ± 0.82 | 3.71 ± 0.59 | <0.001 |
| FVC %-predicted, % | 107.1 ± 14.1 | 108.2 ± 14.1 | <0.001 |
| $FEV_1$/FVC ratio | 0.76 ± 0.05 | 0.77 ± 0.05 | <0.001 |
| **CT-derived volumes** | | | |
| TLV (L) | 6.12 ± 1.20 | 4.71 ± 0.79 | <0.001 |
| Volume LUL (L) | 1.47 ± 0.28 | 1.09 ± 0.18 | <0.001 |
| Volume LLL (L) | 1.37 ± 0.37 | 1.08 ± 0.25 | <0.001 |
| Volume RUL (L) | 1.19 ± 0.23 | 0.89 ± 0.16 | <0.001 |
| Volume RML (L) | 0.56 ± 0.13 | 0.40 ± 0.09 | <0.001 |
| Volume RLL (L) | 1.51 ± 0.40 | 1.24 ± 0.27 | <0.001 |

***Table 8.1*** *- Demographic characteristics of the study population. The demographics are summarized as follows: Data is expressed as the mean ± standard deviation for continuous variables, while participant numbers are presented as counts and percentages relative to the total within each group. p-values were determined using an independent two-sided t-test. $FEV_1$ = Forced Expiratory Volume in one second, FVC = Forced Vital capacity. TLV = Total Lung Volume, LUL = Left Upper Lobe, LLL = Left Lower Lobe, RUL = Right Upper Lobe, RLL = Right Lower Lobe, RML = Right Middle Lobe.*

## Regression Analysis

All volumes were normally distributed. Men demonstrated higher lung and lobar volumes at the same height than women. The regression models fitted for the volumes demonstrated consistent patterns, particularly, positive associations with both age and height, with the exception of the LLL in women as this volume did not seem to be associated with age. The explained variance by the regression models ranged from 7.8% to 19.9%. In general, the RLL was the largest lobe, followed by the LUL and the LLL, which were about equal in size. The RUL was smaller, and the RML was, by a large margin, the smallest.

The volume of the upper lobes was more related to age than the lower lobes; with increasing age the upper lobes comprised an ever-larger proportion of the TLV for both men and women. At advanced age, this led to the LUL on average becoming larger than the RLL in men. The reference equations can be appreciated in Table 8.2. Figure 8.2 demonstrates the volumes for increase age at three different heights. Figure 8.3 demonstrates the volumes for increasing height at three ages.

| Parameter | Reference equation | RSD | $R^2$ |
|---|---|---|---|
| **Men** | | | |
| TLV (L) | -8.514 + 7.090 * H + 0.0287 * A | 1.107 | 0.151 |
| Volume LUL (L) | -2.259 + 1.717 * H + 0.0100 * A | 0.251 | 0.199 |
| Volume LLL (L) | -1.763 + 1.633 * H + 0.0027 * A | 0.354 | 0.078 |
| Volume RUL (L) | -1.469 + 1.148 * H + 0.0094 * A | 0.213 | 0.179 |
| Volume RML (L) | -0.849 + 0.686 * H + 0.0026 * A | 0.123 | 0.116 |
| Volume RLL (L) | -2.143 + 1.883 * H + 0.0039 * A | 0.382 | 0.087 |
| **Women** | | | |
| TLV (L) | -5.626 + 5.664 * H + 0.0133 * A | 0.713 | 0.177 |
| Volume LUL (L) | -1.474 + 1.355 * H + 0.0048 * A | 0.164 | 0.199 |
| Volume LLL (L) | -1.164 + 1.338 * H - 0.0001 * A | 0.236 | 0.107 |
| Volume RUL (L) | -0.959 + 0.897 * H + 0.0057 * A | 0.144 | 0.167 |
| Volume RML (L) | -0.504 + 0.502 * H + 0.0009 * A | 0.088 | 0.098 |
| Volume RLL (L) | -1.510 + 1.556 * H + 0.0021 * A | 0.251 | 0.116 |

***Table 8.2*** *- Regression analysis with the resulting reference equations. RSD = Residual standard deviation, R2 = adjusted regression coefficient squared, TLV = Total Lung Volume, LUL = Left Upper Lobe, LLL = Left Lower Lobe, RUL = Right Upper Lobe, RLL = Right Lower Lobe, RML = Right Middle Lobe. H = height (m), A = age (years).*

## Populations With Lung Health Impairments

The mean percentage predicted TLV using the reference equations of Table 8.2, was 103.1 ± 17.5 % for the current smoking subgroup, and 110.3 ± 16.9 % for the airway obstruction subgroup. Table 8.3 demonstrates these values in addition to the mean percentage predicted values with standard deviations for all the lobar volumes within current smokers and airway obstruction subgroups, all of which follow normal distributions. The percentage predicted values of the lung and lobar volumes of the airway obstruction subgroup were significantly different from the lung-healthy population (all p<0.001). The male current smokers were significantly different to the lung-healthy population regarding percentage predicted values for TLV (p=0.002), LUL and RUL (both p<0.001), but not for LLL (p=0.835), RML (p=1) and RLL (p=0.410). For female current smokers, all lung and lobar predicted volumes were significantly different from the lung-healthy population (all p<0.001, except LLL: p=0.025), with the exception of the RLL (p=1). The largest differences were observed in the upper lobes.

| | Current smokers | CS versus LH<br>Adjusted p | Airway obstruction | AO versus LH<br>Adjusted p |
|---|---|---|---|---|
| **Men** | | | | |
| Participants, N | 603 | | 298 | |
| TLV, % predicted | 103.1 ± 17.5 | **0.002** | 110.3 ± 16.9 | **<0.001** |
| LUL, % predicted | 103.4 ± 17.3 | **<0.001** | 110.1 ± 17.7 | **<0.001** |
| LLL, % predicted | 102.5 ± 25.9 | 0.835 | 110.4 ± 25.5 | **<0.001** |
| RUL, % predicted | 105.2 ± 17.8 | **<0.001** | 113.0 ± 21.6 | **<0.001** |
| RML, % predicted | 101.1 ± 21.7 | 1 | 107.6 ± 25.8 | **<0.001** |
| RLL, % predicted | 102.6 ± 23.9 | 0.410 | 109.2 ± 23.9 | **<0.001** |
| **Women** | | | | |
| Participants, N | 575 | | 398 | |
| TLV, % predicted | 103.1 ± 15.3 | **<0.001** | 108.0 ± 14.7 | **<0.001** |
| LUL, % predicted | 103.2 ± 15.1 | **<0.001** | 108.4 ± 16.4 | **<0.001** |
| LLL, % predicted | 103.2 ± 22.0 | **0.025** | 108.2 ± 22.0 | **<0.001** |
| RUL, % predicted | 104.2 ± 16.9 | **<0.001** | 110.1 ± 18.7 | **<0.001** |
| RML, % predicted | 104.4 ± 22.2 | **<0.001** | 104.8 ± 25.9 | **<0.001** |
| RLL, % predicted | 101.6 ± 20.9 | 1 | 107.4 ± 20.2 | **<0.001** |

***Table 8.3*** *- Percentage of predicted lung and lobar volumes across lung-healthy, current Smokers, and airway obstructed groups. The "current smokers" group consists of the current smokers that were excluded for the lung-healthy group and were filtered for all other exclusion criteria. "Airway obstruction" refers to participants that were excluded for the lung-healthy group based on a Forced Expiratory Volume in one second/Forced Vital Capacity ratio below the lower limit of normal, and subsequently filtered for all other exclusion criteria. The percentage of predicted lung and lobar volumes for all groups was calculated using the reference equations (Table 2). Statistical significance was determined through independent two-sided t-tests. The adjusted p-values were obtained using the Bonferroni method to account for multiple comparisons (24 tests in total). P values larger than 1, which may occur due to the Bonferroni correction, are truncated to 1. TLV = Total Lung Volume, LUL = Left Upper Lobe, LLL = Left Lower Lobe, RUL = Right Upper Lobe, RLL = Right Lower Lobe, RML = Right Middle Lobe, CS = Current Smokers, LH = Lung Healthy, AO = Airway Obstructed.*

## Discussion

In this study we established reference equations for lung and lobar volumes, based on inspiratory chest CT in a large sample of a general population without lung disease, using linear regression analysis. Age and height were positively associated with lung and lobar volumes, except for the LLL in women. The RLL was consistently the largest lobe, followed by the LUL and LLL, then the RUL and lastly the RML. Upper lobes showed a stronger association with age, indicating they comprise more of the total lung volume as individuals age. Men have higher lung volumes than women at the same height. Overall, age and height explained 7.8% to 19.9% of the variation in volumes.

Lung volume measurement by CT has the benefit of allowing regional volume assessment, such as lobar volumes, possibly beneficial for treatments like EBV and lung volume reduction. The only other modality capable of achieving this is VP/SPECT which is much less available[179]. Prior studies, specifically related to lobar volumes, have mostly focused on ventilation or collapsibility of the lobes by comparing scans in in- and expiration[180,181]. In EBV studies, attention regarding lobar volumes centres on pre- and post-treatment changes[182]. A lower limit for important difference in lobar volume reduction between pre- and post-treatment has been established at 563 mL[183]. This metric does not consider variations influenced by patient height, age, and sex and may therefore be refined by an approach similar to that employed in the present study. In terms of reference equations for lobar volumes, to our knowledge, only one study previously established such equations at full inspiration based on a cohort of 469 COPDGene participants without COPD (92 never smokers and 377 current or former smokers), incorporating height, sex, and ethnicity[168]. Unlike our study and the GLI reference equations for TLC, they did not observe a significant relationship between age and any of the volumes, possibly attributed to the small cohort size. They did find similar results regarding the relationship to height and a similar intercept[168]. In our study, ethnicity stratification was not performed, given that 97.5% of the participants identified as having Caucasian origins. Similarly to this prior study, we stratified for sex, justified by our finding that women had consistently smaller lobar volumes for the same height compared to men.

The observation that upper lobes had a greater increase in volume with age, as opposed to lower lobes, suggests a potential susceptibility of upper lobes to damage, even among the lung-healthy population. This aligns with research indicating a higher incidence of emphysema and lung cancer in the upper lobes[184–186]. Therefore, it would be expected that smokers and those with COPD would exhibit relatively larger upper lobes compared to their lower lobes when compared to healthy individuals. In this study, we observed a significant difference between the lung-healthy population and current smokers for every lung or lobar volume, except for the LLL and RML in men and the RLL in men and women. This further supports the idea that the upper lobes may have a greater susceptibility to damage.

Regarding CT lung volumes, previous studies primarily compared TLV measurements obtained at inspiration and/or expiration to plethysmography-derived volumes, showing strong correlations[169–176,187]. Typically, TLC was slightly higher than measured TLV, while RV was lower at expiration[186]. In line with this, a previous study established that there is a substantial discrepancy between the GLI-predicted TLC and TLV, with significantly larger estimated TLC than measured TLV[177]. This difference can only partially be explained by measurement position variations between seated plethysmography and supine CT scans, with a 9.9% smaller volume in the supine position[188].

This study's strengths lie in its extensive lung-healthy sample of 7,306 individuals. Additionally, the current study included a standardized CT scan protocol on third generation dual-source CT, with very short acquisition time due to high-pitch scanning mode. Previous research has shown consistent CT-based measurements for lobar volumes, with TLV being more reproducible than TLC as measured by body-plethysmography[173], which further validates our approach. The reference equations are applicable for assessing lobe-specific hyperinflation in COPD, which is specifically potentially useful in treatments like EBV and lung volume reduction. Furthermore, these equations may be of potential value in assessing other conditions like restrictive pulmonary diseases or surgical planning for lobe removal in lung cancer patients. The application of the derived equations to smokers and subjects with airway obstruction, indeed showed higher volumes (especially in the upper lobes). This shows that the equations are capable of pinpointing differences between groups.

There are some limitations with this study. The study focused on a regionally specific population from the north of the Netherlands, characterized by above-average height, approximately 5 cm above the WHO growth chart median[189] and predominantly Caucasian ethnicity. Additionally, this cohort consisted of individuals between the ages of 45 and 80. Given that EBV is typically used for severe emphysema patients aged around 50-70, these limitations are acceptable for our purposes. However, it is crucial to recognize that these reference equations may therefore not be universally applicable. It would be important to calibrate these reference equations in other populations.

The explained variance for the lobar and lung volumes was relatively low, ranging from 7.8 % to 19.9%. This suggests that other factors, not included in the regression analysis, play a role in the size of the lobes and lungs. However, these factors are unknown, and no other explanatory factors are used in similar approaches to reference equations such as the GLI reference equations for TLC, which reported coefficients of variation of over 10% for their models[165]. These unknown factors are likely related to the shape and size of the chest. While sex and height are now used as crude approximations for these factors, they do not fully capture the complexity of individual variations. Genetic factors could also play a role, as well as aspects like fissure integrity.

In conclusion this study establishes reference equations for lobar volumes and total lung volume at inspiratory chest CT by sex, adjusting for age, and height in a population of lung-healthy individuals between the ages 45 and 80 of Northern European descent. Lobar volumes were higher in taller individuals and in men and increased with age especially for upper lobes.

# CHAPTER 9

## DISCUSSION

CT scans play a pivotal role in the creation of imaging biomarkers beyond visual evaluations, in particular due to CT's volumetric and quantitative nature. For imaging of the chest, CT scans allow comprehensive measurements of both the parenchyma of the lungs and the airway tree. CT scans, acquired as part of lung cancer screening or for clinical indications, can be used for bronchial parameter analysis, offering potential for wider application in population health [33]. However, to leverage this capability effectively, we need clear understanding of reference distributions in a healthy general population, and differences in bronchial parameters between healthy and unhealthy individuals must be discernible.

Our review and meta-analysis of existing literature in Chapter 2 revealed not only significant differences in CT-derived bronchial parameters between never-smokers, smokers, COPD patients, and asthma patients but also an evident scarcity of studies involving large healthy populations. The aim of this thesis was to address this imbalance by targeting the knowledge gap of bronchial parameter measurements within a large, predominantly healthy general population. The thesis further elucidates how factors such as sex, height, weight, and smoking history influence these bronchial parameters, and lung lobe measurements. To accomplish this objective, we first focused on developing and validating an automated method for segmenting the airway lumen and wall, suitable for use in the large set of scans from the Imaging in Lifelines (ImaLife) study.

### AUTOMATED AIRWAY SEGMENTATION AND BRONCHIAL PARAMETER CALCULATION

Airway segmentation historically has been a laborious task, necessitating considerable manual input [9]. Semi-automated approaches improved the speed to process each scan, yet still required intervention from trained technicians and many man-hours [94]. For large-scale studies such as ImaLife, with over 12,000 scanned participants, this would quickly result in months of expensive, dedicated labour. Recently, modern deep-learning methods have enabled the automated and powerful processing of 3D images for specialised tasks such as segmentation. We utilized this deep-learning approach for automatic feature extraction and learning from low-dose CT scans for airway

segmentation.

In Chapter 3, we introduced a method for generating a high-quality training dataset to enhance the performance of deep-learning models when applied to specific scans. Such datasets rely on pairing scans with corresponding accurate "ground truth" segmentations, a task that is both time-consuming and prone to errors. To maximise the quality of training data, time-consuming input from experts in the target domain is needed, this can result in a limited amount of available training data for deep-learning in specific medical-imaging tasks. Additionally, deep-learning models may perform sub optimally when applied outside the scope of their original training. We addressed these challenges by using a deep-learning 3D U-Net model, already trained on data from the Danish lung cancer screening trial (DLCST) [98] and Erasmus MC-Sophia datasets [9], to generate preliminary segmentations of ImaLife scans, albeit incomplete. To refine these segmentations, we manually extended them and added missing branches using open-source software. Consequently, an updated model trained with these improved segmentations achieved more comprehensive airway delineation compared to its predecessor. Given the scarcity of high-quality labelled data for medical imaging segmentation, our strategy not only conserves valuable time but also extends the utility of deep-learning models by supporting their re-training for diverse scanning protocols and applications. Moreover, the use of open-source resources facilitates the swift calibration of AI models to different contexts, streamlining the production of datasets tailored for AI training. Lastly, the deep-learning methodology employed in our investigation delivers good performance even with relatively small training datasets, thereby reducing the labour required to create an effective training dataset [96].

Building on the deep-learning approach for comprehensive airway segmentation, we refined the delineation of the lumen and wall for the entire airway tree. This step was essential for accurate bronchial parameter quantification. To this end, we integrated and validated an optimal-surface graph-cut method for 3D refinement of the airway lumen and concurrent delineation of the airway wall [115]. We presented this in Chapter 4, where we built an automated pipeline for low-dose chest CT that extracts accurate measurements of the airway lumen and wall (when compared against ground truth measurements). This system combines the strengths of our previously trained deep-learning method with fine tuning based on? the graph-cut approach using a standardised imaging phantom scanned using the ImaLife protocol [116]. We validated the pipeline performance on short-term (3-4 month) repeat scans of ImaLife participants and demonstrated that our methods achieved moderate-to-good reproducibility, attaining a comparable level of precision for bronchial parameters such as luminal area and wall thickness to those obtained by earlier methods [10] – while also improving the reproducibility of the Pi10 measurement compared to previous methods [125]. A notable strength of this approach is the absence of the bias, inherent in manual or full-width half-maximum measurements of airway structures, which often results in over-estimation of the airway wall [128]. Both parts of the pipeline are open-source and available to the wider research community (https://github.com/antonioguj/bronchinet and https://bitbucket.org/opfront/opfront). In combination with the research outlined in Chapters 3 and 4 they could be adapted for use with other datasets.

While the rapid advancement in medical imaging analysis has provided more robust measurements of bronchial structures, there is a lack of standardisation across this research field. This may be best highlighted by the inconsistency with how one of the most used bronchial parameters is not always calculated the same way. Pi10 is most often defined as "the square root of the wall area of a hypothetical airway with an internal perimeter of 10mm" and originated from histological analysis of airways [17,121]. Yet, there are studies in which Pi10 is taken as something completely different e.g. the number of airways with an internal perimeter of 10mm [21] or wall thickness at this hypothetical airway [130]. These discrepancies indicate that the field of bronchial parameter research would benefit from concentrated efforts at standardisation as other biomarkers such as CT atherosclerosis has [190]. It is exciting to see early efforts beginning to explore this topic [191]. In the absence of reference methods for bronchial parameter evaluations, we made every effort to ensure that our measurements were accurate and reproducible through our investigations in Chapters 3-4 and provided our methods as open-source code that can be used or adapted down the line.

The steps we took to develop and validate this pipeline demonstrate potential for use in clinical practice. The low-dose CT protocol is a feasible approach for this task, already used in lung cancer screening. The automation of bronchial parameter measurements can reduce the time and labour, allowing for their broader application in clinical settings, which could enhance the efficiency of patient assessments and follow-up. Before integration into a clinical workflow, the software must be approved by regulatory bodies. The European Medicine Agency (EMA) and Food and Drug Administration (FDA) have strict protocols and requirements for software. Both bodies are developing requirements for medical AI alone and in collaboration with each other. The research and development of medical AI should follow their suggestions and

guidelines even from an early research stage [192,193].

## Bronchial parameters in the general population

interest in tracking disease-related airway changes is growing. In smokers at-risk for developing COPD, bronchial parameters have been able to predict who progress to clinical disease and who do not [130]. For asthmatic patients, bronchial parameters have been used to monitor treatment response to medication [194]. However, to adequately interpret bronchial parameter values, it is necessary to know the distribution of normal values within the general population. Based on reference distributions of CT-derived bronchial parameters, abnormal values on the ends of the range can be used for detection of early disease. As with other biometrics, bronchial parameters may be influenced by the individual's height, weight, and age among other things. To separate changes due to illness from changes due to the individual's factors, the influence of demographic factors on bronchial parameters should be elucidated. However, this influence has previously been unclear as the study of healthy individuals was limited to small sets of individuals used as controls, often alongside unhealthy groups, a finding highlighted by our systematic review and meta-analysis from Chapter 3. Previous studies investigating CT-derived bronchial parameters have shown inconsistencies due to variations in study sample characteristics and methods. For example some studies reported thicker airways in healthy men versus women [25,85] while others measured thicker airways in women versus men [27] or no difference by sex [135]. These discrepancies may stem from differences in scan protocol, method for airway measurement, population characteristics and scale of the study.

Using the previously outlined automated bronchial parameter measurement method, in Chapter 5 we obtained measurements from low-dose inspiratory CT scans for all 12,041 participants of the ImaLife study. The ImaLife study consists of a sample of the general population, allowing a comprehensive look at a largely healthy study population. This study population also contained the largest number of never-smoking and respiratory healthy participants yet, granting a unique opportunity to definitively measure a large number of healthy lungs.

Our large-scale study provides conclusive evidence that sex, height, weight, and age influence bronchial parameter measurements. Interestingly, increasing age showed a widening of the lumen and a thickening of the wall, an observation that was not previously made. These changes likely reflect the airway changes that occur with normal ageing. Notably, the association with age was not strongly evident in the wall area percent parameter, where the variance explained by sex, age, height, weight, and smoking history was the lowest (10.4%) among all acquired bronchial parameters. This indicates that changes in wall area percent may be more attributable to other factors such as airway remodelling from disease processes rather than differences in demographics.

We further explored bronchial parameters in Chapter 6, investigating whether long-term smoking cessation relates to airway remodelling. Previous research in heavy smokers and participants with COPD has highlighted significant changes in the airways following smoking cessation in the first one or two years after smoking cessation [18,143,163]. Our results in ex-smokers from the ImaLife dataset demonstrated that there are potential ongoing airway improvements over decades for smokers who quit, particularly those with unhealthy lungs. Once again, in contrast to other parameters wall area percent stood out as a bronchial parameter of note as it changed with differences in smoking habit and unhealthy respiratory state.

With improvements in airway segmentation, additional bronchial parameters such as total airway count (TAC) have received research interest. Simply put, TAC is a sum of all the separate branches identified within the airway segmentation. It is hypothesised that a reduction in TAC could be due to a loss in branches from mucous plugging, destruction of small airways or airway collapse. It is also believed that a more complex branching tree is an indicator of good health, whereas a less complex tree could indicate disease, with complexity measured as TAC or airway fractal dimension [195]. In chapter 7 we expanded current knowledge on TAC with a focus on measurements in the majority, lung-healthy general population. Additionally, we compared TAC to more established CT-based bronchial parameters such as Pi10, wall area percent and luminal area. Our findings confirmed the value of TAC as an additional bronchial parameter to calculate due to its comparable performance in predicting spirometry categories for participants, as well as the ease with which it can be calculated. Yet, as seen with Pi10, the parameter would benefit from standardisation efforts regarding scan protocol and measurement method, as absolute values for TAC differ per study but trends mirror each other when evaluating TAC changes relative to spirometry.

Apart from airway measurements, lung anatomical measurements and parenchymal assessments are of importance in different clinical scenarios. Evaluating individual lung lobe sizes is crucial during the planning and patient selection for lung resection, transplant, and certain COPD treatments. Currently, models from the Global Lung Initiative are used to estimate lung volumes

for procedural planning, however recent studies have highlighted that CT measurements provide better estimates for lung volumes[177]. This finding shows promise for more detailed application of CT measured lung volumes. To study the anatomical lung measures in more depth, we segmented individual lung lobes using the automated pipeline in Chapter 8, to establish reference lobar volumes for a healthy population. We found significant positive associations of age and height with lung and lobar volumes across both sexes, especially for the upper lobes. In men, lung lobe volumes were larger than in women of the same height. Using this information, we developed reference equations for lung and lobar volumes using inspiratory chest CT scans from a substantial sample of the general population without lung disease. As measurement of lung lobes is essential for targeted treatments like endobronchial valve placement and lung volume reduction, reference values for expected normal volumes can prove useful in planning treatment. In combination with our reference bronchial parameter measurements, more targeted treatment could be provided to improved outcomes.

For the research conducted as part of this thesis, there are a number of limitations that apply. The ImaLife dataset is a sample of the general population from the north of the Netherlands. This general population is predominantly white, and is the tallest in the world [152]. Due to this, the reference values established as part of this thesis may require adapting for populations that differ from that within the study. The study sample lacks large numbers of severe airway disease, which limits the applicability of our methods to severe disease cohorts as the reproducibility of measurements on such groups has not been evaluated in our studies yet. As touched upon in the discussion thus far, scan protocols and methods can influence the eventual bronchial parameter measurement, limiting the applicability of our derived reference values for cases where a different scanner or scanning protocol are used.

## Future directions

following the investigations in this thesis there are several promising areas to explore next. AI is advancing at a rapid pace and while the U-Net architecture is yet to be beaten for medical segmentation tasks [196], novel approaches are continuously developed and evaluated for better performance [197]. In addition to improved methods for airway segmentation, new generations of scanners such as photon-counting CT offer higher image quality and spatial resolution at similar radiation dose, which could translate into higher accuracy measurements of the airways as has been seen with lung nodule measurement [198].Alongside this, efforts to standardise bronchial parameters can contribute to their adoption in clinical practice. As this field of research is still relatively new and constantly advancing with novel parameters, focus on a more established and validated bronchial parameter, like Wall Area Percentage, could be good to get started with.

The follow up of our findings with longitudinal studies are pivotal and could offer valuable insights into the evolution of bronchial parameters over time to confirm the associations we have observed with airway changes and ageing. By tracking these changes in both healthy individuals and varied disease cohorts, we stand to gain a deeper understanding of disease progression from an early stage as well as the role bronchial parameters can play in identifying those early stages. This is especially pertinent in validating the bronchial parameter improvements observed following long-term smoking cessation in Chapter 6, which we could so far only evaluate in a cross-sectional manner.

With the size and composition of the ImaLife dataset there is an opportunity to zoom in on the participant sample at the threshold of being lung-unhealthy. There may be discernible differences in bronchial parameters and lung measurements at this early stage that could help guide screening, monitoring, or treatment strategies for improved population health. Another promising avenue lies in exploring the role of environmental factors in respiratory health, such as unravelling the impacts of air pollution and occupational exposures on bronchial health. While the ImaLife dataset is large, it does not cover the diversity in populations across the globe. Towards this, the methods we have outlined can be repeated in other general population samples around the world to establish and contrast their bronchial parameters to those that were derived in this thesis.

Outside of technical and clinical research, future investigations into the useability of bronchial parameters and airway segmentations bear interest. For example, the segmentations could be visualised with automatically labelled branches. Areas of the airway tree with measurements that deviate from reference values could be automatically highlighted, speeding up review by researchers or clinicians in downstream tasks.

## Conclusion

This thesis establishes the use of low-dose chest CT for automated bronchial parameter evaluation with high reproducibility. The research described in this thesis demonstrates that bronchial parameters are influenced by demographic factors such as sex, height, weight, and smoking habits in a healthy population. Using scans from lung healthy ImaLife participants, we gained insights into how bronchial parameters and lung lobe volumes vary across these factors. This work fills a significant gap as previous research in this field centred on individuals with COPD or asthma. Our findings have resulted in reference equations and percentile charts that could enhance the application of bronchial parameters in early disease detection and treatment monitoring. Particularly, wall area percent emerged as a sensitive bronchial parameter for assessing changes in airways due to smoking and disease while not being heavily influenced by demographic factors. Our comprehensive evaluation of the fully segmented airway tree enabled evaluation of new bronchial parameters such as the total airway count which was shown to perform comparably to wall area percent while being easier to calculate.

Given that scan characteristics can influence measurements, dataset-specific optimization may be necessary to apply the automated method developed here to other datasets. Towards this our techniques are open-source, and the methods outlined in this thesis considerably reduce the time required to prepare training data for fine-tuning the deep-learning model. The fully automated approach is highly applicable to large-scale applications such as screening and would not impose significant time demands on radiologists. Thus, this thesis not only advances our understanding of bronchial parameters but also streamlines their potential practical application in medical imaging.

# CHAPTER 10

## REFERENCES


1 Albert RK, Spiro SG, Jett JR. Clinical respiratory medicine, 2nd ed. Philadelphia, Pa.: Mosby, 2004.

2 Weibel ER. Morphometry of the Human Lung. Berlin Heidelberg: Springer-Verlag, 1963 DOI:10.1007/978-3-642-87553-3.

3 Galanski M, Prokop M. Spiral and Multislice Computed Tomography of the Body. Georg Thieme Verlag, 2003 http://public.ebookcentral.proquest.com/choice/publicfullrecord.aspx?p=1250276 (accessed July 19, 2023).

4 Kauczor HU, Kreitner KF. MRI of the pulmonary parenchyma. *Eur Radiol* 1999; **9**: 1755–64.

5 Washko GR, Parraga G. COPD biomarkers and phenotypes: opportunities for better outcomes with precision imaging. *Eur Respir J* 2018; **52**. DOI:10.1183/13993003.01570-2018.

6 Sonka M, Wonkyu Park, Hoffman EA. Rule-based detection of intrathoracic airway trees. *IEEE Trans Med Imaging* 1996; **15**. DOI:10.1109/42.500140.

7 van Rikxoort EM, van Ginneken B. Automated segmentation of pulmonary structures in thoracic computed tomography scans: a review. *Phys Med Biol* 2013; **58**: R187-220.

8 van Ginneken B. Fifty years of computer analysis in chest imaging: rule-based, machine learning, deep learning. *Radiol Phys Technol* 2017; **10**: 23–32.

9 Kuo W, de Bruijne M, Petersen J, *et al.* Diagnosis of bronchiectasis and airway wall thickening in children with cystic fibrosis: Objective airway-artery quantification. *Eur Radiol* 2017; **27**: 4680–9.

10 Petersen J, Nielsen M, Lo P, *et al.* Optimal surface segmentation using flow lines to quantify airway abnormalities in chronic obstructive pulmonary disease. *Med Image Anal* 2014; **18**: 531–41.

11 Hoesein FAAM, Jong PA de, Lammers J-WJ, *et al.* Airway wall thickness associated with forced expiratory volume in 1 second decline and development of airflow limitation. *Eur Respir J* 2015; **45**: 644–51.

12 Konietzke P, Weinheimer O, Wagner WL, *et al.* Optimizing airway wall segmentation and quantification by reducing the influence of adjacent vessels and intravascular contrast material with a modified integral-based algorithm in quantitative computed tomography. *PLOS ONE* 2020; **15**: e0237939.

13 Santos A., Faria E., Geraldes L., *et al.* Parameters for monitoring severe asthma - A prospective study. *Rev Port Imunoalergologia* 2009; **17**: 135–53.

14 Lowe KE, Regan EA, Anzueto A, *et al.* COPDGene(®) 2019: Redefining the Diagnosis of Chronic Obstructive Pulmonary Disease. *Chronic Obstr Pulm Dis Miami Fla* 2019; **6**: 384–99.

15 Lederlin M, Laurent F, Dromer C, Cochet H, Berger P, Montaudon M. Mean bronchial wall attenuation value in chronic obstructive pulmonary disease: comparison with standard bronchial parameters and correlation with function. *AJR Am J Roentgenol* 2012; **198**: 800–8.

16 Zhang Q, Illing R, Hui CK, *et al.* Bacteria in sputum of stable severe asthma and increased airway wall thickness. *Respir Res* 2012; **13**: 35–35.

17 Nakano Y, Wong JC, de Jong PA, *et al.* The Prediction of Small Airway Dimensions Using Computed Tomography. *Am J Respir Crit Care Med* 2005; **171**: 142–6.

18 Wyszkiewicz PV, Sharma M, Desaigoudar V, *et al.* Reduced Total Airway Count and Airway Wall Tapering after Three-Years in Ex-Smokers. *COPD* 2023; **20**: 186–96.

19 Tanabe N, Sato S, Suki B, Hirai T. Fractal Analysis of Lung Structure in Chronic Obstructive Pulmonary Disease. *Front Physiol* 2020; **11**. DOI:10.3389/fphys.2020.603197.

20 Tanabe N, Vasilescu DM, Coxson HO, *et al.* Structural Analysis of the Airway Tree in Explanted Lungs with Severe COPD Using a Combination of MDCT, microCT and Histology. In: B109. ADVANCES IN PULMONARY MEASUREMENTS, MODELING, AND METHODOLOGY. American Thoracic Society, 2017: A4871–A4871.

21 Ma D, Shi H, Tan C, *et al.* Quantitative CT Metrics for the Prediction of Therapeutic Effect in Asthma. *J Clin Med* 2023; **12**: 639.

22 Chaudhary MFA, Hoffman EA, Guo J, *et al.* Predicting severe chronic obstructive pulmonary disease exacerbations using quantitative CT: a retrospective model development and external validation study. *Lancet Digit Health* 2023; **5**: e83–92.

23 Bodduluri S, Puliyakote ASK, Gerard SE, *et al.* Airway fractal dimension predicts respiratory morbidity and mortality in COPD. *J Clin Invest* 2018; **128**: 5374–82.

24 Kirby M, Tanabe N, Tan WC, *et al.* Total Airway Count on Computed Tomography and the Risk of Chronic Obstructive Pulmonary Disease Progression. Findings from a Population-based Study. *Am J Respir Crit Care Med* 2018; **197**: 56–65.

25 Bhatt SP, Bodduluri S, Nakhmani A, *et al.* Sex Differences in Airways at Chest CT: Results from the COPDGene Cohort. *Radiology* 2022; : 212985.

26 Terada S, Tanabe N, Maetani T, *et al.* Association of age with computed tomography airway tree morphology in male and female never smokers without lung disease history. *Respir Med* 2023; **214**: 107278.

27 Hackx M, Francotte D, Garcia TS, Van Muylem A, Walsdorff M, Gevenois PA. Effect of total lung capacity, gender and height on CT airway measurements. *Br J Radiol* 2017; **90**: 20160898.

28 Choi S, Hoffman EA, Wenzel SE, *et al.* Quantitative computed tomographic imaging-based clustering differentiates asthmatic subgroups with distinctive clinical phenotypes. *J Allergy Clin Immunol* 2017; **140**: 690-700.e8.

29 de Koning HJ, van der Aalst CM, de Jong PA, *et al.* Reduced Lung-Cancer Mortality with Volume CT Screening in a Randomized Trial. *N Engl J Med* 2020; **382**: 503–13.

30 Snowsill T, Yang H, Griffin E, *et al.* Low-dose computed tomography for lung cancer screening in high-risk populations: a systematic review and economic evaluation. *Health Technol Assess* 2018; **22**: 1–276.

31 Reduced Lung-Cancer Mortality with Low-Dose Computed Tomographic Screening. *N Engl J Med* 2011; **365**: 395–409.

32 Xia C, Rook M, Pelgrim GJ, *et al.* Early imaging biomarkers of lung cancer, COPD and coronary artery disease in the general population: rationale and design of the ImaLife (Imaging in Lifelines) Study. *Eur J Epidemiol* 2019; published online April 23. DOI:10.1007/s10654-019-00519-0.

33 Behr CM, Koffijberg H, Degeling K, Vliegenthart R, IJzerman MJ. Can we increase efficiency of CT lung cancer screening by combining with CVD and COPD screening? Results of an early economic evaluation. *Eur Radiol* 2022; **32**: 3067–75.

34 Heuvelmans MA, Vonder M, Rook M, *et al.* Screening for Early Lung Cancer, Chronic Obstructive Pulmonary Disease, and Cardiovascular Disease (the Big-3) Using Low-dose Chest Computed Tomography: Current Evidence and Technical Considerations. *J Thorac Imaging* 2019; **34**: 160.

35 The top 10 causes of death. https://www.who.int/news-room/fact-sheets/detail/the-top-10-causes-of-death (accessed April 12, 2023).

36 Reitsma MB, Fullman N, Ng M, *et al.* Smoking prevalence and attributable disease burden in 195 countries and territories, 1990–2015: a systematic analysis from the Global Burden of Disease Study 2015. *The Lancet* 2017; **389**: 1885–906.

37 Quaderi SA, Hurst JR. The unmet global burden of COPD. *Glob Health Epidemiol Genomics* 2018; **3**. DOI:10.1017/gheg.2018.1.

38 Ehteshami-Afshar S, FitzGerald JM, Doyle-Waters MM, Sadatsafavi M. The global economic burden of asthma and chronic obstructive pulmonary disease. *Int J Tuberc Lung Dis* 2016; **20**: 11–23.

39 Shimizu K, Hasegawa M, Makita H, Nasuhara Y, Konno S, Nishimura M. Comparison of airway remodelling assessed by computed tomography in asthma and COPD. *Respir Med* 2011; **105**: 1275–83.

40 Patel BD, Coxson HO, Pillai SG, *et al.* Airway wall thickening and emphysema show independent familial aggregation in chronic obstructive pulmonary disease. *Am J Respir Crit Care Med* 2008; **178**: 500–5.

41 Lynch DA, Austin JHM, Hogg JC, *et al.* CT-Definable Subtypes of Chronic Obstructive Pulmonary Disease: A Statement of the Fleischner Society. *Radiology* 2015; **277**: 192–205.

42 Ross JC, Castaldi PJ, Cho MH, *et al.* Longitudinal Modeling of Lung Function Trajectories in Smokers with and without Chronic Obstructive Pulmonary Disease. *Am J Respir Crit Care Med* 2018; **198**: 1033–42.

43 Oelsner EC, Ortega VE, Smith BM, *et al.* A Genetic Risk Score Associated with Chronic Obstructive Pulmonary Disease Susceptibility and Lung Structure on Computed Tomography. *Am J Respir Crit Care Med* 2019; **200**: 721–31.

44 Dijkstra AE, Postma DS, van Ginneken B, *et al.* Novel genes for airway wall thickness identified with combined genome-wide association and expression analyses. *Am J Respir Crit Care Med* 2015; **191**: 547–56.

45 Hoshino M, Ohtawa J. Effects of budesonide/formoterol combination therapy versus budesonide alone on airway dimensions in asthma. *Respirol Carlton Vic* 2012; **17**: 639–46.

46 Li Y, Dai Y, Guo Y. The pulmonary damage caused by smoking: A longitudinal study. *Technol Health Care Off J Eur Soc Eng Med* 2018; **26**: 501–7.

47 Takayanagi S, Kawata N, Tada Y, *et al.* Longitudinal changes in structural abnormalities using MDCT in COPD: do the CT measurements of airway wall thickness and small pulmonary vessels change in parallel with emphysematous progression? *Int J Chron Obstruct Pulmon Dis* 2017; **12**: 551–60.

48 Liu L, Li G, Sun Y, Li J, Tang N, Dong L. Airway wall thickness of allergic asthma caused by weed pollen or house dust mite assessed by computed tomography. *Respir Med* 2015; **109**: 339–46.

49 Thomson NC, Chaudhuri R, Spears M, *et al.* Poor symptom control is associated with reduced CT scan segmental airway lumen area in smokers with asthma. *Chest* 2015; **147**: 735–44.

50 Gierada DS, Guniganti P, Newman BJ, *et al.* Quantitative CT assessment of emphysema and airways in relation to lung cancer risk. *Radiology* 2011; **261**: 950–9.

51 Ji W, Lim MN, Bak SH, *et al.* Differences in chronic obstructive pulmonary disease phenotypes between non-smokers and smokers. *Clin Respir J* 2018; **12**: 666–73.

52 Kirby M, Pike D, Sin DD, Coxson HO, McCormack DG, Parraga G. COPD: Do Imaging Measurements of Emphysema and Airway Disease Explain Symptoms and Exercise Capacity? *Radiology* 2015; **277**: 872–80.

53 Diaz AA, Bartholmai B, San José Estépar R, *et al.* Relationship of emphysema and airway disease assessed by CT to exercise capacity in COPD. *Respir Med* 2010; **104**: 1145–51.

54 Higami Y, Ogawa E, Ryujin Y, *et al.* Increased Epicardial Adipose Tissue Is Associated with the Airway Dominant Phenotype of Chronic Obstructive Pulmonary Disease. *PloS One* 2016; **11**: e0148794–e0148794.

55 Mohamed Hoesein FAA, Schmidt M, Mets OM, *et al.* Discriminating dominant computed tomography phenotypes in smokers without or with mild COPD. *Respir Med* 2014; **108**: 136–43.

56 Koyama H, Ohno Y, Yamazaki Y, *et al.* Quantitative bronchial luminal volumetric assessment of pulmonary function loss by thin-section MDCT in pulmonary emphysema patients. *Eur J Radiol* 2012; **81**: 384–8.

57 Diaz AA, Han MK, Come CE, *et al.* Effect of Emphysema on CT Scan Measures of Airway Dimensions in Smokers. *Chest* 2013; **143**: 687–93.

58 Gietema HA, Edwards LD, Coxson HO, Bakke PS, ECLIPSE Investigators. Impact of emphysema and airway wall thickness on quality of life in smoking-related COPD. *Respir Med* 2013; **107**: 1201–9.

59 Hong Y, Ji W, An S, Han S-S, Lee S-J, Kim WJ. Sex differences of COPD phenotypes in nonsmoking patients. *Int J Chron Obstruct Pulmon Dis* 2016; **11**: 1657–62.

60 Zach JA, Newell JD, Schroeder J, *et al.* Quantitative Computed Tomography of the Lungs and Airways in Healthy Nonsmoking Adults: *Invest Radiol* 2012; **47**: 596–602.

61 Kim Y-I, Schroeder J, Lynch D, *et al.* Gender Differences of Airway Dimensions in Anatomically Matched Sites on CT in Smokers. *COPD J Chronic Obstr Pulm Dis* 2011; **8**: 285–92.

62 Moher D, Liberati A, Tetzlaff J, Altman DG, Group TP. Preferred Reporting Items for Systematic Reviews and Meta-Analyses: The PRISMA Statement.

*PLOS Med* 2009; **6**: e1000097.

63 Covidence - Better systematic review management. Covidence. https://www.covidence.org/ (accessed Aug 7, 2020).

64 Sterne JAC, Savović J, Page MJ, *et al.* RoB 2: a revised tool for assessing risk of bias in randomised trials. *BMJ* 2019; **366**. DOI:10.1136/bmj.l4898.

65 Cochrane. Formulae for combining groups. https://training.cochrane.org/handbook/current/chapter-06#section-6-5-2-10 (accessed Aug 15, 2021).

66 Larson DA. Analysis of Variance with Just Summary Statistics as Input. *Am Stat* 2012; published online Feb 27. https://www.tandfonline.com/doi/pdf/10.1080/00031305.1992.10475872?needAccess=true (accessed June 24, 2020).

67 Deeks JJ, Higgins JP. Statistical algorithms in Review Manager 5. *Cochrane Collab* 2010; : 11.

68 Egger M, Smith GD, Schneider M, Minder C. Bias in meta-analysis detected by a simple, graphical test. *BMJ* 1997; **315**: 629–34.

69 Boyden EA. A critique of the international nomenclature on bronchopulmonary segments. *Dis Chest* 1953; **23**: 266–9.

70 Nakano Y, Muro S, Sakai H, *et al.* Computed tomographic measurements of airway dimensions and emphysema in smokers. Correlation with lung function. *Am J Respir Crit Care Med* 2000; **162**: 1102–8.

71 Choi S, Haghighi B, Choi J, *et al.* Differentiation of quantitative CT imaging phenotypes in asthma versus COPD. *BMJ Open Respir Res* 2017; **4**: e000252–e000252.

72 Haghighi B, Choi S, Choi J, *et al.* Imaging-based clusters in current smokers of the COPD cohort associate with clinical characteristics: the SubPopulations and Intermediate Outcome Measures in COPD Study (SPIROMICS). *Respir Res* 2018; **19**: 178–178.

73 Subramanian DR, Gupta S, Burggraf D, *et al.* Emphysema- and airway-dominant COPD phenotypes defined by standardised quantitative computed tomography. *Eur Respir J* 2016; **48**: 92–103.

74 Koyama H, Ohno Y, Nishio M, *et al.* Iterative reconstruction technique vs filter back projection: utility for quantitative bronchial assessment on low-dose thin-section MDCT in patients with/without chronic obstructive pulmonary disease. *Eur Radiol* 2014; **24**: 1860–7.

75 Petersen J, Wille MMW, Rakêt LL, *et al.* Effect of inspiration on airway dimensions measured in maximal inspiration CT images of subjects without airflow limitation. *Eur Radiol* 2014; **24**: 2319–25.

76 Kambara K, Shimizu K, Makita H, *et al.* Effect of lung volume on airway luminal area assessed by computed tomography in chronic obstructive pulmonary disease. *PloS One* 2014; **9**: e90040–e90040.

77 Gupta S, Hartley R, Khan UT, *et al.* Quantitative computed tomography-derived clusters: redefining airway remodeling in asthmatic patients. *J Allergy Clin Immunol* 2014; **133**: 729-38.e18.

78 Washko GR, Dransfield MT, Estépar RSJ, *et al.* Airway wall attenuation: a biomarker of airway disease in subjects with COPD. *J Appl Physiol Bethesda Md 1985* 2009; **107**: 185–91.

79 Schmidt M, Kuhnigk J-M, Krass S, M.d MO, Hoop B de, Peitgen H-O. Reproducibility of airway wall thickness measurements. In: Medical Imaging 2010: Computer-Aided Diagnosis. SPIE, 2010: 487–96.

80 Lutey BA, Conradi SH, Atkinson JJ, *et al.* Accurate measurement of small airways on low-dose thoracic CT scans in smokers. *Chest* 2013; **143**: 1321–9.

81 Cho HB, Chae KJ, Jin GY, *et al.* Structural and Functional Features on Quantitative Chest Computed Tomography in the Korean Asian versus the White American Healthy Non-Smokers. *Korean J Radiol* 2019; **20**: 1236–45.

82 Hansel NN, Washko GR, Foreman MG, *et al.* Racial differences in CT phenotypes in COPD. *COPD* 2013; **10**: 20–7.

83 Wan ES, Hokanson JE, Murphy JR, *et al.* Clinical and radiographic predictors of GOLD-unclassified smokers in the COPDGene study. *Am J Respir Crit Care Med* 2011; **184**: 57–63.

84 Inoue H, Niimi A, Takeda T, *et al.* Pathophysiological characteristics of asthma in the elderly: a comprehensive study. *Ann Allergy Asthma Immunol Off Publ Am Coll Allergy Asthma Immunol* 2014; **113**: 527–33.

85 Kim SS, Jin GY, Li YZ, Lee JE, Shin HS. CT Quantification of Lungs and Airways in Normal Korean Subjects. *Korean J Radiol* 2017; **18**: 739.

86 Li Y, Dai Y-L, Yu N, Guo Y-M. Sex-related differences in bronchial parameters and pulmonary function test results in patients with chronic obstructive pulmonary disease based on three-dimensional quantitative computed tomography. *J Int Med Res* 2018; **46**: 135–42.

87 Charbonnier J-P, Pompe E, Moore C, *et al.* Airway wall thickening on CT: Relation to smoking status and severity of COPD. *Respir Med* 2019; **146**: 36–41.

88 Eddy RL, Svenningsen S, Kirby M, *et al.* Is Computed Tomography Airway Count Related to Asthma Severity and Airway Structure-function? *Am J Respir Crit Care Med* 2020; : 10.1164/rccm.201908-1552OC.

89 Oguma T, Hirai T, Fukui M, *et al.* Longitudinal shape irregularity of airway lumen assessed by CT in patients with bronchial asthma and COPD. *Thorax* 2015; **70**: 719–24.

90 Tanabe N, Sato S, Oguma T, *et al.* Associations of airway tree to lung volume ratio on computed tomography with lung function and symptoms in chronic obstructive pulmonary disease. *Respir Res* 2019; **20**: 77–77.

91 Smith BM, Hoffman EA, Rabinowitz D, *et al.* Comparison of spatially matched airways reveals thinner airway walls in COPD. The Multi-Ethnic Study of Atherosclerosis (MESA) COPD Study and the Subpopulations and Intermediate Outcomes in COPD Study (SPIROMICS). *Thorax* 2014; **69**: 987–96.

92 Lo P, van Ginneken B, Reinhardt JM, *et al.* Extraction of Airways From CT (EXACT'09). *IEEE Trans Med Imaging* 2012; **31**: 2093–107.

93 Hammond E, Sloan C, Newell JD, *et al.* Comparison of low- and ultralow-dose computed tomography protocols for quantitative lung and airway assessment. *Med Phys* 2017; **44**: 4747–57.

94 Tschirren J, Yavarna T, Reinhardt J. Airway segmentation framework for clinical environments. In: 2nd international workshop on pulmonary image analysis. 2009: 227–38.

95 Yun J, Park J, Yu D, *et al.* Improvement of fully automated airway segmentation on volumetric computed tomographic images using a 2.5 dimensional convolutional neural net. *Med Image Anal* 2019; **51**: 13–20.

96 Garcia-Uceda A, Selvan R, Saghir Z, Tiddens HAWM, de Bruijne M. Automatic airway segmentation from computed tomography using robust and efficient 3-D convolutional neural networks. *Sci Rep* 2021; **11**: 16001.

97 Garcia-Uceda Juarez A, Tiddens HAWM, de Bruijne M. Automatic Airway Segmentation in Chest CT Using Convolutional Neural Networks. In: Stoyanov D, Taylor Z, Kainz B, *et al.*, eds. Image Analysis for Moving Organ, Breast, and Thoracic Images. Cham: Springer International Publishing, 2018: 238–50.

98 Pedersen JH, Ashraf H, Dirksen A, *et al.* The Danish Randomized Lung Cancer CT Screening Trial—Overall Design and Results of the Prevalence Round. *J Thorac Oncol* 2009; **4**: 608–14.

99 Xu DM, Gietema H, de Koning H, *et al.* Nodule management protocol of the NELSON randomised lung cancer screening trial. *Lung Cancer* 2006; **54**: 177–84.

100 Fedorov A, Beichel R, Kalpathy-Cramer J, *et al.* 3D Slicer as an Image Computing Platform for the Quantitative Imaging Network. *Magn Reson Imaging* 2012; **30**: 1323–41.

101 Virtanen P, Gommers R, Oliphant TE, *et al.* SciPy 1.0: Fundamental algorithms for scientific computing in python. *Nat Methods* 2020; **17**: 261–72.

102 van den Bosch WB, James AL, Tiddens HAWM. Structure and function of small airways in asthma patients revisited. *Eur Respir Rev* 2021; **30**: 1–18.

103 Tiddens HAWM, Donaldson SH, Rosenfeld M, Paré PD. Cystic fibrosis lung disease starts in the small airways: can we treat it more effectively? *Pediatr Pulmonol* 2010; **45**: 107–17.

104 Gove K, Wilkinson T, Jack S, Ostridge K, Thompson B, Conway J. Systematic review of evidence for relationships between physiological and CT indices of small airways and clinical outcomes in COPD. *Respir Med* 2018; **139**: 117–25.

105 Bian Z, Charbonnier J-P, Liu J, Zhao D, Lynch DA, Ginneken B van. Small airway segmentation in thoracic computed tomography scans: a machine learning approach. *Phys Med Biol* 2018; **63**: 155024.

106 Lo P, Sporring J, Ashraf H, Pedersen JJH, de Bruijne M. Vessel-guided airway tree segmentation: A voxel classification approach. *Med Image Anal* 2010; **14**: 527–38.

107 Prevedello LM, Halabi SS, Shih G, *et al.* Challenges Related to Artificial Intelligence Research in Medical Imaging and the Importance of Image Analysis Competitions. *Radiol Artif Intell* 2019; **1**: e180031.

108 Qin Y, Zheng H, Gu Y, *et al.* Learning Tubule-Sensitive CNNs for Pulmonary Airway and Artery-Vein Segmentation in CT. *IEEE Trans Med Imaging* 2021; **40**: 1603–17.

109 Cheng G, Wu X, Xiang W, Guo C, Ji H, He L. Segmentation of the Airway Tree From Chest CT Using Tiny Atrous Convolutional Network. *IEEE Access* 2021; **9**: 33583–94.

110 Zheng H, Qin Y, Gu Y, *et al.* Refined Local-imbalance-based Weight for Airway Segmentation in CT. In: de Bruijne M, Cattin PC, Cotin S, *et al.*, eds. Medical Image Computing and Computer Assisted Intervention – MICCAI 2021. Cham: Springer International Publishing, 2021: 410–9.

111 Nadeem SA, Hoffman EA, Sieren JC, *et al.* A CT-Based Automated Algorithm for Airway Segmentation Using Freeze-and-Grow Propagation and Deep Learning. *IEEE Trans Med Imaging* 2021; **40**: 405–18.

112 Reinhardt JM, D'Souza ND, Hoffman EA. Accurate measurement of intrathoracic airways. *IEEE Trans Med Imaging* 1997; **16**: 820–7.

113 Estépar RSJ, Washko GG, Silverman EK, Reilly JJ, Kikinis R, Westin C-F. Accurate airway wall estimation using phase congruency. *Med Image Comput Comput-Assist Interv MICCAI Int Conf Med Image Comput Comput-Assist Interv* 2006; **9**: 125–34.

114 Dudurych I, Garcia-Uceda A, Saghir Z, Tiddens HAWM, Vliegenthart R, de Bruijne M. Creating a training set for artificial intelligence from initial segmentations of airways. *Eur Radiol Exp* 2021; **5**: 54.

115 Petersen J, Arias-Lorza AM, Selvan R, *et al.* Increasing Accuracy of Optimal Surfaces Using Min-Marginal Energies. *IEEE Trans Med Imaging* 2019; **38**: 1559–68.

116 Sieren JP, Gunderson K, Lynch DA, Newell JD, Judy P, Hoffman EA. COPD-Gene Phantom: Quality Control Of Quantitative Lung Imaging In A Multicenter Trial. In: D27. PUSHING IMAGING TOWARD MICROANATOMY AND ORGAN/CELL PHYSIOLOGY. American Thoracic Society, 2010: A5519–A5519.

117 Akiba T, Sano S, Yanase T, Ohta T, Koyama M. Optuna: A Next-generation Hyperparameter Optimization Framework. In: Proceedings of the 25th ACM SIGKDD International Conference on Knowledge Discovery & Data Mining. New York, NY, USA: Association for Computing Machinery, 2019: 2623–31.

118 Schlathoelter T, Lorenz C, Carlsen IC, Renisch S, Deschamps T. Simultaneous segmentation and tree reconstruction of the airways for virtual bronchoscopy. In: Medical Imaging 2002: Image Processing. SPIE, 2002: 103–13.

119 Merkel D. Docker: lightweight linux containers for consistent development and deployment. *Linux J* 2014; **2014**: 2.

120 Sijtsma A, Rienks J, van der Harst P, Navis G, Rosmalen JGM, Dotinga A. Cohort Profile Update: Lifelines, a three-generation cohort study and biobank. *Int J Epidemiol* 2021; : dyab257.

121 Kuwano K, Bosken CH, Paré PD, Bai TR, Wiggs BR, Hogg JC. Small Airways Dimensions in Asthma and in Chronic Obstructive Pulmonary Disease. *Am Rev Respir Dis* 1993; **148**: 1220–5.

122 Moore DS Notz, William, Fligner, Michael A,. The basic practice of statistics. New York: W.H. Freeman and Co., 2013.

123 Seabold S, Perktold J. statsmodels: Econometric and statistical modeling with python. In: 9th Python in Science Conference. 2010.

124 Dudurych I, Muiser S, McVeigh N, *et al.* Bronchial wall parameters on CT in healthy never-smoking, smoking, COPD, and asthma populations: a systematic review and meta-analysis. *Eur Radiol* 2022; published online Feb 22. DOI:10.1007/s00330-022-08600-1.

125 Pompe E, van Rikxoort EM, Mets OM, *et al.* Follow-up of CT-derived airway wall thickness: Correcting for changes in inspiration level improves reliability. *Eur J Radiol* 2016; **85**: 2008–13.

126 Xu Z, Bagci U, Foster B, Mansoor A, Udupa JK, Mollura DJ. A hybrid method for airway segmentation and automated measurement of bronchial wall thickness on CT. *Med Image Anal* 2015; **24**: 1–17.

127 Weikert T, Friebe L, Wilder-Smith A, *et al.* Automated quantification of airway wall thickness on chest CT using retina U-Nets - Performance evaluation and application to a large cohort of chest CTs of COPD patients. *Eur J Radiol* 2022; **155**: 110460.

128 King GG, Müller NL, Whittall KP, Xiang Q-S, Paré PD. An Analysis Algorithm for Measuring Airway Lumen and Wall Areas from High-Resolution Computed Tomographic Data. *Am J Respir Crit Care Med* 2000; **161**: 574–80.

129 Sun Y, Zhou J. New insights into early intervention of chronic obstructive pulmonary disease with mild airflow limitation. *Int J Chron Obstruct Pulmon Dis* 2019; **14**: 1119–25.

130 Kirby M, Smith BM, Tanabe N, *et al.* Computed tomography total airway count predicts progression to COPD in at-risk smokers. *ERJ Open Res* 2021; **7**. DOI:10.1183/23120541.00307-2021.

131 Koo HJ, Lee SM, Seo JB, *et al.* Prediction of Pulmonary Function in Patients with Chronic Obstructive Pulmonary Disease: Correlation with Quantitative CT Parameters. *Korean J Radiol* 2019; **20**: 683–92.

132 Cheung WK, Pakzad A, Mogulkoc N, *et al.* Automated airway quantification associates with mortality in idiopathic pulmonary fibrosis. *Eur Radiol* 2023; published online July 28. DOI:10.1007/s00330-023-09914-4.

133 Dudurych I, Garcia-Uceda A, Petersen J, Du Y, Vliegenthart R, de Bruijne M. Reproducibility of a combined artificial intelligence and optimal-surface graph-cut method to automate bronchial parameter extraction. *Eur Radiol* 2023; published online April 18. DOI:10.1007/s00330-023-09615-y.

134 Chae KJ, Jin GY, Choi J, *et al.* Generation-based study of airway remodeling in smokers with normal-looking CT with normalization to control inter-subject variability. *Eur J Radiol* 2021; **138**: 109657.

135 Telenga ED, Oudkerk M, van Ooijen PMA, *et al.* Airway wall thickness on HRCT scans decreases with age and increases with smoking. *BMC Pulm Med* 2017; **17**. DOI:10.1186/s12890-017-0363-0.

136 Pride NB. Ageing and changes in lung mechanics. *Eur Respir J* 2005; **26**: 563–5.

137 Wilson JW. Inflammation and remodelling in the ageing airway. *Med J Aust* 2005; **183**. DOI:10.5694/j.1326-5377.2005.tb06915.x.

138 Brandsma C-A, Vries M de, Costa R, Woldhuis RR, Königshoff M, Timens W. Lung ageing and COPD: is there a role for ageing in abnormal tissue

repair? *Eur Respir Rev* 2017; **26**. DOI:10.1183/16000617.0073-2017.

139 Janssens JP, Pache JC, Nicod LP. Physiological changes in respiratory function associated with ageing. *Eur Respir J* 1999; **13**: 197–205.

140 Verleden SE, Kirby M, Everaerts S, *et al.* Small airway loss in the physiologically ageing lung: a cross-sectional study in unused donor lungs. *Lancet Respir Med* 2021; **9**: 167–74.

141 Mok LC, Juárez AG-U, Corput MK-VD, *et al.* The effect of CFTR modulators on CT outcomes in cystic fibrosis. *Eur Respir J* 2019; **54**. DOI:10.1183/13993003.congress-2019.OA2128.

142 Hoshino M., Ohtawa J. Effects of tiotropium and salmeterol/fluticasone propionate on airway wall thickness in chronic obstructive pulmonary disease. *Respiration* 2013; **86**: 280–7.

143 Jobst BJ, Weinheimer O, Buschulte T, *et al.* Longitudinal airway remodeling in active and past smokers in a lung cancer screening population. *Eur Radiol* 2019; **29**: 2968–80.

144 Grydeland TB, Dirksen A, Coxson HO, *et al.* Quantitative computed tomography measures of emphysema and airway wall thickness are related to respiratory symptoms. *Am J Respir Crit Care Med* 2010; **181**: 353–9.

145 Stanojevic S, Wade A, Stocks J. Reference values for lung function: past, present and future. *Eur Respir J* 2010; **36**: 12–9.

146 Nadeem SA, Comellas AP, Hoffman EA, Saha PK. Airway Detection in COPD at Low-Dose CT Using Deep Learning and Multiparametric Freeze and Grow. *Radiol Cardiothorac Imaging* 2022; **4**: e210311.

147 Abozid H, Kirby M, Nasir N, *et al.* CT airway remodelling and chronic cough. *BMJ Open Respir Res* 2023; **10**: e001462.

148 Diaz AA, Orejas JL, Grumley S, *et al.* Airway-Occluding Mucus Plugs and Mortality in Patients With Chronic Obstructive Pulmonary Disease. *JAMA* 2023; **329**: 1832–9.

149 Oguma T, Hirai T, Niimi A, *et al.* Limitations of Airway Dimension Measurement on Images Obtained Using Multi-Detector Row Computed Tomography. *PLOS ONE* 2013; **8**: e76381.

150 Vasilescu DM, Martinez FJ, Marchetti N, *et al.* Noninvasive Imaging Biomarker Identifies Small Airway Damage in Severe Chronic Obstructive Pulmonary Disease. *Am J Respir Crit Care Med* 2019; **200**: 575–81.

151 Usmani OS, Han MK, Kaminsky DA, *et al.* Seven Pillars of Small Airways Disease in Asthma and COPD: Supporting Opportunities for Novel Therapies. *CHEST* 2021; **160**: 114–34.



152 Roser M, Appel C, Ritchie H. Human Height. *Our World Data* 2013.

153 Terzikhan N, Verhamme KMC, Hofman A, Stricker BH, Brusselle GG, Lahousse L. Prevalence and incidence of COPD in smokers and non-smokers: the Rotterdam Study. *Eur J Epidemiol* 2016; **31**: 785–92.

154 James AL, Wenzel S. Clinical relevance of airway remodelling in airway diseases. *Eur Respir J* 2007; **30**: 134–55.

155 Forey BA, Thornton AJ, Lee PN. Systematic review with meta-analysis of the epidemiological evidence relating smoking to COPD, chronic bronchitis and emphysema. *BMC Pulm Med* 2011; **11**: 36.

156 Willemse BWM, Postma DS, Timens W, Hacken NHT ten. The impact of smoking cessation on respiratory symptoms, lung function, airway hyperresponsiveness and inflammation. *Eur Respir J* 2004; **23**: 464–76.

157 Scanlon PD, Connett JE, Waller LA, *et al.* Smoking Cessation and Lung Function in Mild-to-Moderate Chronic Obstructive Pulmonary Disease. *Am J Respir Crit Care Med* 2000; **161**: 381–90.

158 Song H., Lee I.J. Differences of low-dose chest computed tomography findings between smokers and nonsmokers based on smoking cessation program. *Iran J Radiol* 2018; **15**. DOI:10.5812/iranjradiol.64340.

159 Regan EA, Hokanson JE, Murphy JR, *et al.* Genetic Epidemiology of COPD (COPDGene) Study Design. *COPD J Chronic Obstr Pulm Dis* 2011; **7**: 32–43.

160 Donohue KM, Hoffman EA, Baumhauer H, *et al.* Cigarette smoking and airway wall thickness on CT scan in a multi-ethnic cohort: the MESA Lung Study. *Respir Med* 2012; **106**: 1655–64.

161 pulmonary_function_test [Lifelines Wiki]. http://wiki-lifelines.web.rug.nl/doku.php?id=pulmonary_function_test (accessed Aug 24, 2023).

162 Dudurych I, Pelgrim G-J, Sidorenkov G, *et al.* Low-Dose CT–derived Bronchial Parameters in Individuals with Healthy Lungs. *Radiology* 2024; **311**: e232677.

163 Anazawa R, Kawata N, Matsuura Y, *et al.* Longitudinal changes in structural lung abnormalities using MDCT in chronic obstructive pulmonary disease with asthma-like features. *PloS One* 2019; **14**: e0227141–e0227141.

164 Quanjer PH, Tammeling GJ, Cotes JE. Lung volumes and forced ventilatory flows. *Eur Respir J* 1993; **6**: 5–40.

165 Hall GL, Filipow N, Ruppel G. Official ERS technical standard: Global Lung Function Initiative reference values for static lung volumes in individuals of European ancestry. *Eur Respir J* 2021; **57**. DOI:10.1183/13993003.00289-2020.

166 Shah PL, Herth FJ, Geffen WH. Lung volume reduction for emphysema. *Lancet Respir Med* 2017; **5**: 147–56.

167 Klooster K, Slebos DJ. Endobronchial Valves for the Treatment of Advanced Emphysema. *Chest* 2021; **159**: 1833–42.

168 Come CE, Diaz AA, Curran-Everett D. Characterizing functional lung heterogeneity in COPD using reference equations for CT scan-measured lobar volumes. *Chest* 2013; **143**: 1607–17.

169 Tantucci C, Bottone D, Borghesi A. Methods for Measuring Lung Volumes: Is There a Better One? *Respiration* 2016; **91**: 273–80.

170 Garfield JL, Marchetti N, Gaughan JP. Total lung capacity by Plethysmography and high-resolution computed tomography in COPD. *Int J COPD* 2012; **7**: 119–26.

171 Becker MD, Berkmen YM, Austin JHM. Lung Volumes before and after Lung Volume Reduction Surgery. *Am J Respir Crit Care Med* 1998; **157**: 1593–9.

172 Matsumoto AJ, Bartholmai BJ, Wylam ME. Comparison of Total Lung Capacity Determined by Plethysmography with Computed Tomographic Segmentation Using CALIPER. *J Thorac Imaging* 2017; **32**: 101–6.

173 Brown MS, Kim HJ, Abtin F. Reproducibility of Lung and Lobar Volume Measurements Using Computed Tomography. *Acad Radiol* 2010; **17**: 316–22.

174 Kauczor HU, Heussel CP, Fischer B. Assessment of lung volumes using helical CT at inspiration and expiration: comparison with pulmonary function tests. *Am J Roentgenol* 1998; **171**: 1091–5.

175 Zaporozhan J, Ley S, Eberhardt R. Paired inspiratory/expiratory volumetric thin-slice CT scan for emphysema analysis: Comparison of different quantitative evaluations and pulmonary function test. *Chest* 2005; **128**: 3212–20.

176 Bakker JT, Klooster K, Bouwman J. Evaluation of spirometry-gated computed tomography to measure lung volumes in emphysema patients. *ERJ Open Res* 2022; **8**: 00492–2021.

177 Wisselink HJ, Steerenberg DJD, Rook M, *et al.* Predicted versus CT-derived total lung volume in a general population: The ImaLife study. *PloS One* 2023; **18**: e0287383.

178 Hasenstab KA, Tabalon J, Yuan N, Retson T, Hsiao A. CNN-based Deformable Registration Facilitates Fast and Accurate Air Trapping Measurements at Inspiratory and Expiratory CT. *Radiol Artif Intell* 2021; **4**: e210211.

179 Kristiansen JF, Perch M, Iversen M. Lobar Quantification by Ventilation/Perfusion SPECT/CT in Patients with Severe Emphysema Undergoing Lung Volume Reduction with Endobronchial Valves. *Respiration* 2019; **98**: 230–8.

180 Tahir BA, Holsbeke C, Ireland RH. Comparison of CT-based lobar ventilation with 3He MR imaging ventilation measurements. *Radiology* 2016; **278**: 585–92.

181 Kitano M, Iwano S, Hashimoto N. Lobar analysis of collapsibility indices to assess functional lung volumes in COPD patients. *Int J COPD* 2014; **9**: 1347–56.

182 Brown MS, Kim HJ, Abtin FG. Emphysema lung lobe volume reduction: Effects on the ipsilateral and contralateral lobes. *Eur Radiol* 2012; **22**: 1547–55.

183 Welling JBA, Hartman JE, Rikxoort EM. Minimal important difference of target lobar volume reduction after endobronchial valve treatment for emphysema. *Respirology* 2018; **23**: 306–10.

184 Wisselink HJ, Yang X, Rook M. CT-based emphysema characterization per lobe: A proof of concept. *Eur J Radiol* 2023; **160**. DOI:10.1016/j.ejrad.2023.110709.

185 Byers TE, Vena JE, Rzepka TF. Predilection of lung cancer for the upper lobes: An epidemiologic inquiry. *J Natl Cancer Inst* 1984; **72**: 1271–5.

186 Bakker JT, Klooster K, Vliegenthart R, Slebos D-J. Measuring pulmonary function in COPD using quantitative chest computed tomography analysis. *Eur Respir Rev* 2021; **30**. DOI:10.1183/16000617.0031-2021.

187 Coxson HO, V. NFP, Storness-Bliss C. Computed tomography assessment of lung volume changes after bronchial valve treatment. *Eur Respir J* 2008; **32**: 1443–50.

188 Yamada Y, Yamada M, Chubachi S, *et al.* Comparison of inspiratory and expiratory airway volumes and luminal areas among standing, sitting, and supine positions using upright and conventional CT. *Sci Rep* 2022; **12**: 21315.

189 Growth reference data for 5-19 years. https://www.who.int/tools/growth-reference-data-for-5to19-years/indicators/height-for-age.

190 Profiles - QIBA Wiki. https://qibawiki.rsna.org/index.php/Profiles (accessed May 26, 2024).

191 Ohno Y, Akino N, Fujisawa Y, *et al.* Comparison of lung CT number and airway dimension evaluation capabilities of ultra-high-resolution CT, using different scan modes and reconstruction methods including deep learning reconstruction, with those of multi-detector CT in a QIBA phantom study. *Eur Radiol* 2023; **33**: 368–79.

192 Health C for D and R. Artificial Intelligence and Machine Learning in Software as a Medical Device. *FDA* 2024; published online June 13. https://www.fda.gov/medical-devices/software-medical-device-samd/artificial-intelligence-and-machine-learning-software-medical-device (accessed July 14, 2024).

193 Artificial intelligence workplan to guide use of AI in medicines regulation | European Medicines Agency. https://www.ema.europa.eu/en/news/artificial-intelligence-workplan-guide-use-ai-medicines-regulation (accessed July 14, 2024).

194 Hoshino M, Ohtawa J, Akitsu K. Effects of the addition of tiotropium on airway dimensions in symptomatic asthma. *Allergy Asthma Proc* 2016; **37**: 147–53.

195 Kinose D, Ogawa E, Kawashima S, *et al.* An index of the fractal characteristic of an airway tree is associated with airflow limitations and future body mass index reduction in COPD patients. *J Appl Physiol* 2020; **128**: 1280–6.

196 Isensee F, Wald T, Ulrich C, *et al.* nnU-Net Revisited: A Call for Rigorous Validation in 3D Medical Image Segmentation. 2024; published online April 15. DOI:10.48550/arXiv.2404.09556.

197 Antonelli M, Reinke A, Bakas S, *et al.* The Medical Segmentation Decathlon. *Nat Commun* 2022; **13**: 4128.

198 Hop JF, Walstra ANH, Pelgrim G-J, *et al.* Detectability and Volumetric Accuracy of Pulmonary Nodules in Low-Dose Photon-Counting Detector Computed Tomography: An Anthropomorphic Phantom Study. *Diagnostics* 2023; **13**: 3448.

# CHAPTER 11

## Summary


### Part 1: Bronchial parameters on chest CT in context

The ability to extract detailed information from computed tomography scans is increasing with advancements in medical computer vision. This thesis outlines the development, validation and use of such techniques to measure bronchial parameters in a large, generally healthy study cohort from the general population. Starting with the foundational context and a systematic review, Chapter 2 presents an overview of current methodologies employed to assess bronchial wall parameters for patients with chronic obstructive pulmonary disease (COPD), asthma, never smokers and individuals who smoke or smoked. The systematic review and meta-analysis show that existing studies predominately focus on populations diagnosed with COPD or those with smoking history. Only few and mainly small-scale studies concern measurements of healthy individuals.

### Part 2: Automated bronchial parameter evaluation

Advancing into the technological core of the thesis, Chapters 3 and 4 cover our approaches for automated airway segmentation and bronchial parameter calculation. Chapter 3 shows the approach for efficient population-specific training of image segmentation models. Initial airway segmentations were derived from a pre-trained deep-learning model architecture specialised in segmentation based on volumetric CT images (U-Net). We performed manual correction of the initial segmentations in a small dataset and used them as ground truth to retrain the U-Net. The retrained model demonstrates improved accuracy and completeness of airway segmentations compared to the initial segmentations.

Chapter 4 builds on our work for automated bronchial parameter calculation. We introduce an automated pipeline for segmenting the lumen and wall surfaces of the bronchial tree. The pipeline utilizes the U-Net from Chapter 3 for airway extraction and an optimal-surface graph-cut method to segment the wall surrounding the extracted airways. To validate this approach, we measured bronchial parameters from the segmentations of initial and repeat scans of participants in the Imaging in Lifelines (ImaLife) study, taken an average of

3 months apart, and assessed their repeatability. The results demonstrate that the measurements exhibit sufficient reproducibility, and that the overall automated process can be applied to a large-scale dataset.

## Part 3: Airway and lung measurements in the general population

Chapter 5 applies these advanced methodologies to a large, lung-healthy cohort from the ImaLife study, establishing a comprehensive set of reference bronchial parameters. Using low-dose CT scans, bronchial parameters were automatically calculated using the approaches of Chapters 3-5. The results show that all bronchial parameters correlate significantly with characteristics such as age, sex, height, and weight, and smoking history. These population characteristics explain up to 46% of the variation in bronchial parameters. The findings provide a detailed characterisation of healthy airways and reference values for future studies on bronchial parameters.

In Chapter 6 we evaluated the relationship of smoking cessation duration with CT-based bronchial morphology based on a cross-sectional analysis of the general population. We studied whether longer periods of smoking cessation resulted in bronchial measurements approaching normal values. The observed correlation between smoking cessation duration and airway morphology suggests that for participants who had a history of respiratory illness, abnormal spirometry or imaging signs of respiratory disease, the detrimental effects of long-term smoking on the lungs are not entirely permanent and can be ameliorated through sustained cessation, providing an additional compelling argument for sustained smoking cessation efforts from a public health perspective.

Exploratory insights continue in Chapter 7 where we evaluate the Total Airway Count (TAC) and the impact of age, sex, height, weight, and smoking habits on TAC variation between individuals with healthy lungs and those with compromised lung health. Moreover, we determine the relationship between TAC and variations observed in spirometry results and assess TAC's predictive capabilities in differentiating between participant groups based on spirometry thresholds. Our findings reveal significant distinctions in CT-based TAC between lung-healthy and lung-unhealthy groups within the general population. Importantly, our analysis indicates that TAC holds potential as a simpler alternative to wall area percent and luminal area for predicting spirometry thresholds while providing comparable predictive performance.



In Chapter 8, the examination of individual lung lobe volumes further complements the overall thesis by providing reference equations for lung lobe volumes based on demographic attributes. These measurements are potentially useful for precisely planning targeted respiratory treatments, such as lung volume reduction procedures for COPD.

The comprehensive findings are discussed in Chapter 9 with additional commentary on future perspectives. The potential integration of advanced AI tools and an enhanced understanding of environmental impacts on respiratory health stand out as promising areas for future studies.

Overall, this thesis contributes to understanding of CT-based bronchial parameters in the lung healthy population by using state-of-the-art imaging analysis techniques. By establishing reference values of bronchial parameters in a large and healthy population and examining impact of lifestyle factors such as smoking cessation, this work provides valuable insights into healthy respiratory physiology as visualised on low-dose CT and sets the stage for future explorations in CT-based bronchial evaluations.

# SAMENVATTING

## DEEL 1 – BRONCHIALE PARAMETERS OP CT-SCAN IN CONTEXT

De mogelijkheid om gedetailleerde informatie uit een computertomografie (CT) scan te halen neemt toe met de huidige ontwikkelingen in medische computervisie. Deze thesis beschrijft de ontwikkeling, validatie en toepassing van dergelijke technieken om bronchiale parameters te meten in een grote, over het algemeen gezonde onderzoeksgroep uit de algemene bevolking. Beginnend met de basiscontext en een systematische review, presenteert Hoofdstuk 2 een overzicht van de huidige methodologieën die worden toegepast om bronchiale parameters te beoordelen bij patiënten met chronisch obstructieve longziekte (COPD), astma, individuen die roken, gerookt hebben of nooit gerookt hebben. De systematische review en meta-analyse tonen aan dat bestaande studies voornamelijk gericht zijn op populaties met een diagnose van COPD of die een rookgeschiedenis hebben. Slechts enkele en voornamelijk kleinschalige studies hebben betrekking op metingen bij gezonde individuen.

## DEEL 2 – GEAUTOMATISEERDE EVALUATIE VAN BRONCHIALE PARAMETERS

Hoofdstukken 3 en 4 betreffen onze benadering voor geautomatiseerde luchtwegsegmentatie en berekening van bronchiale (luchtwegwand) parameters als start van het technische gedeelte van dit proefschrift. Hoofdstuk 3 beschrijft de benadering voor efficiënte populatiespecifieke training van beeldsegmentatie modellen. De eerste luchtwegsegmentaties werden verkregen vanuit een vooraf getraind deep-learning model gespecialiseerd in segmentatie van volumetrische CT-beelden (U-Net). We voerden handmatige correctie van de initiële segmentaties uit in een kleine dataset en gebruikten deze als gouden standaard om het U-Net model opnieuw te trainen. Het opnieuw getrainde model toont verbeterde nauwkeurigheid en volledigheid van luchtwegsegmentaties vergeleken met de initiële segmentaties.

Hoofdstuk 4 bouwt voort op ons werk voor de geautomatiseerde berekening van bronchiale parameters. We introduceren een geautomatiseerde pijplijn voor het segmenteren van het lumen en de wandoppervlakten van de bronchi. De werkstroom maakt gebruik van de U-Net uit Hoofdstuk 3 voor segmentatie van de luchtwegen en een 'optimal-surface graph-cut' methode om de wanden rondom de luchtwegen te segmenteren. Ter validatie van deze benadering hebben we metingen verricht van de bronchiale parameters op initiële en herhaalde scans van deelnemers van de Imaging in Lifelines (ImaLife) studie, die gemiddeld 3 maanden tussen elkaar zijn gemaakt. Vervolgens beoordeelden we de overeenkomst in bronchiale parameters. De resultaten tonen aan dat de metingen voldoende reproduceerbaarheid vertonen en dat het algehele geautomatiseerde proces kan worden toegepast op een grootschalige dataset.

## DEEL 3 – LUCHTWEG- EN LONGMETINGEN IN DE ALGEMENE BEVOLKING

Hoofdstuk 5 past de hierboven geschreven geavanceerde methodologieën toe op een grote groep deelnemers met gezonde longen uit de ImaLife-studie, waarbij een uitgebreide reeks bronchiale referentieparameters is onderzocht. Met behulp van lage-dosis CT-scans werden bronchiale parameters automatisch berekend met de benaderingen uit Hoofdstukken 3-5. We vonden dat alle bronchiale parameters een relatie vertonen met kenmerken zoals leeftijd, geslacht, lengte en gewicht, en rookgeschiedenis. Deze populatiekenmerken verklaren tot 46% van de variatie in bronchiale parameters tussen verschillende personen. De bevindingen bieden een gedetailleerde karakterisering van gezonde luchtwegen en referentiewaarden voor toekomstige studies over bronchiale parameters.

In Hoofdstuk 6 evalueerden we de relatie tussen de duur van stoppen met roken en de bronchiale parameters op basis van een cross-sectionele analyse van de algemene bevolking. We bestudeerden of personen die al langere tijd gestopt waren met roken bronchiale metingen hadden die dichter bij normale waarden kwamen. De bevindingen suggereren dat in personen met luchtwegziekten, afwijkende longfunctietest of tekenen van luchtwegziekte op CT, de schadelijke effecten van langdurig roken op de longen gedeeltelijk reversibel zijn. Dit biedt vanuit een volksgezondheidsstandpunt een extra overtuigend argument voor voortdurende inspanningen om mensen te laten stoppen met roken.

In Hoofdstuk 7 onderzochten we de zogenaamde Total Airway Count (TAC), het totaal aantal aan gemeten luchtwegtakken op CT. We evalueerden de mpact van leeftijd, geslacht, lengte, gewicht en rookgewoonten op de variatie van TAC tussen individuen met gezonde longen en degenen met verminderde longgezondheid. Bovendien bepaalden we de relatie tussen TAC en longfunctietest resultaten. Als laatsteonderzochten we hoe goed TAC onderscheid kan maken tussen deelnemergroepen op basis van afwijkende longfunctietest resultaten. We vonden significante verschillen in

CT-gebaseerde TAC tussen groepen met gezonde longen of ongezonde longen binnen de algemene bevolking. Onze analyse toont aan dat TAC kansrijk is  als eenvoudiger alternatief voor andere bronchiale parameters zoals wandoppervlakte procent en luminale oppervlakte voor het voorspellen van afwijkende longfunctie.

In Hoofdstuk 8 zijn de referentiewaarden voor volume van individuele longkwabben in de algemene bevolking bepaald . Hierbij wordt rekening gehouden met demografische kenmerken zoals leeftijd en geslacht. Deze metingen zijn mogelijk bruikbaar voor nauwkeurige planning van gerichte behandelingen, zoals longvolume-reductieprocedures in COPD patiënten.

De resultaten van dit proefschrift worden besproken in Hoofdstuk 9 met aanvullend een perspectief op de toekomst. De potentiële integratie van geavanceerde AI-tools en een verbeterd begrip van de omgevingseffecten op de gezondheid van de luchtwegen springen eruit als veelbelovende gebieden voor toekomstige studies.

Concluderend levert dit proefschrift een bijdrage aan de kennis over CT-gebaseerde bronchiale parameters in de longgezonde populatie door gebruik te maken van geavanceerde beeldanalyse technieken. Door referentiewaarden vast te stellen van bronchiale parameters in een grote en gezonde populatie en de impact van levensstijlfactoren zoals rookstop te onderzoeken, biedt dit werk waardevolle inzichten in de luchtwegen zoals gevisualiseerd op lage-dosis CT en legt het de basis voor toekomstig onderzoek van luchtwegen via CT-evaluatie van bronchiale parameters.

# CHAPTER 12
# Appendix

## Supplemental Material

Please scan the QR code or follow the link below to view the supplemental material for each chapter.

https://pixelstoparameters.info/supplemental_material

# Acknowledgements

Before and during the journey towards this thesis, I had the pleasure of interacting with many great people. With their help, input and support I have grown academically, professionally and personally. I would like to thank everyone who in one way or other (sometimes non-knowingly) helped me in this journey with a special mention for some people in particular.

My first promotor, **Prof. Vliegenthart**. Rozemarijn, thank you for your dedication and support. With your outstanding academic experience and skill, I feel that I have greatly grown my own skills in the world of academia. Thank you too for your guidance and your trust in the studies we did together. I have been greatly inspired by your hard work, attention to detail and push for excellence. This is all evident from the excellent and impactful projects you lead, but seeing this from the inside of your lab taught me what it takes to get to such a point. Thank you for the hard work and time that you have dedicated to help me push through and complete this thesis.

My second promotor, **Prof. de Bruijne**. Marleen, it was a real pleasure to work with you and the lab at Erasmus MC. Thanks to you and the skills of people in your lab, I always had the resources I needed to get through the most technical challenges of the thesis. I'm sorry that due to the pandemic we had little opportunity for more in-person interaction, though despite this I could always count on your support and ability to make time for me. Your belief in my abilities helped me stay motivated during the most challenging parts of the thesis.

Thank you to the assessment committee **Prof. P.M.A. van Ooijen**, **Prof. G.H. Koppelman** and **Prof. P.A. de Jong** for their time and dedication in reviewing this thesis. Also, a thank you to the rest of the members of the corona for the opportunity to defend my thesis.

**Antonio**, I am very lucky to have had you as a close colleague and friend on this thesis path. Without your skills and hard work, there would be no backbone for the rest of my research. Your attention to detail and passion to get to the bottom of any issue drove the development of an amazing tool. Always kind and curious, your contribution to the studies and the writing process made me glad I could rely on your help and support.

To **Hendrik Wisselink-Bijker**, Rik it was a very dangerous decision to place us together as office mates. The increased frequency of bad (and sometimes good) puns that the rest of our colleagues had to deal with could somewhat be classified as a work hazard. Whatever topic came up, it was always possible to have a deep and interesting conversation with you about it, or at the very least find a suitable XKCD comic that did all the talking for us. **Leonardus van den Oever**, Daan it's only because I consider you a friend that I didn't ask you to become a paranymph once more. The sword and board games we played together were a great deal of fun every time and displayed your great analytical mind (and very Dutch directness) at full force.

Thank you **Gert Jan** for your cheerful demeanour and willingness to always help out. Inside and outside the main topics of our interests, it was a great deal of fun in seeing the sparks of inspiration result in a patent application that you, **Michiel** Erasmus and I worked on together. It was a pleasure to explore something like this with you. **Stella Noach**, your kindness, guidance and a listening ear were crucial to me throughout the PhD journey. I'll always value the friendship and advice you gave. **Mirjam Wielema** the evenings gathered around your table with a chat over a new or old boardgame to share were some great times I've had over the course of this PhD journey.

Thanks to everyone in the G2 group (then Bloemsingel… then G2 again) in no particular order, **Jingxuan Wang, Nikos Sourlos, Iris Hamelink, Ricardo Rivas Loya, Marleen Vonder, Ludo Cornelissen, Daiwei Han, Yeshu Nagaraj, Congying Xia, Xiaonan Cui, Zhenhui Nie, Luis de la O Arevalo, Alessia de Biase, Xueping Jing, Nils van der Velden, Erfan Darzi Dehkalani, Daan Ties, Randy van Dijk, Jiali Cai, Marly van Assen, Runlei Ma**. My time in Groningen was made all the richer thanks to you all! Thanks for all the coffee breaks and interesting discussions over the years.

Thanks to everyone at the BIGR lab, it was always a great inspiration to see what all of you were working on **Robin, Kim, Hoel** and **Shuai**. I learnt a lot from all of you in both technical and academic skills. While unfortunately due to COVID there was little opportunity for in person visits throughout the years, the few times I got to spend time with you all in person were great!

A great part about working in the UMCG is the ease with which it was possible to meet interesting people with great ideas, and to collaborate on these ideas. **Jens Bakker**, **Joost Hop**, **Maarten van den Berge**, **Dirk Jan Slebos**, **Marcel Greuter**, **Grigory Sidorenkov**, **Martin Dijkhuizen**, it was a pleasure to work on many interesting topics together.

Thank you to my colleagues from the B3Care Project **Nikos Sourlos, Carina Behr**, **Elfie Hoffmeier**, **Lu Liu**, **Sara Roscioni**, **Hans Brouwers** and everyone from Lifelines with a particular mention to **Seija Jansen**, **Trynke de Jong**, **Jurjen van Bolhuis** for the help and support with the ImaLife and B3Care projects.

**Conor, Michael, Stephen, Cian, Jesse, Shane, Patrick** the distance and travel-bans haven't worn away our friendships, and each late-night adventure into the fray with all of you remain highlights in my mind. As always, your friendships have brought many joys into my days that helped push through difficult days and each of you demonstrate so many qualities that I strive to improve in myself. **Niall,** while we never get enough chances to catch up, each time we do is a real treat. I'm always excited at the prospect of grabbing a coffee or two (or three), knowing we'll use up all the time available discussing the latest and greatest until other matters call our attention elsewhere. **Sam**, it's just my luck that as I moved back to Ireland, off you went to Australia and we missed each other again. It's a testament to how good of a friend you are to people around you that I'm sitting here with Tula and Petra on your couch after you ferried us around for a few days all over the Great Ocean Road!

This journey towards a thesis cannot go without mentioning the people instrumental to intriguing me and helping me find my way towards the Netherlands. **Des Winter**, your contagious curiosity and deep discussions sparked my own interest in the academic side of medicine. Your example of establishing international collaboratives to bring insights into serious topics showed me what research can do, and the value of contributing to it. **Emma Bruns**, I'm always in awe of your ability to blend serious science, medicine and philosophy with current events. I always greatly enjoyed our conversations together and am forever grateful for the time you spent in helping me find my way in the Netherlands and showing me the options available. **Joost Huiskens**, the evening lake-side chat in Rotterdam is really a formative memory for me and has helped shape my journey since. Thank you for sharing your path and helping me find mine. **Bart Geerts**, meeting you has shown me what artificial intelligence can really contribute to healthcare beyond the theoretical and academic. With this I had the confidence to jumping into a topic that was new, uncertain and technically challenging, knowing that there really could be something worthwhile at the end.

To all the GSMS and Kolff PhD Council colleagues **Alejandro, Klaudia, Ioana, Tiago, Nad'ka, Ioana, Rita, Frits, Tamara, Noura, Janne, Daniëlle, Andréa**. It's been great to figure things out together and I have learnt a lot from all of you in the process.

**Torben**, lead Bizzy Bee! Your enthusiasm is contagious, the effort you apply to any task is admirable and I'm very glad to have made a friend like you during my studies. I hope we get some opportunity soon to explore some skateparks, by which point I hope to also have learnt an ollie, an achievement almost more daunting than a PhD at this age!

To **Doreen**, **Patricia** and **Brian**, without your support throughout the years I surely would not be where I am now. Words cannot express my gratitude to all of you for all your help.

To my parents **Ivan** and **Dariya**, both of you always show me the example of what it is to be a good person. Your dedication to our family, support, understanding and love are the foundation of all that I am. Despite our separation during Covid, the daily calls and chats have helped me immensely and your support from afar has helped me through the toughest parts of this journey. You even managed to sneak in some engineering into my studies and career after all!

To **Diana** my sister, always a fount of kindness and support in good and bad. Throughoug all our years together, I can count on you for a listening ear. You have this great knack for bringing the best people around you, and without this I wouldn't have half the good friends and new family members in life that I do now. Through you our family is enriched with so many great people, with a very special thanks to my brother-in-law **Dan, Pax, Joanne, Tom, Sam**.

**Becca**, I started on this journey without knowing you, but I can't imagine finishing it without you by my side. My life is so much richer with you in it, and your love and support were key ingredients to take this thesis to the end. Thank you for giving me a listening ear and sage advise on substance (and style) both for the thesis and life.

To my paranymphs **Diana** and **Rebecca**, thank you for your help, support and lending your endless artistic skills towards the beautiful design of this book.

# List of Publications

**2019-2024**

**Low-Dose CT–derived Bronchial Parameters in Individuals with Healthy Lungs**
I. Dudurych, G.-J. Pelgrim, G. Sidorenkov, A. Garcia-Uceda, J. Petersen, D.-J. Slebos, G.H. de Bock, M. van den Berge, M. de Bruijne, R. Vliegenthart, D. Katz, A. Panzer
*Radiology 2024* e232677. https://doi.org/10.1148/radiol.232677.

**Reference Formulas for Chest CT-Derived Lobar Volumes in the Lung-Healthy General Population**
J.T. Bakker, I. Dudurych, S.A. Roodenburg, J.M. Vonk, K. Klooster, M. de Bruijne, M. van den Berge, D.-J. Slebos, R. Vliegenthart
*European Radiology 2024* https://doi.org/10.1007/s00330-024-11123-6.

**Reproducibility of a combined artificial intelligence and optimal-surface graph-cut method to automate bronchial parameter extraction**
I. Dudurych, A. Garcia-Uceda, J. Petersen, Y. Du, R. Vliegenthart, M. de Bruijne
*European Radiology 2023* https://doi.org/10.1007/s00330-023-09615-y.

**Bronchial wall parameters on CT in healthy never-smoking, smoking, COPD, and asthma populations: a systematic review and meta-analysis**
I. Dudurych, S. Muiser, N. McVeigh, H.A.M. Kerstjens, M. van den Berge, M. de Bruijne, R. Vliegenthart
*European Radiology 2022* https://doi.org/10.1007/s00330-022-08600-1.

**Improved precision of noise estimation in CT with a volume-based approach**
H.J. Wisselink, G.J. Pelgrim, M. Rook, I. Dudurych, M. van den Berge, G.H. de Bock, R. Vliegenthart *European Radiology Experimental 2021* https://doi.org/10.1186/s41747-021-00237-x.



**Creating a training set for artificial intelligence from initial segmentations of airways**
I. Dudurych, A. Garcia-Uceda, Z. Saghir, H.A.W.M. Tiddens, R. Vliegenthart, M. de Bruijne
*European Radiology Experimental 2021* https://doi.org/10.1186/s41747-021-00247-9.

**Manual Correction of CT-Derived Airway Segmentations for Artificial Intelligence Applications: A Technical Note**
I. Dudurych, A.G.-U. Juarez, R. Vliegenthart, M. de Bruijne
*European Congress of Radiology 2021* https://epos.myesr.org/poster/esr/ecr2021/C-10975

**Predicting outcomes of pelvic exenteration using machine learning**
I. Dudurych, PelvEx Collaborative
*Colorectal Disease 2020* https://doi.org/10.1111/codi.15235.

**Glyoxal cross-linking of solubilized extracellular matrix to produce highly porous, elastic, and chondro-permissive scaffolds for orthopedic tissue engineering**
D.C. Browe, O.R. Mahon, P.J. Díaz-Payno, N. Cassidy, I. Dudurych, A. Dunne, C.T. Buckley, D.J. Kelly, *Journal of Biomedical Materials Research Part A 2019* https://doi.org/10.1002/jbm.a.36731.